862

LA-9846-PR

Progress Report

Los Alamos National Laboratory is operated by the University of California for the United States Department of Energy under contract W-7405-ENG-36.

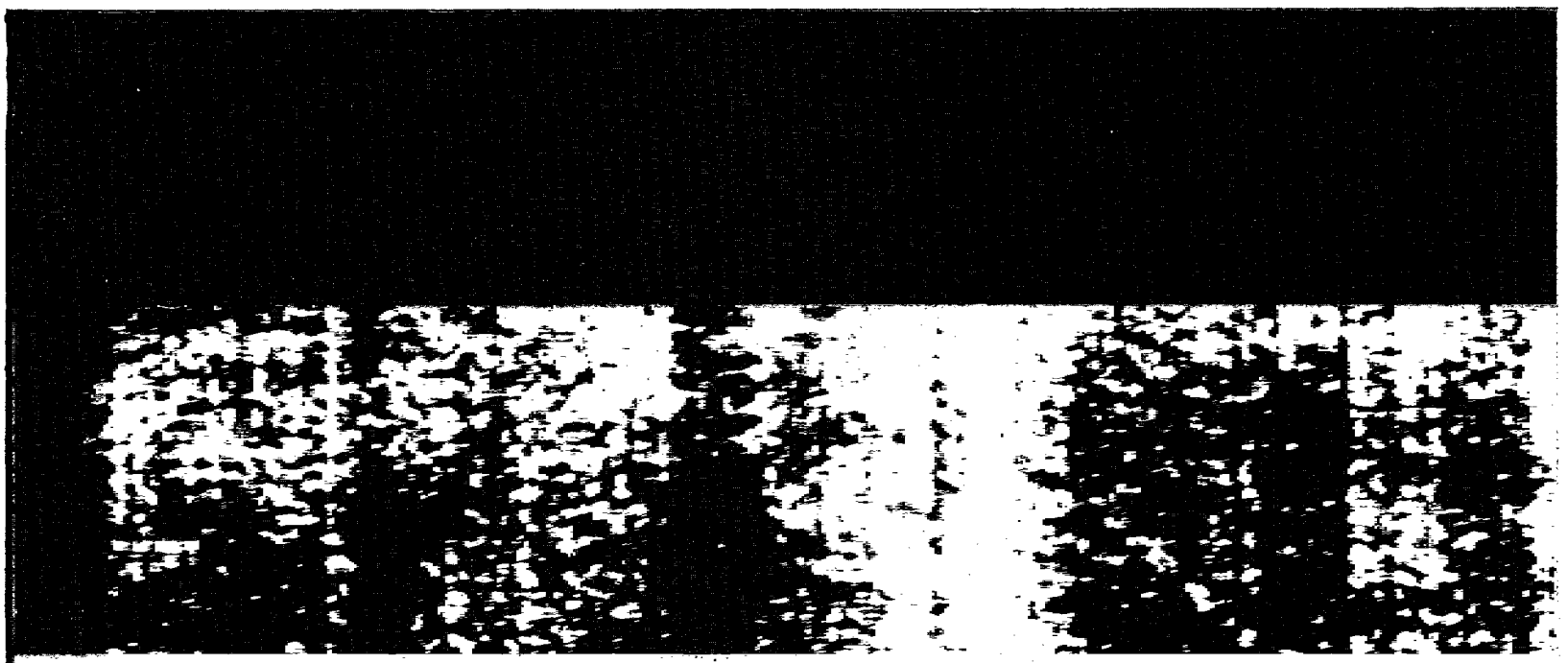

Research and Development Related to the Nevada Nuclear Waste Storage Investigations

April 1—June 30, 1983

Los Alamos

Los Alamos National Laboratory
Los Alamos, New Mexico 87545

An Affirmative Action/Equal Opportunity Employer

The four most recent reports in this series, unclassified, are LA-9484-PR, LA-9577-PR, LA-9666-PR, and LA-9793-PR.

This report was prepared by the Los Alamos National Laboratory as part of the Nevada Nuclear Waste Storage Investigations managed by the Nevada Operations Office of the US Department of Energy. Based upon their applicability to the investigations, some results from the Radionuclide Migration Project, managed by the Nevada Operations Office of the US Department of Energy, are included in this report.

Edited by Jody Heiken, INC Division

DISCLAIMER

This report was prepared as an account of work sponsored by an agency of the United States Government. Neither the United States Government nor any agency thereof, nor any of their employees, makes any warranty, express or implied, or assumes any legal liability or responsibility for the accuracy, completeness, or usefulness of any information, apparatus, product, or process disclosed, or represents that its use would not infringe privately owned rights. Reference herein to any specific commercial product, process, or service by trade name, trademark, manufacturer, or otherwise, does not necessarily constitute or imply its endorsement, recommendation, or favoring by the United States Government or any agency thereof. The views and opinions of authors expressed herein do not necessarily state or reflect those of the United States Government or any agency thereof.

LA-9846-PR
Progress Report

UC-70
Issued: December 1983

Research and Development Related to the Nevada Nuclear Waste Storage Investigations

April 1—June 30, 1983

Compiled by
A. E. Ogard, K. Wolfsberg, and D. T. Vaniman

Contributors

R. D. Aguilar
W. S. Baldridge
B. P. Bayhurst
D. L. Bish
J. D. Blacic
D. E. Broxton
F. M. Byers, Jr.
F. A. Caporuscio
B. A. Carlos
M. R. Cisneros
B. M. Crowe
D. B. Curtis
A. H. Davis
C. J. Duffy
R. R. Geoffrion
R. C. Gooley
L. E. Hersman
J. F. Kerrisk
S. D. Knight
F. O. Lawrence
S. S. Levy
S. Maestas
A. J. Mitchell
E. J. Mroz
C. W. Myers
D. C. Nelson
T. W. Newton
A. E. Norris
A. E. Ogard
D. M. Roy*
V. L. Rundberg
R. S. Rundberg
R. E. Semarge
K. W. Thomas
D. T. Vaniman
R. J. Vidale
P. L. Wanek
K. Wolfsberg
D. A. York

*Materials Research Laboratory, The Pennsylvania State University, University Park, PA 16802.

Los Alamos
Los Alamos National Laboratory
Los Alamos, New Mexico 87545

CONTENTS

ABSTRACT 1

EXECUTIVE SUMMARY 2

I. INTRODUCTION 9

II. GEOCHEMISTRY OF TUFF 9

A. Groundwater Chemistry of Yucca Mountain 9

B. Variations of Groundwater Chemistry in Contact with Tuffs . 14

C. Variations with Temperature of Groundwater Composition in Contact with Tuff 18

D. Groundwater Analysis 20

E. Microbiological Activity in the Yucca Mountain Environment. 21

F. Plutonium Chemistry in Near-Neutral Solutions 22

G. Solubility of Actinide Solids in the pH Range of 5 to 10 . 27

H. Batch Sorption Experiments 31

I. Geochronology 36

J. Matric Potential Determinations 42

K. Fracture-Flow Experiments 43

L. New Thermodynamic Data for EQ3/6 43

M. Analcime Solid-Solution Model 53

III. MINERALOGY-PETROLOGY OF TUFF 54

A. Studies of Drill Hole UE-25p#1 54

B. Fibrous Zeolites at Yucca Mountain 56

C. Effects of Composition on Thermal Expansion/Contraction in Clinoptilolite. 58

IV. VOLCANISM STUDIES 59

V. ROCK PHYSICS 60

VI. SHAFT AND BOREHOLE SEALING 64

VII. EXPLORATORY SHAFT 68

A. Design 68

B. Test Plan 69

VIII. QUALITY ASSURANCE 71

A. Los Alamos 71

B. US Geological Survey 72

REFERENCES 72

APPENDIX A 77

APPENDIX B 104

RESEARCH AND DEVELOPMENT RELATED TO THE NEVADA NUCLEAR WASTE STORAGE INVESTIGATIONS

April 1--June 30, 1983

Compiled by

A. E. Ogard, K. Wolfsberg, and D. T. Vaniman

Contributors

R. D. Aguilar
W. S. Baldridge
B. P. Bayhurst
D. L. Bish
J. D. Blacic
D. E. Broxton
F. M. Byers, Jr.
F. A. Caporuscio
B. A. Carlos
M. R. Cisneros
B. M. Crowe
D. B. Curtis
A. H. Davis
C. J. Duffy
R. R. Geoffrion
R. C. Gooley
L. E. Hersman
J. F. Kerrisk
S. D. Knight
F. O. Lawrence
S. S. Levy
S. Maestas
A. J. Mitchell
E. J. Mroz
C. W. Myers
D. C. Nelson
T. W. Newton
A. E. Norris
A. E. Ogard
D. M. Roy
V. L. Rundberg
R. S. Rundberg
R. E. Semarge
K. W. Thomas
D. T. Vaniman
R. J. Vidale
P. L. Wanek
K. Wolfsberg
D. A. York

ABSTRACT

This report summarizes the contribution of the Los Alamos National Laboratory to the Nevada Nuclear Waste Storage Investigations for the third quarter of 1983.

EXECUTIVE SUMMARY

This report summarizes some of the technical contributions from the Los Alamos National Laboratory to the Nevada Nuclear Waste Storage Investigations (NNWSI) project managed by the Nevada Operations Office of the US Department of Energy (DOE) during the period from April 1 through June 30, 1983. The report is not a detailed technical document but does indicate the status of many investigations being performed at Los Alamos.

GEOCHEMISTRY OF TUFF (WBS 1.3.2.2.1)

The chemistry of the groundwater in Yucca Mountain at the Nevada Test Site (NTS) is important for several reasons. (1) The speciation of nuclear wastes that may dissolve in the groundwater will largely be controlled by the groundwater chemistry. The speciation, in turn, will affect the precipitation reactions, complexing, and other retardation mechanisms. (2) The corrosion rate of the waste package is greatly affected by groundwater composition. (3) The definition of water flow paths can be aided by a knowledge of the groundwater chemistry. The composition of groundwater from wells pumped and sampled in the vicinity of Yucca Mountain has been analyzed; data are included for water from Wells USW H-1, H-4, H-5, H-6, J-13, UE-29a#2, and UE-25b#1. The sodium, potassium, and calcium contents fall into the following three groups.

(1) Analyses from Wells USW H-5 and USW H-6 are highest in sodium and lowest in calcium content. These are also the two wells farthest to the west; they lie beyond a fault 1500 ft west of Drill Hole USW G-4 in Yucca Mountain.

(2) The second group includes waters from Drill Holes USW H-1, H-4, G-4, and UE-29a#2; they show a lower sodium and a higher calcium content.

(3) The third group includes analyses for Wells UE-25b#1 and J-13, which are east of Yucca Mountain; they show the lowest sodium content.

Whether these differences have any physical significance for water flow paths or water travel times is not known. Groundwater can be expected to change somewhat in composition as it migrates down through a different strata of the unsaturated zone and along various water pathways in the saturated zone. Information that can be used to model these changes has been obtained by pretreating groundwater with tuff before each sorption experiment. This

pretreatment step revealed that contact between groundwater and glassy tuff increases the magnesium and potassium content of the water as the glass dissolves, whereas contact with a zeolite such as a clinoptilolite further along the pathway will decrease the magnesium content. Although the changes are not large and probably have no significant effect on retardation of waste elements, this information is needed to model groundwater flow paths and to predict changes in groundwater.

As a result of waste loading in the repository, the tuff of the Topopah Spring Member and possibly a portion of the tuff of the Calico Hills will be subjected to temperature increases for a long time. These changes could alter the composition of any water in contact with the tuff and, in turn, could affect reactions between the water and waste cannister. The change in composition of distilled water in contact with the tuff of Calico Hills at 150 and 325°C for periods of 1 to 21 weeks was studied. (The Topopah Spring Member tuff had been studied earlier.) Distilled water was used because water from condensed steam--essentially distilled water--from the loaded repository will be a lower bound on the dissolved-solids content in water/tuff interactions. The most notable result is the high silicon content that is rapidly achieved in the water (>200 mg/ℓ at 150°C and >500 mg/ℓ at 325°C). These high silicon concentrations could result in precipitation of silica in the tuffs at a lower temperature and would also cause a decrease in the tuff's porosity.

Several microbiological oxygen-uptake experiments were done with the drilling polymer and detergent currently used at Yucca Mountain. These experiments will provide information about any microbiological activity caused by site characterization activities; the data will be used to quantify the effect on retardation. If significant quantities of polymer or detergent are introduced, the oxygen consummed by microbial growth on the polymer and/or detergent could cause a significant reduction in the Eh of the repository site.

A number of precipitates of hydrous plutonium dioxide have been prepared for x-ray powder diffraction studies. The data from the precipitations are useful because they provide upper limits for the solubility. The precipitates were prepared by adding Pu(IV) in acid solution, Pu(IV) polymer, or Pu(III) to an excess of a well-stirred solution of a base. The phases were then

separated by centrifugation and analyzed. The results agree quite well with Rai and Swanson's equation $\log C = -2.55 + 0.75\ pH$.

Additional information on the solubility of plutonium solids at ~pH 8 can be obtained from plutonium sorption experiments done at Los Alamos over the past 3 years. The initial plutonium tracer for sorption experiments was prepared by adding $NaNO_2$ to an aliquot of Pu(III) in HCl, which was then air dried. For sorption experiments, the solid is then dissolved in representative waters. When the amount of a particular solid going into solution is constant, regardless of any additional amount of solid available, the solubility limit for that particular solid has been reached. Under oxidizing conditions in Well J-13 water, this solubility was 3×10^{-7} M ± a factor of 10. Similar experiments on americium did not give a solubility limit.

Sorption of radioactive waste elements on minerals in tuff is one of the most important retardation mechanisms in Yucca Mountain tuffs. The majority of available data on the sorption properties of tuff come from batch or static laboratory measurements; these are valid results for an equilibrium system. Sorption results for uranium, radium, and selenium on tuff are now available. The sorption ratios for barium and radium on various tuffs are high—within a factor of 2 of each other. Therefore, barium can be used as an analogue for radium sorption, and the sorption ratios determined previously for barium can be applied to calculations for radium sorption. Sorption ratios for uranium under aerobic conditions range from 0 on tuffs largely composed of alkali feldspars to 54 mℓ/g on tuffs containing the zeolite clinoptilolite as the major mineral. Selenium tested with similar conditions and tuff minerals exhibited somewhat lower sorption ratios: from 0 to 25 mℓ/g. Additional sorption ratios for americium and plutonium on unsaturated tuffs are presented in this report.

Measurements of ^{36}Cl can be used to date vadose water older than ~6×10^4 years. These measurements, used with carbon dating techniques, will provide information on the rate of water infiltration through the unsaturated zone. Techniques are being developed to quantitatively leach chlorides from tuffs for this analysis.

To model the flow and transport characteristics in tuff, it is necessary to know their matric potential as a function of saturation. Both mercury intrusion and pressure membrane extraction methods are used to determine the

matric potential of Topopah Spring Member tuff, and the results are in agreement.

The EQ3/6 thermodynamic data base is being expanded and updated to include the minerals and groundwater species found at Yucca Mountain and the elements needed for chemical modeling of waste radionuclides that are listed in Environmental Protection Agency (EPA) document 40 CFR 191. New data for manganese and strontium have been compiled and added to the data base. In some cases, this information replaced existing data and in others it added new solids or aqueous species to the data base.

A model for the formation of analcime solid solutions in the environs of Yucca Mountain has been developed. Based on observed compositions of the analcime that coexists with quartz there, this model will help predict the future stability of tuff minerals at Yucca Mountain.

MINERALOGY-PETROLOGY (WBS 1.3.2.2.2)

Mineralogy-petrology studies concentrated on the stratigraphy and mineralogy of Drill Hole UE-25p#1, the question of possible health hazards from fibrous zeolites at Yucca Mountain, and the thermal expansion/contraction of clinoptilolite. Modal analyses and electron-microprobe analyses were used to help identify the Tram, Lithic Ridge, and older tuff (Unit A and Unit C) samples. Modal and microprobe studies also led to a correlation of the deepest ash flow encountered with the tuff of Yucca Flat. The studies of fibrous zeolites were examined in light of current research that suggests these minerals might cause lung disease. Erionite and mordenite are the zeolites of particular interest. Erionite has not been detected at Yucca Mountain; if present, it must occur only in abundances less than 2%. Mordenite is abundant only below the breakout horizon in the Topopah Spring unit; some mordenite also occurs along fractures within the breakout horizon, but its overall abundance is very small. It is very unlikely that fibrous zeolites will be of concern during repository construction or operation. Abundant mordenite might be encountered if the exploratory shaft is mined below 1470-ft (448-m) depth. The behavior of clinoptilolite at elevated temperatures is highly composition dependent. Contractions range up to 8.5% in sodium-clinoptilolite but do not exceed 3.5% in calcium-clinoptilolite and 1.6% in potassium-clinoptilolite.

VOLCANISM STUDIES (WBS 1.3.3.4)

Volcanism studies are nearly complete, and activities during the quarter were devoted to writing the final volcanic hazards report.

Field sampling by helicopter at the Nellis Bombing and Gunnery Range filled in missing information for the geochemical data base. The basalt of Nye Canyon was mapped in detail to verify that the opening eruptive activity of the southern two centers was phreatomagmatic.

The volcanism sections of the Site Characterization Plan (SCP) were revised and the report "Summary of Volcanism Studies for the Nevada Nuclear Waste Storage Investigations" by B.M. Crowe, D.T. Vaniman, and W.J. Carr was published.

ROCK PHYSICS STUDIES (WBS 1.4.8.1)

The first long-term creep test of Calico Hills zeolitized tuff have been started. Improvements in the sample-grinding technique have eliminated sample-cracking problems, and an inventory of five finished samples was produced for further testing. The creep curve can be characterized as showing a slow but accelerating dilation. Average strain rate over the last 50 hours is about $1 \times 10^{-9} s^{-1}$. If it is possible within a reasonable time, the tests should continue until the sample is taken to failure. However, because of the limited time available to test the Calico Hills sample, this experiment will probably be cut off at 500 hours.

SHAFT AND BOREHOLE SEALING (WBS 1.4.5.1)

The report "Preliminary Accelerated Reaction Studies of the Hydrothermal Alteration of a Tuff-Bearing Concrete" by B. E. Sheetz and D. M. Roy describes a series of accelerated hydrothermal experiments that were run on the concrete CL-40 CON-14. The concrete was prepared by the Waterways Experiment Station and contains, as aggregate, indigenous sand and tuffaceous rock from the NTS. Characterization of the solid and liquid reaction products of the experiments indicated that chemical reaction took place in both the tuff aggregate and the cementatious matrix of the concrete. The accelerated tests provided preliminary information on the stability of this particular concrete formation. The next phase of experimentation, which is now under way, uses coarser fractions of crushed material and single blocks of concrete to investigate possible interfacial reactions between tuff and the cementatious matrix. A more silica-rich

matrix, #82-22, has also been formulated and should be less reactive with the tuff; experiments are now under way to test the new formulation.

The report "Low-Temperature Equilibria in the System Concrete-Tuff: Thermodynamic Calculations, Experimental Studies, and Natural Assemblages" by W. P. Freeborn, M. W. Barnes, and D. M. Roy applies three different sources of information to determine the thermodynamic stability of the phases and phase assemblages in the concrete/tuff system; only limited data were available from each source. The conclusions, although tentative, suggest strongly that siliceous concretes may be compatible with tuff (whereas high-lime concretes are probably not), that tuffs are compatible with aluminous clays, but that neither high-lime nor siliceous concretes are compatible with aluminous clays. Therefore, it is important to use siliceous concrete mixes, such as #82-22, in a tuff repository and to avoid placing aluminous clays in direct contact with concrete.

EXPLORATORY SHAFT (WBS 1.6.4.2)

A. Design

The Title II design of the Exploratory Shaft (ES) surface and subsurface facilities has continued. Construction of the site-access road and water line has been completed to the NTS boundary. All construction work has ceased. The Finding of No Significant Impact and the Land Use Agreement between DOE and the US Air Force have been signed. The ES site preparation construction is now scheduled to begin in January 1984.

B. Test Plan

The Exploratory Shaft Test Plan (ESTP) proposals for construction-phase Testing in the ES were completed. Most of the proposals were approved; some were tentatively approved pending modification. Approval was given to proceed on the data-acquisition portion of the integrated data system. Plans for tests that will be performed during shaft sinking are still being developed.

QUALITY ASSURANCE (WBS 1.6.4.3)

A. Los Alamos

An internal audit was performed of the Los Alamos Group INC-11 Count Room. A quality assurance (QA) training program was presented at Los Alamos.

The Exploratory Shaft Quality Assurance Program Plan draft was distributed for external review. Quality Assurance Manuals from Fenix and Scisson, Holmes and Narver, and REECo were reviewed; comments will be sent to the Waste Management Project Office.

B. USGS

A response was prepared for DOE audit 83-01. Two audits were performed of geophysics records at the Menlo Park, California, and Denver, Colorado, US Geological Survey (USGS) offices. A systems audit of the overall QA program was also performed in Denver.

I. INTRODUCTION

This report summarizes some of the technical contributions from the Los Alamos National Laboratory to the NNWSI project managed by the Nevada Operations Office of the US DOE during the period from April 1 through June 30, 1983. The report is not a detailed technical document but does indicate the status of the investigations being performed at Los Alamos.

II. GEOCHEMISTRY OF TUFF

A. Groundwater Chemistry of Yucca Mountain (A. E. Ogard, P. L. Wanek, R. D. Aguilar, A. J. Mitchell, S. Maestas, and M. R. Cisneros)

There have been additional tests of the groundwater chemistry for wells in the vicinity of Yucca Mountain. All results to date for the wells that have been pumped, sampled, and analyzed are included in Tables I and II. Water from these wells shows a range of alkali metal and alkaline earth contents (see Table I). The relative sodium, potassium, and calcium contents of these waters can be compared on a ternary diagram (see Fig. 1). The points plotted for the 10 well analyses show a comparatively constant relative potassium content, a relative calcium content in the range of 1 to 20%, and a relative sodium content in the range of 75 to 97%. The shaded area in Fig. 1 represents relative sodium, potassium, and calcium contents of interstitial waters from Rainier Mesa, which is located in the north-central part of the NTS.[1] These interstitial waters tend to grade from high calcium contents at shallow depths (100 to 250 m) to very low calcium contents below 450-m depth. The results from Yucca Mountain are lower in potassium than are the Rainier Mesa results.

Reaction-path calculations of groundwater chemistry and studies of mineral formation at Rainier Mesa have been done to model volcanic glass dissolution, water chemistry evolution, and secondary-mineral precipitation.[2] Figure 2 shows some results in which the relative sodium, potassium, and calcium content of the water is also plotted on a ternary diagram for calculations at four temperatures. The calculated compositions start at 40% sodium, 57% calcium, and 3% potassium at the beginning of glass dissolution and move toward the sodium apex as glass dissolution proceeds. Direction changes in the reaction-path lines are associated with secondary-mineral precipitation. The shaded area is the same as that shown on Fig. 1,

TABLE I

ELEMENTAL CONCENTRATIONS OF GROUNDWATERS FROM THE VICINITY OF YUCCA MOUNTAIN

Well No.	Field pH	Concentration[a] (mg/ℓ) Ca	Mg	Na	K	Li	Fe	Mn	Al	Si
USW H-1	—	7.2	0.40	75	5.1	0.07	0.03	0.06	0.03	—
USW H-5	7.1	1.6	0.05	93	3.2	0.13	0.05	0.02	0.05	26.4
USW H-6	7.4	3.6	0.05	88	1.7	0.11	0.08	0.03	0.07	21.1
UE-29a#2	7.0	11.1	0.34	51	1.2	0.10	0.05	0.03	0.04	25.8
UE-25b#1										
Unfiltered	7.7	17.3	0.62	54	3.2	0.26	0.34	0.004	0.02	28.1
Filtered[b]	7.7	19.7	0.68	56	3.3	0.28	0.04	0.004	0.03	31.5
USW G-4	7.1	9.2	0.15	56	2.5	0.08	0.04	0.02	0.02	19.6
USW H-4	7.4	10.8	0.19	84	2.6	0.16	0.03	0.005	0.04	25.9
J-13	6.9	11.5	1.76	45	5.3	0.06	0.01	0.01	0.02	31.8
UE-25b#1 Isolated Bullfrog Unit										
2nd day	7.4	18.6	0.74	43	2.8	0.31	0.93	0.43	0.06	28.9
28th day	7.3	17.9	0.01	37	3.0	0.17	0.08	0.07	0.06	28.8
USW H-1 Depth (ft)										
2000	7.2	3.5	0.20	106	6.4	0.07	0.02	0.11	0.02	3.6
3000	7.0	5.2	0.09	153	1.4	0.09	0.14	0.08	0.03	11.5
4000	8.0	1.7	0.07	166	1.4	0.11	0.03	0.04	0.02	12.9
5900	7.6	6.2	0.15	120	2.2	0.14	0.21	0.15	0.02	16.1

[a]Ionic or molecular species are not listed; concentration is based on the element.

[b]Filtered through a 0.05-μm Nuclepore membrane.

TABLE II
CONCENTRATIONS IN GROUNDWATERS FROM
THE VICINITY OF YUCCA MOUNTAIN

Well No.	Concentration (mg/ℓ)									
	F^-	Cl^-	SO_4^{2-}	HCO_3^-	NO_2^-	NO_3^-	O_2	Eh[a]	S^{2-}	Deter-gent
USW H-1				No Analysis						
USW H-5	1.27	5.7	14.6	122	N.D.[b]	8.6	6.3	353		<0.005
USW H-6	4.1	7.7	27.5	168	N.D.	5.3	5.6	395	N.D.	--
UE-29a#2	0.56	8.3	22.7	108	N.D.	18.7	5.7	305	N.D.	--
UE-25b#1	1.2	7.1	20.6	134	N.D.	0.6	1.8	220	N.D.	--
USW G-4	2.4	5.5	15.7	143	N.D.	5.5	6.4	402	N.D.	--
USW H-4	4.5	6.2	23.9	172	N.D.	4.7	5.8	215	N.D.	>2
J-13	2.1	6.4	18.1	143	N.D.	10.1	5.7	--	N.D.	N.D.
UE-25b#1	Isolated Bullfrog Unit									
2nd day	1.5	8.4	20.5	147	0.5	2.1	<0.1	-40	N.D.	>2
28th day	1.2	6.6	20.3	130	N.D.	4.5	1.8	156	N.D.	0.02
USW H-1 Depth (ft)										
2000	2.7	24.6	13.9	210	N.D.	N.D.	3.4	270	N.D.	--
3000	17.7	8.3	34.4	354	N.D.	N.D.	1.3	-40	6.4×10^{-2}	--
4000	13.1	8.4	60.9	354	N.D.	N.D.	1.2	-25	6.4×10^{-5}	--
5000	16.8	9.5	50.0	258	N.D.	N.D.	<1.2	-150	3.2×10^{-2}	--

[a]An MV vs hydrogen electrode.

[b]N.D. = not detected.

representing interstitial water compositions from Rainier Mesa; however, the scale of the plot is different. The reaction-path calculations and Fig. 2 indicate a correlation between increasing depth of interstitial water at Rainier Mesa and the greater extent of glass dissolution. This relation may mean that water at greater depth has been in contact with glass for a longer time.

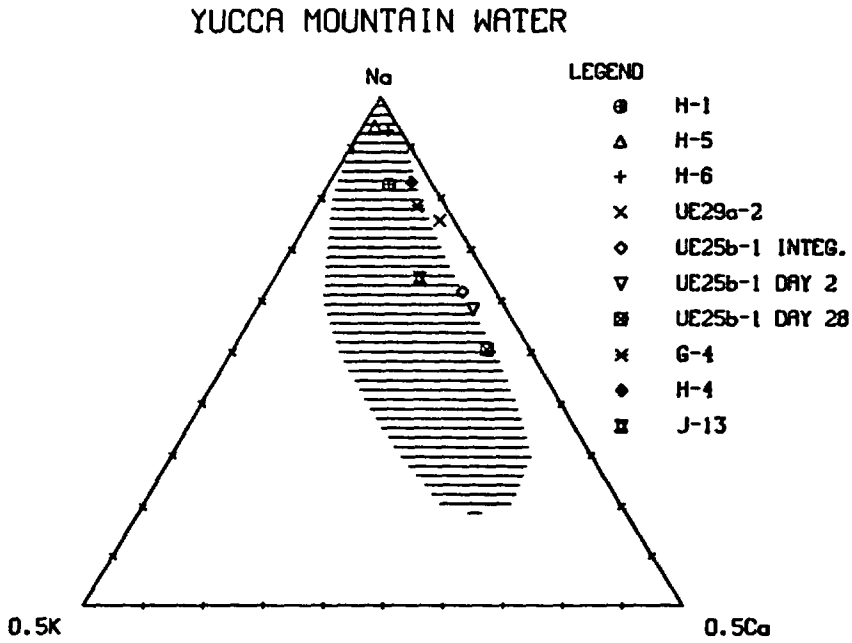

Fig. 1. Sodium, potassium, and calcium content of Yucca Mountain water.

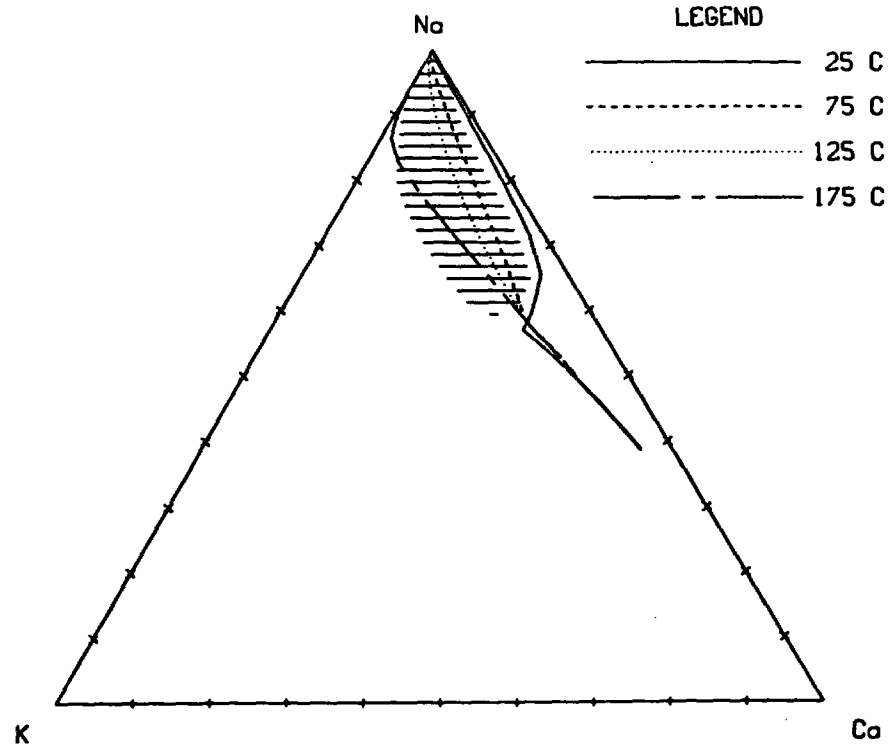

Fig. 2. Sodium, potassium, and calcium content of Yucca Mountain water calculated at four temperatures.

A connection between these concepts and the water analyses from the vicinity of Yucca Mountain is not as clear. The 10 relative sodium, potassium, and calcium contents plotted in Fig. 1 fall into 3 groups. (1) Analyses from Wells USW H-5 and H-6 are nearest the sodium apex; that is, they are highest in sodium and lowest in calcium content. They are also the two wells farthest to the west; they lie beyond a fault 1500 ft to the west of USW G-4 in Yucca Mountain. (2) The second group in Fig. 1 includes analyses from Wells USW H-1, H-4, G-4, and UE-29a#2. They show lower sodium content and higher calcium content. Except for UE-29a#2, which is ~10 km northeast of Yucca Mountain, these wells lie along a north-south line near the eastern edge of the exploration block. (3) The third group in Fig. 1 includes analyses for Wells UE-25b#1 and J-13; they show the lowest sodium content. Both wells are still farther east. It is not clear whether these trends have any physical significance for water flow paths or water travel times.

Additional preliminary conclusions have been drawn from the data to date.

(1) Integral water samples are oxidizing; this results in very low iron and manganese contents. Deep isolated zones, such as the Bullfrog zone sampled in UE-25b#1, can be reducing and exhibit high iron and manganese concentrations. (Details on this test are given in an earlier report.)[3] However, the reason that the reducing character changes with duration of pumping has not been determined. Over-pumping and flow through fractures or microorganism growth could be used to explain the results.

(2) The NO_3^- concentrations, which (to a first approximation) enter the water system from the air or surface, may be useful in pathway identification. Large differences in NO_3^- concentration occur from well to well; they may help to identify the mixing of different water pathways as more wells are drilled and sampled.

(3) Detergent concentration is a useful tracer of the original drilling fluids.

(4) Variations observed in Fl^-, Cl^-, and SO_4^{2-} are not consistent and may be caused by localized fracture-fill materials.

(5) The composition of at-depth samples taken from a stagnant well (USW H-1) can exhibit large changes from the norm. These changes may be caused by reactions of sulfides exposed to air-saturated water.

B. Variations of Groundwater Chemistry in Contact with Tuffs (P. L. Wanek, A. J. Mitchell, and A. E. Ogard)

Before each sorption experiment, groundwater from Well J-13 is equilibrated with crushed tuff from the core that is being examined for sorption properties. In this way, any changes in composition caused by water/tuff reactions will not be attributed to the sorption process. The change in groundwater composition during these equilibrations could also be used to model changes in composition that might be expected as water flows through the unsaturated zone, along the pathways in the saturated zone, and on to the accessible environment. Tables III and IV list the composition of the water after a 2-week equilibration (pretreatment) between Well J-13 water at ambient temperature and selected tuffs. Table V lists the tuff compositions used in these equilibrations.

A number of preliminary conclusions can be drawn from the results listed on these tables.

(1) Contact of groundwater with glassy tuff increases the magnesium and potassium content of the water as the glass dissolves.

(2) Calcite in contact with the groundwater increases the calcium content, as one would expect from the dissolution of the calcite.

(3) Contact with crushed vitrophyre from the lower Topopah Spring Member tuff increases the iron content of the groundwater. The vitrophyre contains unoxidized iron minerals that, after crushing, are exposed to the water and dissolve. In the natural state, groundwater would probably flow through fractures that were surrounded by oxidized iron minerals, and its iron concentration would not change as much as is shown here.

(4) Zeolites, such as clinoptilolite, decrease the magnesium content through ion exchange. In the process, sodium is released to the water but would not change the relatively large sodium concentration now in the water.

(5) Any changes in silicon and sulfate concentrations are masked by the concentrations in the groundwater.

(6) Fluoride, chloride, and manganese contents either are not changed by these equilibrations or are small compared to the concentrations now in the water.

(7) Changes in potassium do not appear to be related to the mineralogy.

TABLE III

COMPOSITION OF TUFF-PRETREATED GROUNDWATER[a]

Sample / Analysis	Composition (mg/ℓ)									
	YM-5	YM-22	YM-30	YM-38	YM-42	YM-45	YM-46	YM-48	YM-49	YM-54
Ca	15	13	14	14	15	14	15	18	20	14
Mg	4.1	2.4	1.5	0.1	0.5	1.2	1.1	1.2	1.2	1.4
Na	51	54	53	57	59	53	51	50	49	56
K	8.2	5.3	2.5	5.8	2.2	5.6	3.9	2.5	2.6	5.9
Fe	0.01	0.01	0.01	0.01	0.04	0.04	0.02	0.03	0.03	-
Mn	0.001	0.001	0.001	0.001	0.001	0.001	0.002	0.03	0.002	0.001
Si	35	34	30	32	28	34	34	37	36	37
F^-	2.5	2.6	2.5	2.5	2.4	2.5	2.5	2.5	2.5	2.6
Cl^-	7.9	7.3	7.0	7.5	6.9	6.8	7.5	6.7	6.9	6.8
SO_4^{2-}	23	24	23	26	27	24	24	24	25	24

[a]The pH of the final solution varied from 8.1 to 8.4. (Taken from Ref. 4.)

TABLE IV

COMPOSITION OF TUFF-PRETREATED GROUNDWATER[a]

Sample Analysis	Composition (mg/ℓ)							
	Fran Ridge Topopah	GU-3-433	GU-3-1301	GU-3-1203	G-2-547	G-2-723	G-2-1952	G-2-3933
Ca	9.7	9.3	11.1	11.9	8.7	13.2	12.8	10.2
Mg	1.3	2.1	1.0	1.8	2.5	3.0	1.4	0.9
Na	51.4	49.8	45.7	50.9	43.3	45.2	45.2	62.8
K	11.6	9.5	6.2	5.1	4.3	7.4	5.8	9.7
Fe	0.07	0.06	0.05	0.14	0.04	0.06	0.05	0.05
Mn	0.03	0.02	0.03	0.03	0.02	0.02	0.02	0.04
Si	21.2	22.4	25.7	25.5	30.0	25.8	26.7	18.3
F^-	2.6	2.8	2.7	2.8	2.7	2.4	2.4	2.7
Cl^-	10.1	9.2	8.8	8.7	8.1	7.5	7.7	7.3
SO_4^{2-}	19.0	19.3	19.0	19.3	17.3	16.6	16.1	21.7
NO_3^-	8.5	7.1	8.1	8.2	5.8	7.6	7.3	7.7

[a]The pH of the final solutions was at 8.5.

TABLE V

PETROLOGIC CHARACTERIZATION OF TUFF SAMPLES[a]

Sample	Depth (m)	Abundance (%) Smectite	Illite Mordenite	Clinoptilolite	Quartz	Cristobalite	Alkali Feldspar	Glass
YM-5	77				<5	<5	10-20	~70
YM-22	258	5-10			40-60		40-60	
YM-30	385	5-10	5	5-10	40-60	5-15	30-50	
YM-38	459	5-10	<2	30-50	15-30	10-20	5-15	
YM-42	556	Tr	<5	20	35-40		40	
YM-45	588	1-5			40-60	Tr	30-50	
YM-46	611	<5	<5		40-60		35-55	
YM-48	644	Tr		10-20			20-30	40-60
YM-49	678	Tr	Tr	10-20			20-30	40-60
YM-54	759	Tr	Tr		50-70		20-40	

Sample[b]	Depth (m)	Abundance (%) Smectite	Mordenite	Clinoptilolite	Quartz	Cristobalite	Alkali Feldspar	Glass	Calcite
GU-3-433	131					10-15	75-85		
GU-3-1301	397	1-3			2-6	10-15	35-45	30-60	
GU-3-1531	472	2-4		1-3	15-20	2-6	45-55	10-30	
GU-3-1203	115 ± 3	3-6			2-4	2-8	45-55	30-50	
G-2-547	167	5-15				5-15	10-20	40-60	
G-2-723	220	5-15				<5	5-10	15-30	30-50
G-2-1952	595		40-60	5-10	10-20	10-20	10-20		
G-2-3933	1199	10-20	Analcime 20-40		20-40		20-40		5-10

[a]Taken from Refs. 5-7. Tr = trace.

[b]Topopah Spring Member tuff from Fran Ridge has not been examined.

C. Variations with Temperature of Groundwater Composition in Contact with Tuff (C. J. Duffy)

Because of waste loading in the repository, the tuff of the Topopah Spring Member and possibly a portion of the tuff of the Calico Hills will be subjected to a temperature rise for a long period of time. Conceivably, this change will alter the composition of any water in contact with the tuff and affect the reactions between the water and the waste cannister.

The composition change of water in contact with the tuff of the Topopah Spring Member and of the Calico Hills at 152°C was reported earlier.[5] In the present study, the change of composition of water with the tuff of Calico Hills has been studied at two temperatures (150 and 325°C). Although the repository tuffs will not experience temperatures as high as 325°C, this temperature was chosen to accelerate the changes in mineralogy and serve as a limit on the changes expected. The sample of Calico Hills tuff was primarily clinoptilolite with minor amounts of alkali feldspar and even smaller amounts of cristobalite. Distilled water was used as the starting water (results are listed in Table VI) because water (condensed steam) from the loaded repository will be a lower bound for dissolved solids in the water composition for water/tuff interactions.

The experiments at 150°C did not show any observable change in mineralogy, whereas after 11 weeks at 325°C and 350 bars of fluid pressure, the clinoptilolite had been transformed completely to mordenite, small amounts of alkali feldspar, and smaller amounts of cristobalite. The major change in water composition shown by these experiments is the highly increased concentration of silicon. It is conceivable that these high silicon concentrations would cause precipitation of silica in the tuffs at a lower temperature, which would result in a less porous tuff.

The kinetics of reaction between flowing water and tuff is also being studied. The first experiments, at 80°C and pressures between 1 and 72 bars, used distilled water flowing through 1-in.-diam by 1-in.-long cylinders of Topopah Spring Member tuff from cores of Well USW GU-3. Results are shown in Table VII. The sample, from 770-ft depth, comprised largely cristobalite and alkali feldspars. There is insufficient data to draw firm conclusions; it appears that calcium, sodium, and silicon increase in concentration as the flow rate decreases, as one would expect. The flow rate at which the maximum dissolution occurs has not been reached.

TABLE VI

VARIATION WITH TEMPERATURE IN COMPOSITION OF WATER IN CONTACT WITH THE TUFF OF CALICO HILLS

Contact Time (weeks)	Concentration[a] (mg/ℓ)									
	Ca	Mg	Na	K	Li	Fe	Al	Si	F^-	Cl^-
150°C										
1	0.05	0.03	8.8	2.2	0.02	0.45	0.36	236	2.7	1.3
6	0.04	0.05	11.5	4.1	—	0.45	1.22	234	1.5	1.0
13	0.07	0.02	11.8	4.3	—	0.24	—	217	0.9	0.4
21	0.06	0.03	13.1	5.1	—	0.38	1.29	199	1.9	0.5
325°C										
6	0.03	0.05	24.5	6.4	0.04	0.67	3.98	541	11.6	1.3
8	0.04	—	23.1	5.8	—	0.66	3.81	526	11.5	0.9
11	0.13	—	20.1	5.0	—	0.65	3.31	504	12.0	1.3
After cooling to room temperature										
5 days	5.75	0.04	11.3	2.1	0.16	0.52	1.33	358	7.4	1.0
17 days	6.59	0.05	10.1	1.8	0.14	0.44	1.01	372	3.8	0.5

[a]Unfiltered samples.

TABLE VII

COMPOSITION OF WATER FLOWING THROUGH TOPOPAH SPRING MEMBER TUFF

Flow Rate (cm^3/second)	Concentration (mg/ℓ)				
	Ca	Na	K	Si	F^-
5.78×10^{-4}	0.66	1.73	2.10	22.6	2.6
5.66×10^{-4}	0.87	2.04	1.70	22.4	2.1
2.67×10^{-4}	1.03	1.64	1.98	22.1	2.6
1.89×10^{-4}	0.74	1.24	2.76	42.0	3.9
1.42×10^{-4}	1.33	2.17	1.79	28.7	2.6
5.29×10^{-5}	1.86	3.16	1.36	35.3	1.7

D. Groundwater Analysis (P. L. Wanek)

Minor improvements have been made for water analysis. The autotitrator was reprogrammed to use a drift kinetic method that allows for longer solution stabilization between acid additions and also more closely resembles the standard field hand-titration method. A minimum sample volume of 10 m ℓ was established using the 0.04 normal HCl titrant. (Results on smaller volumes are not reproducible.) A data base of analytical data has been established on the central computer; some modifications still must be made to ensure standardization.

Further experimentation on various types of potential groundwater tracers was performed to provide a choice of types and corresponding analytical data for each. Iodine-131 has been used fairly successfully in relatively short-term, short-flow-path studies of groundwater movement in the field. The analysis is performed by using high-performance liquid chromatography to separate nonradioactive iodide from other anionic water components, and UV or electrochemical detection. The chromatographic character of the large iodide anion precludes its coincidental use with the potential fluorobenzoate salt tracers. Under conditions favorable to iodide analysis, the fluorobenzoates elute essentially at the same time as nitrate (a natural groundwater component). There was some variation with iodide response relative to the presence of sodium hydroxide in the solution, which indicates a possible pH dependence on the state and/or behavior of iodide in a chromatographic detection scheme. The detection limit is approximately 50 ppb when this method is used.

Analysis of the thiocyanate ion was also investigated. A detection limit of approximately 50 ppb was attained by using chromotographic separation and electrochemical detection. No interference with normal groundwater components was observed. However, the thiocyanate ion, like iodide, cannot be used under these analysis conditions with the fluorobenzoate salts, although it could be used simultaneously with iodide. The possible complexation of thiocyanate with components of the experimental system, such as plastic or rubber, must be considered further.

A literature search was undertaken to gather recent data on nonradioactive tracers. Large, areal groundwater studies have been done by measuring ratios of stable isotopes, such as $^{18}O/^{16}O$ and $^{13}C/^{12}C$, to study flow paths. Short-term tests using radioactive tracers such as ^{198}Au, ^{51}Cr-EDTA, and ^{131}I

as well as tritium have been conducted on small areas, both down hole and on the surface. However, there seems to be a paucity of written material on nonradioactive tracers. Much of the work on underground fluid tracers has apparently been done in the field of oil and gas exploration, and the data is not readily accessible to the public. Often experimentors were interested in tracing flow paths on a gross scale and were not concerned by small-to-moderate amounts of tracer adsorped onto minerals along the way.

Disadvantages of certain tracers now under consideration have been suggested:* expense, unavailability for large-scale tests (fluorobenzoates), volatility in unsaturated media (fluorocarbons), and metal complexation (SCN^-, CN^-). According to the literature,[9] thiocyanate appears to complex less tightly to metals than does the cyanide ion and, therefore, should be advantageous. Thiocyanate also appears to be less toxic than cyanide.

A very stable, anionic cobalt-cyanide complex ($Co(CN)_6^{3-}$) was suggested as a groundwater tracer if a method could be devised to detect it in a nonradioactive form.** It has been used in the field in the ^{60}Co form, and it apparently behaves much as tritium does. This compound may be investigated further if an additional tracer type is needed.

E. Microbiological Activity in the Yucca Mountain Environment (L. E. Hersman)

Several oxygen-uptake (respiration) experiments were performed on the drilling polymer and detergent currently in use at Yucca Mountain. A 2-mℓ amount of sterile drilling fluid was added to Warburg reaction flasks, innoculated with bacteria, and incubated at 30°C until oxygen consumption could no longer be detected. Measurements were made every 3 hours for the first 24 hours and then once a day for the duration of the experiment. Generally, for the polymer samples, maximum oxygen consumption occurred during the first 24 hours; 863 μmole O_2 were consumed per hour per gram of polymer concentrate. Over the duration of the experiments (8 days), a total of 8.12×10^4 μmole O_2 was consumed per gram of polymer. When this rate is converted to gallons of diluted polymer (1 to 42, polymer to water), it is conceivable that under ideal conditions and for this particular bacterium, 7.31 moles of oxygen could be consumed during the biodegradation of 1 gal. of drilling polymer.

---

* From information provided by S. Jensen, Department of Hydrology and Water Resources, University of Arizona, Tucson, AZ 85721.

** Information given by P. Grant, Lawrence Livermore National Laboratory, P. O. Box 808, Livermore, CA 94550.

Thus, there is a very strong potential for significant reduction in Eh after drilling fluid is introduced into a rock stratum. Similar results were obtained with the drilling detergent.

Nalco Chemical Company,* reports that the composition of the polymer being used is 29% acrylimide copolymer, which is 65% acrylimide and 35% sodium acrylimide (WT/WT); 27.8% light hydrocarbons, which are 91% paraffinic solvents, 3.42% emulsifying agents, and a small amount of EDTA (0.0135%); and 43.2% water.

The chemical composition of the detergent (Turco** 5622) is 10 to 20% isopropyl alcohol, <0.5% gelatin, <0.5% ammonia (28% concentrated NH^+), <0.5% sodium nitrite, 2% surfactant (sodium salt of linear dodecyl benzene sulfonic acid), and water.

For both the polymer and the detergent, the most likely biodegradable constituent is the emulsifying agent (surfactant). This observation is supported by other investigators,† who concur that the polymeric acrylimide, light hydrocarbons, paraffinic solvents, and isopropyl alcohol are, for the most part, too refractory to support the rate of oxygen uptake reported here. However, the long-term biodegradability of these compounds has yet to be determined. The presence of small amounts of EDTA is interesting because of the effects that this strong chelating agent may have on actinide mobility.

Two new experiments have been initiated. The first will determine the availability of the drilling fluids to anaerobic microbial biodegradation. Because it is uncertain that aerobic conditions could persist after the introduction of the fluids, it is necessary to determine the susceptibility of these materials to anaerobic decay. The second set of experiments will determine the relative influence of microorganisms on plutonium sorption onto finely ground tuff particles.

F. Plutonium Chemistry in Near-Neutral Solutions (T. W. Newton and V. L. Rundberg)

These studies are being continued because not enough is known about possible species and equilibria to make convincing predictions about the

---

*Nalco Chemical Company, P. O. Box 89, Sugar Land, TX 77478.

**Turco, 24600 South Main St., Carson, CA 90749.

†F. Hagy, Turco; M. Grula, Oklahoma State University; and R. Gabel and M. Litmann, Nalco.

behavior of plutonium in the Yucca Mountain environment. In particular, the reactions that occur when Pu(IV) is brought into near-neutral solutions are important because Pu(IV) species are probably more readily adsorbed than are species of the other oxidation states. Thermodynamic data[10] indicate that disproportionation of Pu(IV) to give Pu(III) and Pu(V) will be important in the pH range of about 2 to 6.5. However, the reaction rates in this pH range have not been measured before, and extrapolation of previous data for much lower pH values is very uncertain. Another important reaction is polymerization of Pu(IV). Although rates of polymerization have been determined in more concentrated solutions,[11,12] the rate of polymer formation in very dilute solutions and the nature of the product formed are unknown. Therefore, studies have continued of the reactions that occur when Pu(IV) in acid solution is diluted to less than 4×10^{-6} M in the pH range from about 3 to 4.5. In the future, the experiments will be extended to the pH 7 to 8 range.

Current experiments, in agreement with earlier ones, indicate that Pu(IV) disappears by both disproportionation and polymerization. Unreacted Pu(IV) is determined spectrophotometrically, as before, with an Os(II) complex such as $Os(dimethylbipyridine)_3^{2+}$, but the method has been improved by using hydroquinone to reduce the Os(III) back to Os(II), which provides an internal absorbance blank. The Pu(III) and Pu(V), formed by disproportionation, are reducing agents; the sum of these was determined by using Ce(IV). After adding a known excess of Ce(IV) in H_2SO_4, that part remaining was determined by a spectrophotometric titration at 320 nm with standard Pu(III). The results are summarized in Table VIII. The values for the logarithm of the apparent second-order rate constant are consistent with those in Ref. 1, but the current disproportionation fractions are considerably larger than those reported earlier. This fact may be the result of higher plutonium concentrations used in the earlier experiments; that possibility will be explored soon.

Samples from six of the solutions described in Table VIII were studied using zirconium phosphate (ZP-1) columns. The elution patterns clearly show the presence of both Pu(III) and Pu(V), but quantitative conclusions can not be reached because both these oxidation states appear to be oxidized and they reproportionate on the columns.

The behavior of plutonium oxidation states on zirconium phosphate columns (Bio-Rad, ZP-1) are still being studied; these experiments will improve the

TABLE VIII

DISPROPORATIONATION AND POLYMERIZATION OF

Pu(IV) AT ROOM TEMPERATURE

pH	Pu Concentration ($M \times 10^6$)	Log k[a]	Fractionation Disproportionated[b]
2.92	3.3	4.14	0.8
2.97	3.3	--	0.84 ± 0.04
3.00	3.0	4.25	0.87
3.29	3.3	--	0.35
3.56	3.0	5.46	0.33
3.56	1.7	5.51	0.56
3.66	3.3	--	0.32
3.96	3.3	--	0.20
4.09	3.3	--	0.14

[a]Logarithm of observed second-order rate constant; units are M^{-1}/minute.
[b]Fraction of the initial Pu(IV) that formed reducing agent.

conclusions to be drawn from the elution patterns. The general procedure is unchanged: a sample is placed on top of the column and eluted with successive 2-mℓ portions of HCl of increasing concentration. Typically, three portions each of 0.05, 0.10, 0.2, and 0.3 M; two portions each of 0.5, 1.0, and 2.0 M, four portions of 2 M HCl containing hydroquinone; two portions of 3 M; and three portions each of 6 M and 9 M HCl are used. Each portion is collected separately, taken to dryness, heated to about 300°C, and alpha-counted. Elution occurs in several distinct bands; the results are reported in terms of the fraction of the total in each band. The results of these current experiments are summarized as follows:

(1) About half of a sample of Pu(VI), 3×10^{-7} M in 0.05 M HCl, in the first band is eluted by using 0.05 and 0.1 M HCl. The remainder tails out in the other bands.

(2) Pu(V) undergoes reaction on the column. When a sample is placed on the column and allowed to stand for 4 hours before elution is begun,

only 44% is eluted in the 0.05 and 0.1 M band, compared with 85% when elution is started immediately.

(3) Previous work showed that a significant fraction of Pu(IV) is eluted in the second band, using 0.2 to 1.0 M HCl, which suggests a Pu(III) impurity. This band has been confirmed by using a sample of Pu(IV) that contained no reducing agent.

(4) In earlier work,[7] it was noted that Pu(III) appears to be oxidized when left on a column of ZP-1. Current experiments show that this oxidation is not caused by oxygen from the air; all solutions were flushed with argon before use without affecting the results.

(5) Hydroquinone in 2 M HCl is used for eluting Pu(IV) by reducing it to Pu(III). Hydroquinone concentrations as low as 10^{-6}M will elute most of the Pu(IV), but 10^{-4} M is more effective. Using a minimum concentration of hydroquinone will probably help distinguish between Pu(IV) and fresh polymer that is formed in very dilute solutions.

The ZP-1 procedure has been tried on four samples that were used to help develop methods for preparing well-characterized groundwater actinide solutions. The solutions are used in the distribution experiments that are discussed in the next section. The results are summarized in Table IX with those for definite oxidation states.

The elution patterns indicate that no sample contains a single oxidation state, although sample 4 might be predominantly Pu(III). Samples 1, 2, and 3 contain significant fractions of Pu(V) or possibly Pu(VI). Samples 3 and 4 show relatively large amounts of Band 4 material. This is probably similar to the material formed in the mixtures: probably fresh polymer.

A preliminary investigation has been made of BioRex-9, an anion exchange resin designed to be resistant to strong oxidizing agents. It was selected because ordinary AG-1 resins can be oxidized by Pu(VI). Either Pu(IV) or Pu(VI) can be adsorbed from 0.1 M NH_4HCO_3 solutions and eluted with more concentrated solutions of the same salt or of $(NH_4)_2CO_3$. A 20-cm by 4-mm-diam ion exchange column was used. The elution patterns were determined using increasing concentrations of NH_4HCO_3. Most of a sample of Pu(IV) made up in 0.1 M NH_4HCO_3 was eluted in a sharp peak by using 0.75 M. About 90% of a sample of aged Pu(IV) polymer was retained on the column even when 2 M NH_4HCO_3 was used for elution. Plutonium(V) and fresh polymer were eluted as broad

TABLE IX

ELUTION PATTERNS OBTAINED FROM VARIOUS SAMPLES

	Plutonium Concentration (M)	Sample pH	Elution (%) Band Number[a] 1	2	3	4	Remainder (Not eluted) (%)
Samples							
(1) Air-dried stock dissolved in de-ionized water	7×10^{-6}	4.3	35	36	20	4	5
(2) $NaNO_2$ used	3×10^{-8}	5.9	32	14	48	6	--
(3) Air-dried stock treated with $NaNO_2$, dried and in groundwater	8×10^{-9}	8.35	30	16	30	24	--
(4) HNO_3-treated stock air-dried, dissolved in de-ionized water	3×10^{-8}	4.04	3	52	19	26	--
Standards							
Pu(V), by hydroquinone-reduction of Pu(VI)	3×10^{-7}	1.3	85	6	6	3	--
Pu(VI), by $HClO_4$-oxidation	3×10^{-7}	1.3	51	28	15	6	--
Pu(III), by Zn-Hg reduction	2.5×10^{-7}	1.3	0	63	24	13	--
Pu(IV), by reproportionation in 3 M HCl	3.4×10^{-7}	1.0	0	13	69	16	2
Polymer, aged	2.8×10^{-7}	1.3	2	3	4	6	85
Mixtures							
Pu(III) + Pu(V)	3×10^{-7}	4	30	23	25	22	--
Pu(IV) diluted to 1.7×10^{-6}M, pH 3.56; stood 24 hours; 56% reducing agent found	3.4×10^{-7}	3.56	16	26	34	25	--

[a]Band 1 eluted with 0.05 and 0.1 M HCl; Band 2 eluted with 0.2, 0.3, 0.5, and 1.0 M HCl; Band 3 eluted with 2 M HCl, 2 M HCl with hydroquinone, and 3 M HCl; and Band 4 eluted with 6 and 9 M HCl.

peaks with 0.4 and 0.5 M NH_4HCO_3. The patterns were very similar, so distinction between these species would be essentially impossible. In future experiments, the use of $(NH_4)_2CO_3$ will be investigated.

G. Solubility of Actinide Solids in the pH range of 5 to 10 (T. W. Newton, V. L. Rundberg, F. O. Lawrence, and A. E. Ogard)

A number of precipitates of hydrous plutonium dioxide have been prepared for x-ray powder diffraction studies. The data obtained from the precipitations is useful itself because it provides upper limits for the solubility under the conditions employed. The observed plutonium concentrations in precipitation experiments may be greater than equilibrium values because the initial precipitate may be metastable with respect to the final solid formed and because very small solid particles may be included with the solution.

The experiments were done by adding Pu(IV) in acid solution, Pu(IV) polymer sols, or Pu(III) (in one case) to an excess of a well-stirred solution of a base. The phases were separated by centrifugation, and the plutonium concentration in the supernatent was determined by alpha counting. The pH of the supernatent was determined using a Beckman Model 4500 pH meter, which was calibrated with standard buffers. The results of many such experiments are collected in Table X.

Rai and Swanson[13] have reported the solubilities of Pu(IV) polymer in chloride solutions with pH values between 3 and 7. They find their data is approximated by $\log C = -2.55 - 0.75$ pH, where C is the measured concentration of plutonium [primarily Pu(V)]. Values for $-\log C$ that were calculated using this function are given in the last column in Table X. The experimental log C values for runs 1, 3, and 4 fall very close to the calculated values, whereas all the others show higher concentrations. Most higher values are associated with lower centrifugation speeds or with carbonate solutions. The supernatent in run 3 was predominantly Pu(V), in agreement with the published observations. The oxidation state analysis was done by zirconium phosphate ion exchange.

The data obtained so far are preliminary, but they do indicate that a systematic study of plutonium precipitation should be carried out using all four plutonium oxidation states and the polymer as starting material. These experiments should involve a wide range of pH values, high-speed centrifugation, and ion exchange characterization of the plutonium in the supernatents.

TABLE X

$PuO_2 \cdot nH_2O$ PRECIPITATION EXPERIMENTS

Starting Material	Base	Heating Temp. (°C)	Heating Time (minutes)	pH	Centrifugation Time (hours)	Centrifugation rpm x 10^{-3}	-Log C[a]	Calculated[b]
Polymer[c]	$NaHCO_3$	23 ± 2	—	5.1	2	12	6.4	6.4
Pu(IV)	C_5H_5N	"	—	5.5	0.3	6	4.9	6.8
"	NH_4OH	"	—	6.7	2	12	7.6[g]	7.6
"	$(C_2H_4OH)_2NH$	"	—	6.9	1.2	12	8.0	7.7
"	NH_4OH	"	—	8.7	2	12	8.5	9.1
Pu(III)	NH_4OH	"	—	9.5	0.5	6	7.5	9.7
Pu(IV)	"	"	—	9.8	0.3	6	7.5	9.9
"	"	"	—	10.2	0.3	6	6.6	10.2
Polymer[d]	$NH_4(HCO_3)$	"	—	(8.5)	3	12	6.9	8.5
Pu(IV)	"	"	—	(8.5)	1	12	5.1	8.5
Pu(IV) CO_3[e]	diluted	"	—	(8.5)	1	12	5.5	8.5
Pu(IV)	C_5H_5N	85	20	5.2	0.5	7	5.8	6.5
Pu(IV) CO_3	$NH_4(HCO_3)$[f]	92	15	8.8	0.3	12	5.3	9.2
"	"	92	28	9.0	0.5	6	5.9	9.3
Pu(IV)	NH_4OH	85	30	9.7	0.3	6	7.5	9.8

[a] C was the concentration of Pu in the supernatent.

[b] Calculated using $-\log C = 2.55 + 0.75\ pH$ (Ref. 13).

[c] Fresh polymer prepared at pH 3 and 6×10^{-5} M Pu.

[d] Polymer prepared in 0.04 M HCl and 0.02 M Pu, purified by ion exchange, and aged 6 months at room temperature.

[e] Pu(IV)-carbonate complex, 8×10^{-4} M Pu in 0.5 M $NH_4(HCO_3)$, diluted by a factor of 20 with water to give the ppt.

[f] Pu(IV)-carbonate complex prepared as above and boiled to give the precipitate.

[g] Supernatent was principally Pu(V).

The results of such experiments would provide only upper limits for the true solubility but would avoid the alpha irradiation problems associated with long-term experiments.

Reference 5 describes a procedure that was adopted for preparing plutonium tracers used in sorption experiments. In this procedure, not all the dried plutonium compound dissolved in the groundwater. Table XI lists all the plutonium solutions prepared for sorption experiments by this method, the intended concentration (if all the solids went into solution), the resulting final concentration, the final pH of the solution, and the ratio of the intended concentration to the final concentration. The final concentration is always lower than the intended concentration; in addition to not dissolving totally, plutonium always sorbs to some extent on the walls of the container and especially in the filter. By comparing the solutions in Table XI that were intended to be of equal composition, the reproducibility within a factor of 2 to 3 is determined. Further examination of the final concentrations shows that for all intended concentrations greater than 5×10^{-8} M, the quantity of air-dried material that dissolved does not increase to any great extent. The conclusion can be drawn that at pH ~8.3 the maximum solubility of a plutonium solid (unknown composition) in Yucca Mountain groundwater has been reached: 10^{-6} to 10^{-8} M. This value should be compared to the estimated solubility of $Pu(OH)_4$ at pH 8.2 from the Rai and Swanson results of 10^{-8} M (Ref. 13). Compare this value also with the plutonium solubility of a spent fuel element in contact with water at pH 4 of 3×10^{-7} M, postulated by Ogard et al.[14]

The above results suggest that an upper limit for the solubility of plutonium solids in Yucca Mountain groundwater at pH ~8 is 10^{-6} M in the presence of air. Unfortunately, nothing can be said with certainty at this time about the species in solution or the composition of the solid.

A similar series of measurements, but less extensive, has been performed for preparation of americium tracers in groundwater. Initial quantities of americium solids from solutions 1.6×10^{-7} to 3.9×10^{-7} M yielded final solutions less than 2.4×10^{-7} M. Approximately 50 to 70% of the americium sorbed on the container walls or on the filter membrane, but in no case did it appear that a solubility limit was reached as it was in the previously described plutonium experiments. The solubility of the most soluble americium solid at ~pH 8 in air is certainly greater than 2.4×10^{-7} M.

TABLE XI

PLUTONIUM TRACER SOLUTIONS

Concentration (mg/ℓ)			
Intended	Actual	pH	Ratio Intended/Actual
6.9×10^{-5}	1.3×10^{-9}	8.3	5.3×10^{4}
6.2×10^{-6}	9.9×10^{-7}	-	6.3
4.8×10^{-6}	7.8×10^{-7}	8.5	8.2
	3.6×10^{-8}	8.7	133
	6.1×10^{-7}	8.8	7.9
	8.3×10^{-7}	8.5	5.8
	6.2×10^{-7}	4.8	7.7
	6.5×10^{-7}	4.8	7.4
	7.8×10^{-7}	5.4	6.2
	5.7×10^{-7}	8.6	8.1
	5.3×10^{-7}	8.6	8.4
1.2×10^{-6}	2.4×10^{-8}	7.7	50
	2.6×10^{-8}	8.4	46
	4.6×10^{-8}	8.2	26
9.3×10^{-7}	4.8×10^{-8}	8.5	19
	7.1×10^{-9}	8.3	131
	2.6×10^{-8}	8.2	36
	4.1×10^{-8}	8.5	23
5.4×10^{-8}	2.9×10^{-8}	8.4	1.9
3.9×10^{-8}	2.6×10^{-8}	8.1	15
	1.1×10^{-8}	8.4	3.5
3.0×10^{-8}	1.3×10^{-8}	-	2.3
2.7×10^{-8}	9.7×10^{-9}	8.1	2.8
3.9×10^{-9}	1.3×10^{-8}	8.1	3
	1.8×10^{-9}	8.4	2.2
2.5×10^{-9}	5.7×10^{-10}	8.5	4.4
4.5×10^{-10}	1.3×10^{-10}	8.3	3.5
4.4×10^{-10}	1.9×10^{-10}	8.1	2.3
3.7×10^{-10}	1.5×10^{-10}	8.7	2.5
	1.4×10^{-10}	8.4	2.2

TABLE XI (cont)

Concentration (mg/ℓ)			
Intended	Actual	pH	Ratio Intended/Actual
5.6×10^{-11}	7.5×10^{-12}	8.3	7.5
	2.9×10^{-11}	8.4	1.9
4.7×10^{-11}	2.9×10^{-11}	8.0	1.6
4.4×10^{-11}	2.0×10^{-11}	7.8	2.2
1.2×10^{-11}	8.0×10^{-12}	8.4	1.5
	1.4×10^{-12}	8.7	3.6
7.3×10^{-12}	5.9×10^{-13}	8.2	12
7.2×10^{-12}	3.1×10^{-12}	8.8	2.3
	4.1×10^{-12}	8.7	1.8
	4.8×10^{-12}	8.8	1.5
	4.1×10^{-12}	8.7	1.8
3.5×10^{-12}	1.5×10^{-12}	8.1	2.3

H. Batch Sorption Experiments (F. O. Lawrence, S. D. Knight, B. P. Bayhurst, M. R. Cisneros, K. W. Thomas, and K. Wolfsberg)

The last progress report described new experiments to investigate the sorptive behavior of tuffs composed largely of mordenite, glass, calcite, and analcime.[7] Tests were begun on a series of samples of the Topopah Spring Member tuff from Drill Hole USW GU-3 in the unsaturated zone. A series of experiments to round out the study of sorption of uranium under aerobic conditions also included a study of the sorption of selenium. Selenium is one of the waste elements whose total quantity is near but slightly below the limits given in the EPA listing 40 CFR 191. A few selenium sorption experiments were performed; information will be available if it is needed. Radium sorption is also being studied for comparison with barium sorption on tuff. Results of all these studies to date are presented in this section, and preliminary x-ray diffraction analyses for samples are given in Table XII.

The migration of radium must be considered when storing certain types of nuclear wastes.[7] The interactions of tuff and radium have not yet been studied in the laboratory; because of the volatility of the radon daughter,

TABLE XII

X-RAY DIFFRACTION ANALYSES OF TUFF SAMPLES

Sample	Smectite	Mica	Clino-ptilolite	Mordenite	Analcime	Quartz	Cristo-balite	Alkali Feldspar	Calcite	Glass
G-1-1292[a,b]							22 ± 8	15 ± 5		50 ± 10
G-1-1436[a,b]	<5	<5	82 ± 8			8 ± 3		~5		
G-1-2289[a,b]		8 ± 3	40 ± 10			<5		40 ± 10		
G-1-2363[b,c]	5	<2				40 ± 10	5 ± 5	40 ± 10		
G-2-547[a,d]	24 ± 10					5 ± 2	5 ± 3	53 ± 10		
G-2-723[a]	5 ± 3	3 ± 2					3 ± 2	25 ± 10	50 ± 10	15 ± 6
G-2-1952[a]		1	20 ± 10	30 ± 10		7 ± 2	8 ± 3	36 ± 10		
G-2-3933[a]	7 ± 3				15 ± 5	34 ± 5		44 ± 10		
GU-3-433[a]		4 ± 2				4 ± 2	12 ± 4	80 ± 20		
GU-3-855[e]	2 ± 1					20 ± 4	7 ± 3	70 ± 20		
GU-3-1203[a,f]	1	1				5 ± 2	12 ± 4	45 ± 10		40 ± 20
GU-3-1301[a]	2 ± 1	4 ± 2				6 ± 2	15 ± 6	35 ± 20		40 ± 20
GU-3-1436[e]		1				4 ± 2	6 ± 3	50 ± 20		40 ± 20
GU-3-1531[e]		5 ± 2				20 ± 5	6 ± 3	40 ± 20		30 ± 20

[a]Size range 75 to 500 μm.

[b]From LA-9238-MS.

[c]Size range 106 to 500 μm.

[d]Plus 11 ± 5% tridymite.

[e]Size <500 μm. Sorption work was done with 75 to 500 μm. Those samples will be analyzed.

[f]Topopah Spring vitrophyre.

special care must be taken to avoid contamination of the laboratory and counting equipment. It has been suggested that barium is a good analogue for radium in sorption studies because of the similarity of their chemical properties; therefore, a series of experiments was performed to validate that behavior. The experiments with radium were conducted in a glove box, and counting was performed in specially constructed gastight containers.

Preliminary results, given in Table XIII, indicate that the sorptive behavior of radium is indeed very similar to that of barium; sorption data for the two elements are comparable for glassy, devitrified, and zeolitized tuffs, with variations in sorption ratios of more than 2 orders of magnitude for the different types of tuff. It is anticipated that the final results for both sorption and desorption will confirm this behavior, and no more experiments with radium will be required. Of the radium precursors, only the thorium parent has yet to be tested.

Studies of selenium migration, although of some interest for high-level repositories, are not as high a priority as migration studies of other hazardous waste elements.[7] (The experiments reported here were begun before publication of the recent draft of environmental standards[15] and the Los Alamos evaluation of hazard ranking.[7]) Selenium normally exists in the (IV)

TABLE XIII

COMPARISON OF SORPTION RATIOS FOR RADIUM AND BARIUM

	Sorption Ratio (mℓ/g)				
	Ra[a]				
Sample	Experimental		Average[b]	Ba[b]	Ratio (Ra/Ba)
G-1-1292	1500	1400	1500(100)	2100(300)	0.7 ± 0.1
G-1-1436	79 000	130 000	100 000(30 000)	150 000(24 000)	0.7 ± 0.2
G-1-2289	70 000	22 000	50 000(20 000)	66 000(9000)	0.8 ± 0.3
G-1-2363	480	590	540(60)	235(9)	2.3 ± 0.3

[a]Particle-size distribution 75 to 500 μm. Solutions were 3.6×10^{-7} M in radium. Contact time 6 weeks.

[b]Numbers in parentheses are standard deviations of the means.

[c]Reference 5.

oxidation state in nature but may also exist in the (VI) state, particularly in basic conditions. It is easily reduced to the metal. The selenite and selenate anions are not expected to sorb on tuffs, but mild reducing conditions would enhance sorption by reduction of the (IV) or the (VI) oxidation state.[16] A series of sorption experiments was conducted with ^{75}Se (10^{-10} M) and normal uranium (10^{-6} M); the ^{75}Se was counted on a Ge(Li) detector and uranium was determined by neutron activation analysis. Results for selenium are given in Table XIV. The samples cover the representative range of tuff types and mineralogies. There are no clear correlations of sorption with abundances of zeolites, clays, glass, or devitrification minerals, nor is there any correlation with the oxidation state of phenocrysts in the sample. The average value of sorption ratios, 9 ± 8 mℓ/g, is low but is higher than values for iodine and technetium.

Uranium results for these samples are presented in Table XV. The sorption ratios for these samples are generally low, as was stated in an earlier report.[5]

Sorption ratios for strontium, technetium, cesium, barium, and europium for samples GU-3-433 and GU-3-1301 were reported last quarter;[7] desorption experiments have been completed and are reported in Table XVI. The sorption ratios for americium and plutonium on crushed-rock samples from USW G-2 and GU-3 are given in Table XVII. For strontium, cesium, and barium, the values obtained from the sorption experiments[7] are quite similar to those from the desorption experiments. Those for europium, americium, and plutonium agree within a factor of 3, and the values from desorption experiments are higher.

The results for vertically and horizontally shaken samples are similar (Tables XVI and XVII here and Table V of Ref. 7). The horizontal position will be used in ambient-temperature experiments in the future because mixing appears to be better and equilibrium may be attained more rapidly.

Sorption ratios for americium and plutonium at 85°C compare to those at room temperature. At elevated temperatures, several values are significantly greater and a few are as much as a factor of 2 lower. Similar observations were made for sorption of several other elements at 70°C (Ref. 5).

Average sorption ratios obtained recently (this quarter and last quarter)[7] are consolidated in Table XVIII. In addition to the above comments concerning radium, selenium, and uranium, the following points can be made.

TABLE XIV

SORPTION RATIOS FOR SELENIUM

Sample	Sorption Ratio[a] (mℓ/g) Experimental		Average[b]
G-1-1436	11	14	13 (2)
G-1-2289	9	8	9 (1)
G-1-2363	30	19	25 (5)
G-2-547	3	1	2 (2)
G-2-723	20	17	19 (2)
G-2-1952	2	1	2 (1)
G-2-3933	1	0	0 (1)
GU-3-433	18	12	15 (3)
GU-3-1203	0	2	1 (1)
GU-3-1301	5	8	7 (2)

[a]Contact time was 6 weeks under ambient conditions. Solutions were 10^{-10} M in selenium. Particle size of the tuff was 75 to 500 μm.

[b]Values in parentheses are standard deviations of the means.

(1) The zeolites mordenite and clinoptilolite appear to be equal in their ability to sorb cesium and barium. Strontium, plutonium, and americium sorption rates do not appear to be greater for mordenite than for devitrification minerals. These conclusions are based on experiments with sample G-2-1952, which contains ~30% mordenite and ~20% clinoptilolite. The effect of mordenite on samples G-1-2233 and G-1-2289, studied previously,[5] was masked by higher relative abundances of clinoptilolite.

(2) Calcite in sample G-2-723 appears to be responsible for very high sorption ratios of europium, plutonium, and americium. The mechanism for this very high sorption will be investigated.

(3) Analcime in sample G-2-393 does not appear to enhance sorption of strontium, cesium, or barium. Similar observations were made earlier for samples JA-26 and JA-28.

(4) Sorption on glassy tuffs does not correlate with glass content and, instead, may be related to texture. Further examination and description of glassy samples is required.

TABLE XV

SORPTION RATIOS FOR URANIUM UNDER AMBIENT CONDITIONS

Sample	Sorption Ratio[a] (mℓ/g) Experimental		Average[b]
G-1-1292	0.2	-1.6	0[c]
G-1-1436	12	10	11 (1)[b]
G-1-2289	2.5	2.6	2.5 (0.1)
G-1-2363	-0.7	0.5	0
G-2-547	9.4	9.5	9.4 (0.1)
G-2-723	1.8	2.9	2.4 (0.6)
G-2-1952	-0.7	0.6	0[c]
G-2-3933	-1.4	0.9	0[c]
GU-3-433	-0.7	-1.1	0[c]
GU-3-1203	-3.2	-1.9	0[c]
GU-3-1301	-1.7	-1.7	0[c]

[a]Contact time was 6 weeks under ambient conditions. Solutions were 5×10^{-6} M in uranium. Particle size was 75 to 500 μm.
[b]Values in parentheses are standard deviations of the means.
[c]Zero was selected.

(5) All tuff samples taken from above the water tables were tested under aerobic conditions for 6-week periods; technetium sorption was zero or very low.

(6) As expected, sorption of cesium and barium on sample G-2-547, which contains ~24% smectite, is relatively high because of the high sorption ratio for clays. Sorption of strontium, however, is not enhanced for this sample. Sorption of plutonium and americium is quite high and may be related to the increased surface area of clays.

I. Geochronology (A. E. Norris)

Measurements of ^{36}Cl can be used to date vadose zone pore water by using the known ^{36}Cl half-life of 3.01×10^5 years. This technique will date water

TABLE XVI

SORPTION RATIOS FOR DESORPTION OF STRONTIUM, TECHNETIUM, CESIUM, BARIUM, AND EUROPIUM ON USW GU-3 SAMPLES

Sample	Shaking Position	Element	Sorption Ratio[a] (mℓ/g) Experimental		Average[b]
GU-3-433	Horizontal	Sr	39	49	44 (5)
"	"	Cs	482	576	530 (50)
"	"	Ba	450	486	470 (10)
"	"	Eu	103	144	120 (20)
"	Vertical	Sr	36	32	34 (2)
"	"	Cs	531	499	510 (20)
"	"	Ba	508	413	460 (50)
"	"	Eu	166	138	150 (20)
GU-3-1301	Horizontal	Sr	110	76	90 (20)
"	"	Cs	216	153	180 (40)
"	"	Ba	757	562	660 (100)
"	"	Eu	147	75	110 (40)
"	Vertical	Sr	28	88	60 (30)
"	"	Cs	159	211	180 (30)
"	"	Ba	596	786	690 (100)
"	"	Eu	51	131	90 (40)

[a]Desorption time was 6 weeks.
[b]Numbers in parentheses are standard deviations of the means.

older than ~6×10^4 years; therefore, the detection of vadose water that is older than this limit will provide information about the rate of water infiltration through the zone. The dating will be performed on samples collected as the ES is mined. The dating process involves measuring the ratio of ^{36}Cl to total inactive chlorine in each sample. The sample of tuff required for each measurement depends, among other things, on the pore water extraction efficiency and on the mass of the inactive chlorine in each sample. The inactive chlorine is now being assayed in the pore water of Topopah Spring Member tuff from the USW G-4 core at the 1067-ft depth. The tuff was crushed and contacted with de-ionized water overnight. The measured chloride concentration in the water was 1.9 mg/ℓ in one sample and 7.4 mg/ℓ in a second sample. Additional experiments will be performed to measure the chloride concentration as a function of contact time and to obtain more consistent results from similar samples.

TABLE XVII

SORPTION RATIOS FOR AMERICIUM AND PLUTONIUM FOR USW GU-3 AND USW G-2 CRUSHED ROCKS

				R_d (mℓ/g)			
				Sorption[a]		Desorption	
Core	Element	Sample Position	Temperature	Experimental	Av of Duplicates	Experimental	Av of Duplicates
GU-3-1203	Am	Horizontal	Ambient	860		990	
		"	"	970	920 (60)	1400	1200 (200)
		Vertical	"	1400		900	
		"	"	1200	1300 (110)	1800	1400 (460)
		"	85°C	4200		7200	
		"	"	4300	4250 (30)	10 500	8900 (1600)
	Pu	Horizontal	Ambient	330		920	
		"	"	480	410 (70)	880	900 (20)
		Vertical	"	300		920	
		"	"	340	320 (20)	950	930 (10)
		"	85°C	440		620	
		"	"	940	700 (300)	830	720 (100)
GU-3-433	Am	Horizontal	Ambient	3300		9500	
		"	"	2900	3100 (200)	6000	7800 (1700)
		Vertical	"	3500		7800	
		"	"	3800	3600 (150)	14 000	11 000 (3300)
		"	85°C	2100		6700	
		"	"	4200	3200 (1000)	3500	5100 (1600)
	Pu	Horizontal	Ambient	340		960	
		"	"	500	420 (80)	810	890 (100)
		Vertical	"	240		1000	
		"	"	240	240 (2)	890	960 (80)
		"	85°C	1700		4500	
		"	"	1800	1750 (50)	7800	6100 (1700)

TABLE XVII (cont)

Core	Element	Sample Position	Temperature	R_d (mℓ/g) Sorption Experimental	Sorption Av of Duplicates	Desorption Experimental	Desorption Av of Duplicates
GU-3-1301	Am	Horizontal	Ambient	2000		1500	
		"	"	2050	2000 (40)	1500	1500 (5)
		Vertical	"	1600		3800	
		"	"	1400	1500 (120)	3200	3500 (320)
		"	85°C	8600		23 000	
		"	"	11 000	9600 (1000)	19 000	21 000 (1700)
	Pu	Horizontal	Ambient	200		560	
		"	"	250	210 (30)	600	580 (20)
		Vertical	"	380		1800	
		"	"	330	360 (20)	2400	2100 (330)
		"	85°C	2500		1300	
		"	"	7600	5000 (2500)	1600	1400 (110)
G-2-547	Am	Horizontal	Ambient	13 000		18 500	
		"	"	13 000	13 000 (110)	16 000	17 000 (1400)
	Pu	"	"	1100		1100	
		"	"	1300	1200 (120)	1300	1200 (80)
G-2-723	Am	"	"	930 000		>2 800 000	
		"	"	840 000	890 000 (50 000)	>2 800 000	>2 800 000
	Pu	"	"	>4500		>4700	
		"	"	>4500	>4500	>4700	>4700

TABLE XVII (cont)

Core	Element	Sample Position	Temperature	R_d (mℓ/g) Sorption Experimental	Sorption Av of Duplicates	Desorption Experimental	Desorption Av of Duplicates
G-2-1952	Am	Horizontal	Ambient	1850		4000	
		"	"	1700	1800 (70)	3800	3900 (100)
		Vertical	"	1700		7100	
		"	"	1500	1600 (100)	8100	7600 (500)
	Pu	Horizontal	"	72		460	
		"	"	80	76 (4)	380	420 (40)
		Vertical	"	57		310	
		"	"	55	56 (1)	250	280 (30)
	Np	Horizontal	"	2.8		17	
		"	"	2.6	2.7 (0.1)	13	15 (2)
G-2-3933	Am	Horizontal	"	7000		12 000	
		"	"	6200	6600 (400)	11 000	11 500 (500)
	Pu	"	"	1600		650	
		"	"	1600	1600 (30)	330	490 (160)

[a]Numbers in parentheses are standard deviations of the means.

TABLE XVIII

SUMMARY OF SORPTION RATIOS

Sample	Sorption Ratio[a] (ml/g)[a]									
	Se	Sr	Tc	Cs	Ba	Eu	Ra	U	Pu	Am
G-1-1292					2100 (300)		1500 (100)			
G-1-1436					150 000 (24 000)		100 000 (30 000)	11 (1)		
G-1-2289	9 (1)				66 000 (9000)		46 000 (20 000)	2.5 (0.1)		
G-1-2363	25 (5)				235 (9)		540 (60)	0		
G-2-547	2 (2)	265 (10)	0	13 300 (1500)	3490 (30)	390 (30)		9.4 (0.1)	1200 (200)	13 000 (110)
G-2-723	19 (2)	290 (40)	0	4100 (600)	3500 (400)	>10 000		2.4 (0.6)	>4500	890 000 (50 000)
G-2-1952[b]	2 (1)	2200 (400)	0	63 300 (1100)	25 000 (4000)	89 (14)		0	76 (4)	1800 (70)
G-2-3933	0 (1)	240 (60)	0.1 (0.06)	2500 (1000)	1700 (500)	1500 (700)		0	1600 (30)	6600 (400)
GU-3-433	15 (3)	61 (6)	0	630 (20)	810 (100)	100 (14)		0	420 (80)	3100 (200)
GU-3-855	10 (4)							10.0 (0.1)		
GU-3-1203	1 (1)							0	410 (70)	920 (60)
GU-3-1301	7 (2)	32 (8)	0.03 (0.004)	160 (40)	570 (60)	75 (12)		0	210 (30)	2000 (40)
GU-3-1436	3 (0)							20 (2)		
GU-3-1531	5 (1)							54 (9)		

Sample	Comments[c]
G-1-1292	Glassy
G-1-1436	Clinoptilolite
G-1-2289	Clinoptilolite
G-1-2363	Devitrified, 5% clay
G-2-547	24% clay
G-2-723	Calcite, glass, 10% clay
G-2-1952[c]	Mordenite, clinoptilolite
G-2-3933	Analcime, 15% clay
GU-3-433	Devitrified
GU-3-855	Devitrified, 2% clay
GU-3-1203	Glass, vytrophyre
GU-3-1301	Glass, 12% clay
GU-3-1436	Glass
GU-3-1531	Devitrified

[a]Average value for sorption. Horizontal shaking position used where available. Values from this report and Ref. 7. Numbers in parentheses are standard deviations of the means.

[b]Sorption ratio for Np is 2.7 (0.1).

[c]See Table XII for more details.

J. Matric Potential Determinations (E. J. Mroz, R. S. Rundberg, and A. J. Mitchell)

The matric potential as a function of saturation was determined for samples of welded tuff of the Topopah Spring Member from Fran Ridge. Two methods were used and compared: matric potentials were (1) calculated using mercury intrusion data and (2) measured directly using pressure membrane extractions.

Matric potential and mercury intrusion porosimetry depend on the surface tension of a fluid in a pore. The relationship between the pressure and the radius of curvature of the liquid surface can be described by the Washburn equation,

$$P = \frac{\gamma \cos \alpha}{r} \quad ,$$

where

P = applied pressure,

γ = surface tension coefficient,

α = wetting angle, and

r = pore radius.

The relationship can be applied either to mercury by using $\gamma = 375$ dynes/cm and $\alpha = 140°$ or to water by using $\gamma = 72$ dynes/cm and $\alpha = 0°$ (note the change in sign for the pressure). The fractioned volume of mercury intruded into the rock corresponds to the water extracted ($1-\theta$) for matric potential. Quanta Chrome Corporation* performed Mercury intrusion up to 60 000 psi on samples from Fran Ridge. The matric potential curve, which is calculated using the Washburn equation, is shown in Fig. 3 as a solid line.

The matric potential was also determined using a pressure membrane extractor. The saturation was determined by weighing the samples fully saturated, dry, and after water extraction. The low permeability of Topopah Spring tuff made it difficult to perform these measurements because the time required to extract water was so long that the membrane dried out. When the

*Quanta Chrome Corporation, 6 Aerial Way, Syosset, NY 11791.

cellulose membrane dries, it becomes permeable to gas; the ensuing gas flow dries the rock samples by evaporation, which causes erroneous saturation values. This problem was mitigated by slicing the tuff samples to a thickness of about 2 mm. The results are plotted as points in Fig. 3. The agreement between the two methods is good; both measurements show a step at about 20 bar. The measurements from the pressure membrane extractor appear to fall below the curve at pressures less than 2 bar, which may be the result of evaporation, as described above. The good agreement between the mercury intrusion porosimetry and the actual matric potential measurements means that much of the characterization of the unsaturated zone can be accomplished using porosimetry. This method is much cheaper to perform (~$180 per sample) and can be accomplished in a short time. This method should be adequate for developing a satistical distribution of the matric potential.

K. Fracture-Flow Experiments (E. J. Mroz, R. S. Rundberg, and A. J. Mitchell)

Six samples of drill core that contain natural fractures have been surface-sealed and capped for fracture-flow experiments. The apertures of the fractures have been determined by measuring the permeability of the fractures and applying Darcy's law. The permeabilities are measured by applying a liquid head to the fracture, monitoring the inlet and outlet pressure with piezoresistive transducers, and simultaneously measuring the flow rate. The fracture apertures in these cores vary from 57 to 252 m and are listed in Table XIX. Tests of radionuclide elution through these fractures have been started, and some results will be reported next quarter.

L. New Thermodynamic Data for EQ3/6 (J. F. Kerrisk)

The EQ3/6 thermodynamic data base is being expanded and updated to include those elements needed for chemical modeling of waste radionuclides, local minerals, and groundwater at Yucca Mountain. New data for manganese and strontium have recently been compiled and added to the EQ3/6 data base. In some cases the information replaced existing data, and in other cases new solids or aqueous species were added to the data base.

The data needed in chemical equilibrium calculations are equilibrium constants for reactions involving the species of interest and the aqueous basis species employed by the program. However, thermodynamic data are usually not compiled in this way. The MCRT computer program was written by

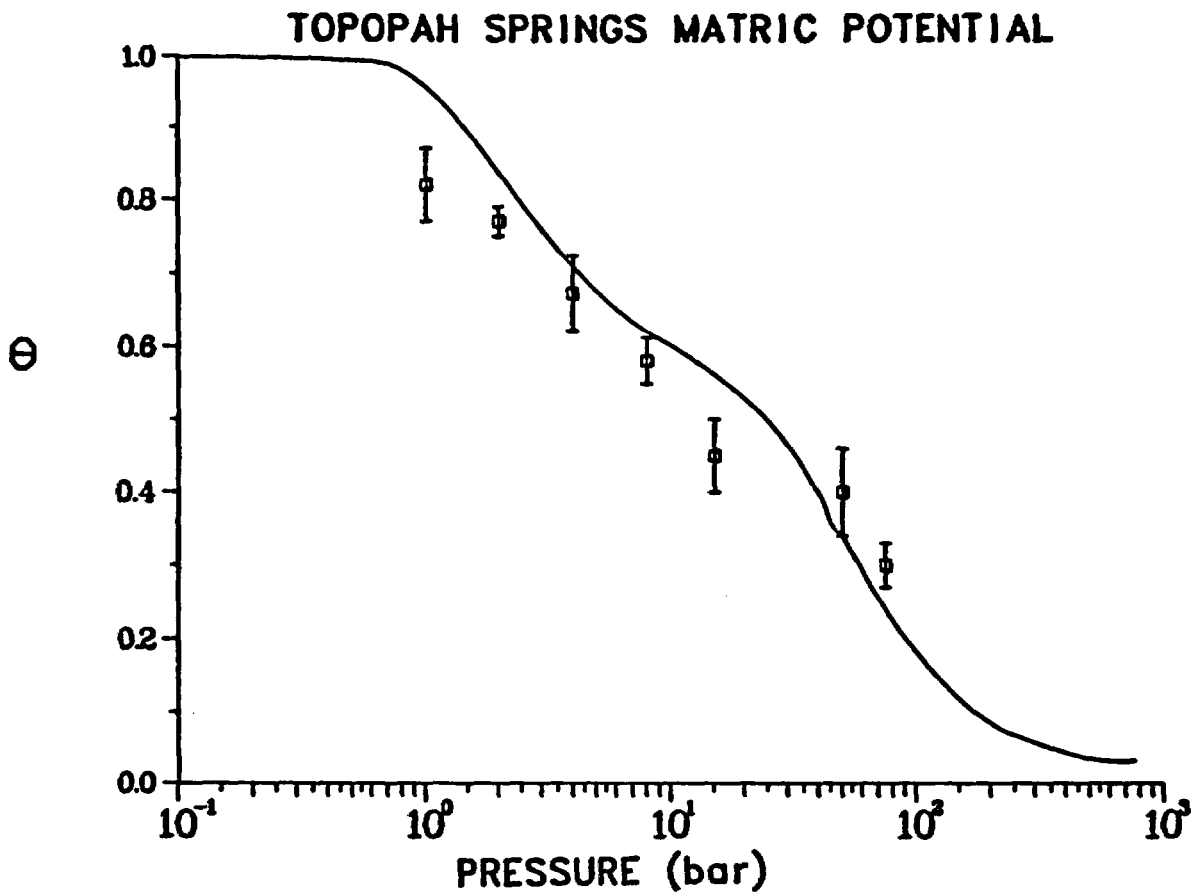

Fig. 3. Topopah Spring tuff matric potential.

TABLE XIX

FRACTURE APERTURES

Sample	Aperture
G-1-103	151 ± 4 μm
G-1-753	57 ± 4 μm
G-1-1221	252 ± 43 μm
GU-3-751	169 ± 10 μm
GU-3-2114	250 ± 26 μm
GU-3-2359	133 ± 6 μm

T. J. Wolery (Lawrence Livermore National Laboratory) to prepare basic thermodynamic data, such as free energies of formation, entropies, and heat capacities in the form needed for EQ3/6 calculations.[17] For aqueous species, the free energy of formation of the species from the elements in their standard states at one temperature is required as a minimum. Data usually exist at 298.15 K, and an equilibrium constant can be calculated at that temperature from this information. If, in addition, the entropy of the species is known at the same temperature, various extrapolation techniques can be used to calculate equilibrium constants at temperatures up to 300°C.[18,19] For solids, the free energy of formation of the species from the elements in their standard states at one temperature is also the minimum required data. This gives an equilibrium constant at that temperature. If heat-capacity data or heat of reaction data are also available, equilibrium constants at other temperatures can be determined.

Basic thermodynamic data for the species of an element are entered in the MCRT program in three files: (1) the MDAQS file contains information on aqueous species, (2) the MDSOL file contains information on solid species, and (3) the REAC file defines the chemical reactions that form the aqueous and solid species from the set of basis species used by EQ3/6. The notation for the REAC file uses negative coefficients for reactants (on the left in a reaction) and positive coefficients for products (on the right). Output from MRCT is a file (DFILE) that lists the reactions and equilibrium constants at eight temperatures (0, 25, 60, 100, 150, 200, 250, and 300°C). Copies of the files for manganese and strontium are contained in Appendix A; references to the sources of the data are included in the files. Summary comments on the data and comparisons with other sources are given below.

1. Manganese Data. Recent analyses of water from wells in the vicinity of Yucca Mountain have shown higher manganese concentrations than were previously observed in these waters. These findings, in addition to the observations of manganese minerals in the unsaturated zone at Yucca Mountain, indicate that manganese may be important when determining the redox state of the water. The existing data base for EQ3/6 contains data for only a few manganese aqueous species and solids. There are no data for aqueous species in oxidation states higher than the (II) state; for this reason, thermodynamic data for manganese species have been collected from various literature sources. Data for 18 aqueous species and 18 solids of manganese are listed in

Appendix A. Where possible, data were taken from National Bureau of Standards (NBS)[20] and USGS[21] compilations.

Investigations in the unsaturated zone at Yucca Mountain have found manganese minerals that have been tentatively identified as todorokite. Minerals with mixed oxidation states of manganese, such as todorokite, are found in various environments, particularly in marine deposits.[22] These minerals have varying compositions; because of the difficulty in defining compositions, thermodynamic data have not been measured for todorokite. Crerar and Barnes have estimated the stability of todorokite and birnessite relative to that of better known manganese minerals such as manganite [MnO(OH)], hausmannite (Mn_3O_4), and pyrolusite (MnO_2).[23] Manganite, todorokite, and birnessite are metastable compared with bixbyite (Mn_2O_3) and pyrolusite. If bixbyite and pyrolusite are ignored, the manganese oxide stability fields change from hausmannite to manganite to todorokite to birnessite as Eh increases at constant pH. Based on these qualitative considerations, thermodynamic data were estimated for todorokite and birnessite. For the estimate, it was assumed that todorokite has the composition $Mn(II)_2Mn(IV)_5O_{12}\cdot 3H_2O$ and birnessite has the composition $Mn(II)_2Mn(IV)_6O_{14}\cdot 5H_2O$ (Ref. 22). Both of these compositions are idealized; in addition to Mn(II), the minerals also contain alkaline earth and alkali metal cations.[22] However, only data for the pure manganese compounds can be estimated by comparisons with other manganese compounds. For the estimates, it was assumed that at pH 10 and 25°C, the manganite-todorokite stability line is at Eh = 0.36 V, and the todorokite-birnessite stability line is at Eh = 0.58 V (Ref. 23). Using these estimates, equilibrium constants can be determined as $\log_{10}K = 18.31$ for the reaction

$$Mn_7O_{12}\cdot 3H_2O + 14H^+ = 7Mn^{2+} + 10H_2O + 2.5O_2(g) \quad ,$$

and $\log_{10}K = 20.38$ for the reaction

$$Mn_8O_{14}\cdot 5H_2O + 16H^+ = 8Mn^{2+} + 13H_2O + 3O_2(g) \quad .$$

The free energy of formation of todorokite is -923.4 kcal/mole and of birnessite is -1145.1 kcal/mole. Neglecting the water of hydration, todorokite

would have the formula $MnO_{1.714}$ with a free energy of formation of -107.6 kcal/mole of manganese; birnessite would have a formula $MnO_{1.750}$ with a free energy of formation of -107.7 kcal/mole of manganese. The value for birnessite is close to Bricker's measurement of -108.2 kcal/mole of manganese for δ-MnO_2 (birnessite).[24]

Data for three aqueous species ($MnPO_4^-$, $MnHPO_4^\circ$, and $MnH_2PO_4^+$) and two solid species [$Mn_3(PO_4)_2$ and $MnHPO_4$] of manganese with phosphate were prepared in this manner for a phosphate thermodynamic data file. These species are in the current version of the EQ3/6 data base and were not recalculated here.

Equilibrium constant data at 25°C for the manganese reactions listed in Appendix A have been compared with data from a number of other sources.[25-30] Table XX lists $\log_{10}K$ values developed as part of this work (in the column labeled EQ3/6) and the other data, most of which are from WATEQ2,[25] WATEQF,[26] and the compilation of Benson and Teague.[27] In general, there is good agreement among the various data bases, although some exceptions exist. The data for $MnCl^+$, $MnCl_2^\circ$, and $MnCl_3^-$ from Mattigod and Sposito[28] are quite different from the data developed as part of this work and from the WATEQ2 (Ref. 25) data, but there is no apparent reason for this difference. Also, smaller differences exist among the MnF^+ and $Mn(NO_3)_2^\circ$ data developed as part of this work, WATEQ2,[25] and Benson and Teague.[27] The only significant difference in the solid data is for alabandite; WATEQ2[25] uses a green MnS precipitate that is less stable than alabandite.

2. Strontium Data. Strontium is one of the waste elements that may be stored at a Yucca Mountain repository, and the EPA has established a release limit for ^{90}Sr (see Ref. 15). The existing EQ3/6 data base has thermodynamic data for four aqueous complexes (SrF^+, $SrPO_4^-$, $SrHPO_4^\circ$, and $SrH_2PO_4^+$) and five solids [strontianite, celestite, $SrF_2(c)$, $Sr_3(PO_4)_2(c)$, and $SrHPO_4(c)$] containing strontium. Literature sources have been reviewed, and data have been collected for 8 new aqueous complexes and 15 new solids that contain strontium. In addition, data for SrF^+, $SrF_2(c)$, strontianite, and celestite were revised. When possible, data were taken from NBS[31] and USGS[21] compilations. For the aqueous species $SrSO_4^\circ$, the free energy of formation from the NBS compilation was disregarded because it gave results that differed from a number of other compilations. Data for the three aqueous species $SrPO_4^-$, $SrHPO_4^\circ$, and $SrH_2PO_4^+$ were recently prepared in this manner for a phosphate data file; they were not recalculated here. Tabular heat capacity

TABLE XX

COMPARISON OF MANGANESE SPECIES THERMODYNAMIC DATA AT 25°C

Species[a]	$Log_{10}K$ [b] EQ3/6	Other Sources
$MnCl^+$	-0.6010	+0.14 (Ref. 28) -0.607 (Ref. 25)
$MnCl_2^\circ$	-0.0586	+1.80 (Ref. 28) -0.041 (Ref. 25)
$MnCl_3^-$	+0.2712	+3.61 (Ref. 28) +0.305 (Ref. 25)
$MnSO_4^\circ$	-2.3082	-2.26 (Ref. 25)
$MnOH^+$	+10.5447	+10.59 (Ref. 29)
$Mn(OH)_2^\circ$	+22.1889	+22.20 (Ref. 29)
$Mn(OH)_3^-$	+34.1996	+34.80 (Ref. 29)
$Mn(OH)_4^{2-}$	+48.2626	+48.30 (Ref. 29)
$MnCO_3^\circ$	+3.8716	+3.83 (Ref. 27) +4.02 (Ref. 28)
MnF^+	-1.3758	-0.85 (Ref. 25)
$Mn(NO_3)_2^\circ$	-0.2067	-0.60 (Ref. 25) +0.40 (Ref. 27)
$MnHCO_3^+$	-0.8928	-1.27 (Ref. 25) -1.95 (Ref. 28) -0.92 (Ref. 27)
Mn^{3+}	+19.2247	+18.908 (Ref. 25)
MnO_4^{2-}	+35.3093	+35.302 (Ref. 25)
MnO_4^-	+95.6662	+95.696 (Ref. 25)
Rhodochrosite	-0.1891	-0.08 (Ref. 25) -0.21 (Ref. 27)

TABLE XX (cont)

Species[a]	$Log_{10}K$ [b] EQ3/6	Other Sources
Alabandite	-0.3811	-0.43 (Ref. 27) -0.20 (Ref. 30) +3.8 (Ref. 25)[c]
Manganosite	+17.9259	+17.938 (Ref. 26) +17.91 (Ref. 27)
$MnSO_4(c)$	+2.6717	+2.669 (Ref. 26) +2.68 (Ref. 27)
$Mn(OH)_2(c)$	+15.2989	+15.088 (Ref. 25) +15.09 (Ref. 27)
Hausmannite	+19.7671	+19.980 (Ref. 25) +19.72 (Ref. 27).
Bixbyite	+8.6434	+8.843 (Ref. 25) +8.61 (Ref. 27)
Manganite	+18.5562	+17.956 (Ref. 25) +17.96 (Ref. 27)
$Mn(OH)_3(c)$	+44.6094	+44.308 (Ref. 26) +44.24 (Ref. 27)
Pyrolusite	+0.0235	-0.384 (Ref. 25) -0.02 (Ref. 27)
Rhodonite	+9.7289	+9.522 (Ref. 26) +9.72 (Ref. 27)
Tephroite	+23.0612	+23.122 (Ref. 26) +23.47 (Ref. 27)
Scacchite	+8.7738	+8.760 (Ref. 26) +8.77 (Ref. 27)
$MnCl_2 \cdot H_2O$	+5.5311	+5.520 (Ref. 26) +5.51 (Ref. 27)
$MnCl_2 \cdot 2H_2O$	+3.9816	+3.974 (Ref. 26) +3.96 (Ref. 27)

TABLE XX (cont)

Species[a]	$Log_{10}K$ [b] EQ3/6	Other Sources
$MnCl_2 \cdot 4H_2O$	+2.7150	+2.710 (Ref. 26) +2.68 (Ref. 27)
Todorokite	+18.3100	--
Birnessite	+20.3755	--

[a]Species formula in EQ3/6 data base.

[b]$Log_{10}K$ for reactions shown in Appendix A.

[c]Data is for MnS (green), which is probably different from alabandite.

data for six of the solids [$SrF_2(c)$, $SrI_2(c)$, $Sr(OH)_2(c)$, $SrBr_2(c)$, $Sr(NO_3)_2(c)$, and strontianite] were fit as a function of temperature to the Maier-Kelley equation

$$C_p = a + bT + c/T^2 \quad ,$$

where T is the temperature (K); C_p is the heat capacity (cal/mole K); and a, b, and c are the parameters determined by the least squares fit. This equation is used in MCRT, and the heat-capacity equation parameters are listed in Appendix A. Data for the solids $Sr_3(PO_4)_2(c)$ and $SrHPO_4(c)$ were recently prepared in this manner for a phosphate data file; they were not recalculated here.

Four species originally in the data base were reconsidered here: (1) the new data for celesite are quite similar to the old, (2) new data for SrF^+ are similar at 25°C but have a slightly different temperature dependence, (3) the new data for $SrF_2(c)$ are about one $log_{10}K$ unit lower, and (4) the new data for strontianite are about two $log_{10}K$ units lower than the original data.

Equilibrium constant data at 25°C for the strontium reactions listed in Appendix A have been compared with data for the same reactions from four other compilations.[25-27,32] Table XXI lists $log_{10}K$ values developed at Los Alamos

TABLE XXI

COMPARISON OF STRONTIUM SPECIES THERMODYNAMIC DATA AT 25°C

Species[a]	$Log_{10}K$ [b] EQ3/6	Other Sources
$SrOH^+$	13.1908	+13.19 (Ref. 27) +13.29 (Ref. 32) +13.178 (Ref. 26)
$SrCl_2^o$	0.0147	0.0 (Ref. 27) 0.0 (Ref. 32)
$SrBr_2^o$	0.0235	--
SrI_2^o	0.1202	--
$SrSO_4^o$	-2.5501	-2.55 (Ref. 27) -2.55 (Ref. 32)
$SrNO_3^+$	-0.7992	-0.82 (Ref. 27)
$Sr(NO_3)_2^o$	-0.1481	-0.80 (Ref. 27)
$SrCO_3^o$	10.3429	--
SrF^+	-0.7528	-0.80 (Ref. 27)
SrO(c)	41.1175	+41.39 (Ref. 27)
SrF_2(c)	-7.3621	-8.54 (Ref. 27) -8.54 (Ref. 25)
$SrCl_2$(c)	7.1613	+7.15 (Ref. 27)
$SrCl_2 \cdot H_2O$	3.9992	+3.98 (Ref. 27)
$SrCl_2 \cdot 2H_2O$	2.5229	+2.50 (Ref. 27)
$SrCl_2 \cdot 6H_2O$	0.6714	+0.63 (Ref. 27)
$SrBr_2$(c)	12.3449	+12.53 (Ref. 27)
$SrBr_2 \cdot H_2O$	8.8163	+8.79 (Ref. 27)
$SrBr_2 \cdot 6H_2O$	2.8279	+2.78 (Ref. 27)
SrS(c)	17.3204	+17.31 (Ref. 27)
Celestite	-6.4788	-6.42 (Ref. 27) -6.465 (Ref. 25)

TABLE XXI (cont)

Species[a]	$Log_{10}K$ [b] EQ3/6	Other Sources	
$Sr(NO_3)_2(c)$	0.1965	+0.59	(Ref. 27)
$Sr(NO_3)_2 \cdot 4H_2O$	-0.1305	+0.05	(Ref. 27)
Strontianite	1.0936	+1.08 +1.08	(Ref. 27) (Ref. 25)
$SrSiO_3(c)$	14.0630	+14.06	(Ref. 27)
$Sr_2SiO_4(c)$	41.2538	-	
$SrI_2(c)$	18.3202	-	

[a]Species formula in EQ3/6 data base.

[b]$Log_{10}K$ for the reactions shown in Appendix A.

(in the column labeled EQ3/6) and the other data, most of which are from Benson and Teague.[27] In general, there is good agreement among the various compilations. The largest differences are for $Sr(NO_3)_2$, $SrF_2(c)$, and $Sr(NO_3)_2(c)$; in only one case [$SrF_2(c)$] is the difference greater than one $log_{10}K$ unit.

3. Speciation and Solubility Calculations. Speciation calculations were done for Well J-13 water with EQ3 and the new manganese data. It was assumed that the water was at pH 6.9; Eh values of 700, 400, 100, and -100 mV were used. Under strongly oxidizing conditions (700 mV Eh), the water was saturated with respect to pyrolusite; at lower Eh, the water was not saturated with any manganese solid. The primary aqueous species at all values of Eh were Mn^{2+} and $MnCO_3$.

Speciation calculations for Well J-13 water were also done with EQ3 using the new strontium data. The total strontium content of the water is 4.6 x 10^{-7} molal (0.04 mg/ℓ). The predominant aqueous species is Sr^{2+}, with a small amount of $SrSO_4^{\circ}$ present. No solids containing strontium were supersaturated.

Calculations of the solubility of strontium in Well J-13 water were also done at pH 6, 7, and 8. Strontianite [$SrCO_3(c)$] was the solid phase controlling strontium solubility under these conditions. Strontium solubilities

were 5.8×10^{-2} molal at pH 6, 9.4×10^{-4} molal at pH 7, and 7.9×10^{-5} molal at pH 8. At pH 6, celestite [$SrSO_4$(c)] was also near saturation.

Strontium solubilities calculated from the old EQ3/6 data base were about a factor of 100 lower than the values reported above. The primary cause of this difference is the strontianite data. The original data base used strontianite thermodynamic data from the SUPCRT compilation.[33] More recent compilations have reduced the free energy of formation of strontianite, which leads to higher calculated solubilities.

M. Analcime Solid-Solution Model (C. J. Duffy)

The analcime solid-solution model developed this quarter is an ideal solid-solution model that takes into consideration the coupled substitution of silica and water of hydration for sodium and aluminum. The model represents analcime as an ideal solid solution between $NaAlSi_2O_6 \cdot H_2O$ and $Si_3O_6 \cdot 1.5H_2O$. Thermodynamic parameters, consisting of the molar Gibbs energy, the molar entropy and the molar volume at 298K, and the heat capacities at constant pressure as a function of temperature, have been derived for the two end members. From these data, the Gibbs energy of the end members at any pressure and temperature ($\Delta G_{P,T}$) can be calculated. The Gibbs energy of any composition in the solid solution ($\Delta G^{SS}_{P,T}$) is then expressed as

$$\Delta G^{SS}_{P,T} = x_1 \Delta G^1_{P,T} + (1-x) \Delta G^2_{P,T} + 0.5\ RT\ [x, \ln x, + (1-x_1) \ln(1-x_1)] \quad ,$$

where x_1 is the mole fraction of one of the end members. (The superscript 1 on the ΔG refers to the same end member, and the 2 refers to the other end member.) R is the gas constant and T is the temperature (K). This is then combined with thermodynamic data for other compounds of interest to calculate phase relationships for analcime. The model is based on the observed compositions of analcimes that coexist with quartz in Yucca Mountain, recently published calorimetric data on the analcime $Na_{0.96}Al_{0.96}Si_{1.04}O_6 \cdot H_2O$ (Ref. 34), and solubility data on analcime plus albite in aqueous solution. The model predicts that the transition from analcime plus quartz to low albite is very insensitive to water pressure and that it takes place at about 135°C. This is in good agreement with the field observations of Iijima,[35] where analcime plus quartz was transformed to low albite at about 125°C; there was little variation with water pressure.

The model predicts that analcime in equilibrium with quartz has a composition of about $Na_{0.85}Al_{0.85}Si_{2.15}O_6$ $1.075H_2O$. There is little variation with temperature and water pressure; therefore, the relative constancy of analcime composition in Yucca Mountain does not provide any information on the pressure-temperature history of the tuffs. However, it does indicate that the analcime was probably formed in equilibrium with quartz.

Calculations of the equilibrium between analcime plus cristobalite predicts that cristobalite plus analcime will be stable (metastable) to slightly over 200°C; however, the predicted composition of the analcime (about $Na_{0.5}Al_{0.5}Si_{2.5}O_6$ $1.25H_2O$) is more silica rich than any known analcime. This suggests that another phase (quite possibly clinoptilolite) is more stable than either analcime or albite in the presence of cristobalite in this temperature range. This conclusion is consistent with cold-seal hydrothermal experiments; however, it is not yet proven that these experiments are in metastable equilibrium.

III. MINERALOGY-PETROLOGY OF TUFF (D. L. Bish, D. E. Broxton, F. M. Byers, Jr., F. A. Caporuscio, B. A. Carlos, R. C. Gooley, S. S. Levy, R. E. Semarge, and D. T. Vaniman)

The interrelation of geochemistry and mineralogy-petrology research for developing a waste repository in tuff was described for the International Conference on Radioactive Waste Management, in Seattle.[36] This presentation emphasized the correlation of technetium, strontium, cesium, barium, cerium, europium, uranium, neptunium, plutonium, and americium sorption with the alteration mineralogy of tuffs. In addition to the continued study of Yucca Mountain mineralogy to define its role in overall sorption, mineralogy-petrology studies this quarter were also applied to the problems of stratigraphy and alteration in Drill Hole UE-25p#1, to the potential toxic hazards of fibrous zeolites during construction at Yucca Mountain, and to the effects of composition on thermal expansion/contraction in clinoptilolite.

A. Studies of Drill Hole UE-25p#1

Under the supervision of M. Carr, USGS, samples of cuttings from Drill Hole UE-25p#1 were analyzed optically and by electron microprobe. To determine the unit stratigraphy in this drill hole, optical petrographic analysis of 50 intervals was combined with modal analysis of 2000 to 5000

points in 40 of those intervals. The identification of Unit A of the older tuffs (equal abundance of potassium feldspar and plagioclase) and Unit C of the older tuffs (plagioclase predominant, abundant biotite) below the Lithic Ridge Tuff is straightforward using the data already available for Drill Hole USW G-1. Two more ash-flow tuffs occur at greater depth, between a carbonate fan and the Silurian dolomite. The lowermost of these ash flows is moderately welded and, therefore, relatively unaltered; feldspar compositions and abundances suggest that this ash flow is correlative with the tuff of Yucca Flat.

Biotite analyses by electron microprobe were used to confirm that the contact between the Tram Member of the Crater Flat tuff and the underlying Lithic Ridge tuff is between 2760 and 2900 ft (842 and 885 m) in Drill Hole UE-25p#1. This distinction is based on the higher average Mg/(Mg+Fe) ratio in biotites of the Lithic Ridge Tuff (0.60) than in biotites of the Tram Member (0.45), as determined by electron microprobe analysis. This interval also appears to coincide with the first appearance of analcime with depth in Drill Hole UE-25p#1.

Mineralogy-petrology studies have confirmed the occurrence of depth-related zones of alteration mineralogy at Yucca Mountain. With increasing depth, these zones progress from relatively unaltered tuff into tuff with open-channel zeolites (clinoptilolite and mordenite), then into analcime-bearing tuff, and then into a zone where authigenic albite occurs. In Drill Hole UE-25p#1, analcime first occurs between the Tram Member and the Lithic Ridge Tuff, as noted above. The first appearance of authigenic albite is within the Lithic Ridge Tuff in a sample from 3453 ft (1053 m). These depths are about 500 ft (150 m) shallower than in the closest hole studied from Drill Hole Wash (Drill Hole UE-25b#1) (Ref. 6). Because the difference in well-head elevation between these two holes is also just under 500 ft, with p#1 being lower, the relative elevation of these mineral zones is the same in Drill Hole UE-25p#1 as it is in Drill Hole Wash.

Clinoptilolite compositions in Drill Hole UE-25p#1 are somewhat different than samples around and north of the exploration block. Clinoptilolite is calcium rich at all depths in UE-25p#1, rather than following the general trend toward potassium, then sodium enrichment. These data, the first on zeolite compositions along potential flow paths away from the repository, suggest that some variability in composition may be expected.

B. Fibrous Zeolites at Yucca Mountain

The question of possible health hazards from fibrous zeolites at Yucca Mountain was first addressed in 1982 (see Appendix B). Concern was specifically directed at the zeolite erionite after the publication of research that suggested a correlation between lung disease and exposure to erionite-bearing tuffs in south-central Turkey. Although asbestos fibers have now also been found in some Cappadocian villages of the region[37] and the correlation of human lung disease with erionite is in doubt, there are experimental data to implicate erionite in the development of malignant peritoneal tumors in mice.[38] Because of the possible dangers of erionite exposure, samples from Well J-13 (where erionite was previously suspected) were re-analyzed by x-ray diffraction in June 1982.[39] No erionite was found in those samples, nor has erionite been identified in any samples from the Yucca Mountain region. Because erionite has not been detected, it can not be present in amounts greater than the bulk rock x-ray diffraction detection limits (about 2%). Erionite is not a mineral to be concerned about at Yucca Mountain.

Although erionite is not a problem for NNWSI, much of the research into erionite toxicity (for example, Suzuki)[38] has also emphasized the potential hazards of other fibrous zeolites. The fibrous crystalline habit is the mineralogic feature associated with toxicity, and therefore this broader emphasis is justified. At Yucca Mountain, the fibrous zeolite mordenite is abundant in some areas and at fairly restricted depths beneath the surface. Mordenite is an abundant component of zeolitized intervals in the northern part of Yucca Mountain; unexpectedly, however, it was absent (except within fractures) at the southern end of the exploration block.[40] Mordenite does not occur in the whole rock (bulk rock) above a depth of 1300 ft (400 m) in any of the drill holes at Yucca Mountain. Only in Drill Hole Wash has mordenite been found in the rock matrix as high as the base of the Topopah Spring Member,[41] and that occurrence is below the basal vitrophyre; therefore, it is also below the host rock for repository development within the Topopah Spring Member. Mordenite does occur as a fracture-filling mineral in Drill Hole USW G-4 within the breakout zones of the Topopah Spring Member. It first appears at 1008-ft depth and generally increases in abundance with depth in fractures of the Topopah Spring host rock. Total abundance is determined by the frequency of fractures within the interval.

Because mordenite, the only fibrous zeolite of significance at Yucca Mountain, is not abundant within the host rock, it is unlikely to be of any concern for repository construction and operation. However, exploratory shaft excavations are presently expected to extend well below the host rock horizon and into the underlying zeolitized intervals. Figure 4 summarizes the distributions of the secondary minerals smectite, clinoptilolite, and mordenite that will be encountered if the exploratory shaft excavations extend to 1600-ft (488 m) depth. These data are based on recently completed analyses of samples from Drill Hole USW G-4. The hachured zones labeled "glass" bound the moderately to densely welded, devitrified portion of the Topopah Spring Member that contains the host rock horizon. Zeolites become abundant in the rock matrix immediately below the lower glass zone, which represents the basal vitrophyre of the Topopah Spring Member. Clinoptilolite is abundant immediately below the vitrophyre, but the fibrous zeolite mordenite does not occur until a depth between 1470 and 1544 ft (448 and 471 m) is reached. If

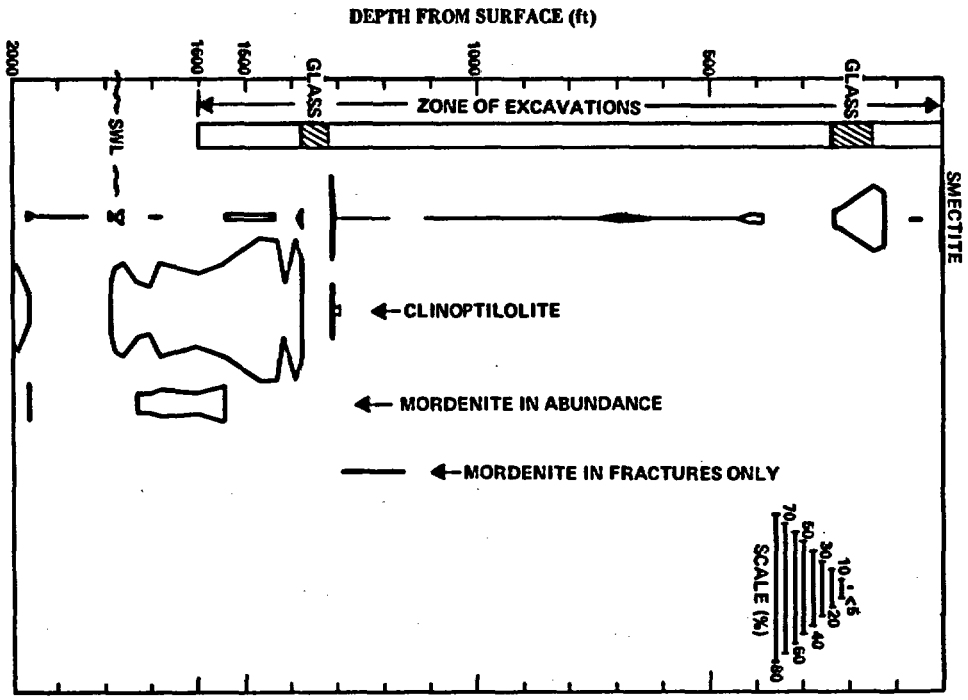

Fig. 4. Distribution of smectite, clinoptilolite, and mordenite expected below 1600-ft depth.

the excavation is extended to 1600 ft (488 m), a distance of more than 56 ft (17 m) of rock averaging 16% mordenite content will be mined. It is uncertain whether the exploratory shaft will extend so far into the zeolitized intervals. If the exploratory shaft is terminated at some depth above 1470 ft (448 m), fibrous zeolites should not be considered a potential health hazard for any exploration or construction activities in the currently proposed host rock at Yucca Mountain. Personnel of the Health, Safety, and Environment Division at Los Alamos are searching the Toxline data base to identify any other possible toxic minerals that may be of concern for NNWSI operations at Yucca Mountain.

C. Effects of Composition on Thermal Expansion/Contraction in Clinoptilolite.

Six natural and three cation-exchanged (sodium, potassium, and calcium) clinoptilolites have been examined from 20 to 300°C in a heated sample holder by x-ray powder diffraction. Unit cell parameters were refined from x-ray data every 50°C to determine the compositional effects on thermal expansion/contraction. The effects of exchangeable cations were very pronounced; sodium-saturated clinoptilolite contracted about 8.5% between 20 and 300°C, calcium-saturated clinoptilolite contracted about 3.5%, and potassium-saturated clinoptilolite contracted about 1.6%. The bulk of the contraction occurred upon evacuating the potassium-saturated material at 20°C (0.1 torr), and the sodium-saturated clinoptilolite contracted most between 50 and 100°C, reaching a relatively constant volume by 150°C. Calcium-saturated clinoptilolite continued to contract up to 300°C. Natural samples with mixed exchangeable-cation compositions exhibited intermediate amounts of thermal contraction but generally continued to contract up to 300°C. In all samples, cation-exchanged and natural, a reduction in the *b* cell dimension was primarily responsible for the decrease in volume. This is probably caused by the collapse of the channels parallel to *c* and *a*. Expansion behavior upon cooling in a vacuum was variable, but most samples rapidly reexpanded and the calcium-rich samples completely expanded to the preheating *in-vacuo* volume. Sodium-rich samples reexpanded completely in a few minutes in the room atmosphere. These data provide information on the nature of the channels at elevated temperatures and explain the variability in macroscopic thermal expansion data obtained for zeolitic tuffs from the NTS. This is true in particular for the natural potassium-, sodium-rich zeolites of the Calico

Hills unit. Future studies will investigate the effects of temperature on sorption by zeolites.

IV. VOLCANISM STUDIES (B. M. Crowe, D. T. Vaniman, F. A. Caporuscio, W. S. Baldridge, and D. B. Curtis)

Helicopter reconnaissance of selected sites in the Nellis Bombing and Gunnery Range at the NTS was completed. Basalt sites were sampled and examined within a zone extending northwest from Black Mountain to Stonewall Mountain. Samples were returned to Los Alamos for thin-section studies and geochemical analyses. Detailed geologic mapping of the southern two centers of the basalts of Nye Canyon has shown that both sites are lava-infilled tuff rings that were formed when basalt magma erupted through a river and mixed with water to form phreatomagmatic explosions. In both cases, elongate tuff rings were formed that were subsequently infilled by Strombolian scoria and thick intracrater lava flows. This is the third recognized phreatomagmatic eruption in the NTS region for the basalt centers of the younger and older rift basalts (0.3 to 9 Myr). Three additional basalt sites were sampled following examinations of aerial photographs and observations made during the helicopter reconnaissance. The easternmost locality of the basalts of Silent Canyon, a series of basalts erupted along the ring-fracture zone of the Silent Canyon cauldron was field mapped and sampled. This site consists of scattered outcrops of scoria rubble, the probable remnants of one or a number of highly eroded scoria cones. This basalt is moderately porphyritic, with phenocrysts and megacrysts of olivine, black clinopyroxene, and plagioclase. The basalt of Buckboard Mesa was sampled along a linear rift extending southeast from Scruggam Peak. The rift vented lava and scoria along its length; the sampled basalts will be examined to determine if the rift may have been the source for the quartz-normative lavas of Buckboard Mesa. A basalt site west of Black Mountain and along the border of the Nellis Bombing and Gunnery Range was examined to determine if a scoria cone noted on color aerial photographs might be a relatively young basalt (<4 Myr). Field mapping showed that the scoria cone underlies a related basalt lava, which in turn is overlain by the Thirsty Canyon Tuff. The scoria cone is, thus, at least 8 Myr or older.

Core samples from a basalt lava intersected in USW VH-2 were examined and sampled at the USGS core library. The basalt is similar megascopically to a 10.5 Myr lava at the south end of Crater Flat, and if the two basalts are

correlative, these lavas should underlie much of southern Crater Flat. Both the surface basalt (10.5 Myr) and the basalt in Drill Hole VH-2 are reversely magnetized; thus, this buried basalt may account for the reversed aeromagnetic anomalies in Crater Flat.

The volcanism sections of the SCP have been revised and checked for consistency with the volcanism summary report,[42] which includes a fold-out map showing the distribution and ages of basaltic volcanism in the southcentral Great Basin. "Aspects of Potential Magmatic Disruption of a High-Level Radioactive Waste Repository in the Southcentral Great Basin" was published in the May issue of the Journal of Geology.[43] B. M. Crowe and D. T. Vaniman presented joint talks at the University of California at Los Angeles;* the talks concerned the geology and geochemistry of basaltic volcanism in the southcentral Great Basin. Discussions were held with a number of faculty and graduate students at UCLA concerning the interpretation of anomalous strontium, neodymium, and trace-element data for basalts of the NTS region. Currently, no model explains adequately the derivation of the isotopic ratios and is completely consistent with the field, geochronology, and major- and trace-element compositional constraints for the basalts.

V. ROCK PHYSICS (J. D. Blacic)

The first long-term creep test of Calico Hills zeolitized tuff has been started. Improvements in sample grinding technique have eliminated sample cracking problems, and an inventory of five finished samples was produced for further testing this summer.

The first test is described here in considerable detail to illustrate the interesting properties of this rock; later tests will be summarized. Figure 5 shows the early period of the test during which saturation, pressurization, and heating were achieved; the early part of creep strain is also shown (point marked S). The sample required nearly 150 hours (6+ days) to saturate; this was an unexpectedly long time. The procedure (1) raised confining pressure (PC) and pore pressure (PP) in steps to 5 MPa and 0.7 MPa, respectively, (2) periodically valved-off the sample from a constant pressure reservoir, and (3) determined if the pore pressure dropped over time as a result of water inflow. When the pore pressure no longer drops during a valve-off test, the sample is

*"A Belt of Late-Cenozoic Basalt Volcanism in the Southcentral Great Basin: Tectonic Setting [B. Crowe] and Geochemistry [D. Vaniman]."

assumed to be saturated. In practice, this is quite a sensitive way of determining when 100% saturation is achieved. Initially, the volume strain (EV) of the sample shows an elastic compression as the pressure is increased, which is followed by a further time-dependent compression (compressive stresses and strains are taken as positive). However, as water flows into the sample, the sign of the volume strain reverses, and a large dilation occurs over several days as the sample slowly saturates and zeolite minerals rehydrate. After about 5 days, the pore pressure was increased to about 3.5 MPa in an attempt to speedup the saturation; saturation was eventually obtained at about 146 hours.

At this point, the pore pressure at one end of the sample was quickly reduced about 20%, and the pulse decay was recorded over time. From this data, a permeability of 0.7 microDarcy was calculated. This low permeability, coupled with the large porosity of the sample (about 73 mℓ of water was required to fill the pore space), explains the long saturation time. In future tests, a high pore pressure will be used from the beginning so that saturation time can be reduced to about 2 days.

Pore pressure was then reduced to 0.1 MPa and the sample was left in a drained condition. After equilibrium was regained, temperature was raised at about 2° per minute to 75°C. The jitter shown in Fig. 5 is caused by SCR noise; the temperature variation is actually much smoother than shown.) Volume strain first increased as the temperature was raised then decreased so that there was a net volume thermal contraction giving an average coefficient of -7×10^{-6}/degree.

After waiting about 1 day to establish equilibrium, the stress was raised to 20 MPa and held constant thereafter. In view of the low permeability and large water content of the sample, the rate of stress increase was of particular concern. It seemed possible that a too rapid stress increase could cause a buildup of pore pressure. Figure 6 shows some detail of the loading. The pore pressure only increased about 0.1 MPa at an average axial strain rate of about 3×10^{-6}/second, so a rate of about 1×10^{-5}/second seems safe for future tests. After the final creep stress was attained, the sample was placed in a drained condition and remained so from then on. The early transient creep is dominated by slow contraction caused by the outflow of pore water. Most of this contraction is completed in about 5 hours, and then the sample slowly dilates.

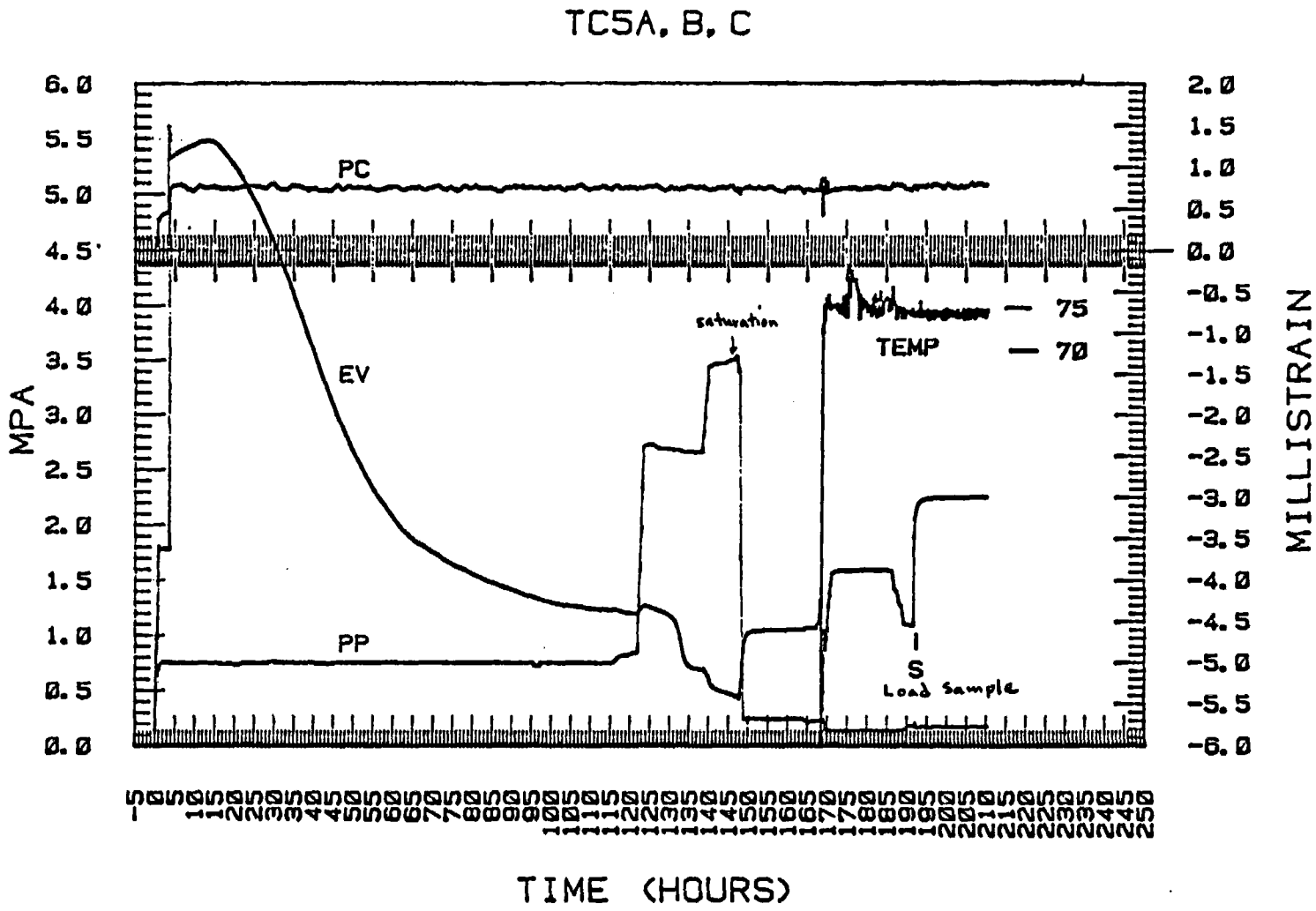

Fig. 5. Confining pressure (PC), volume strain (EV), pore pressure (PP), and temperature vs time.

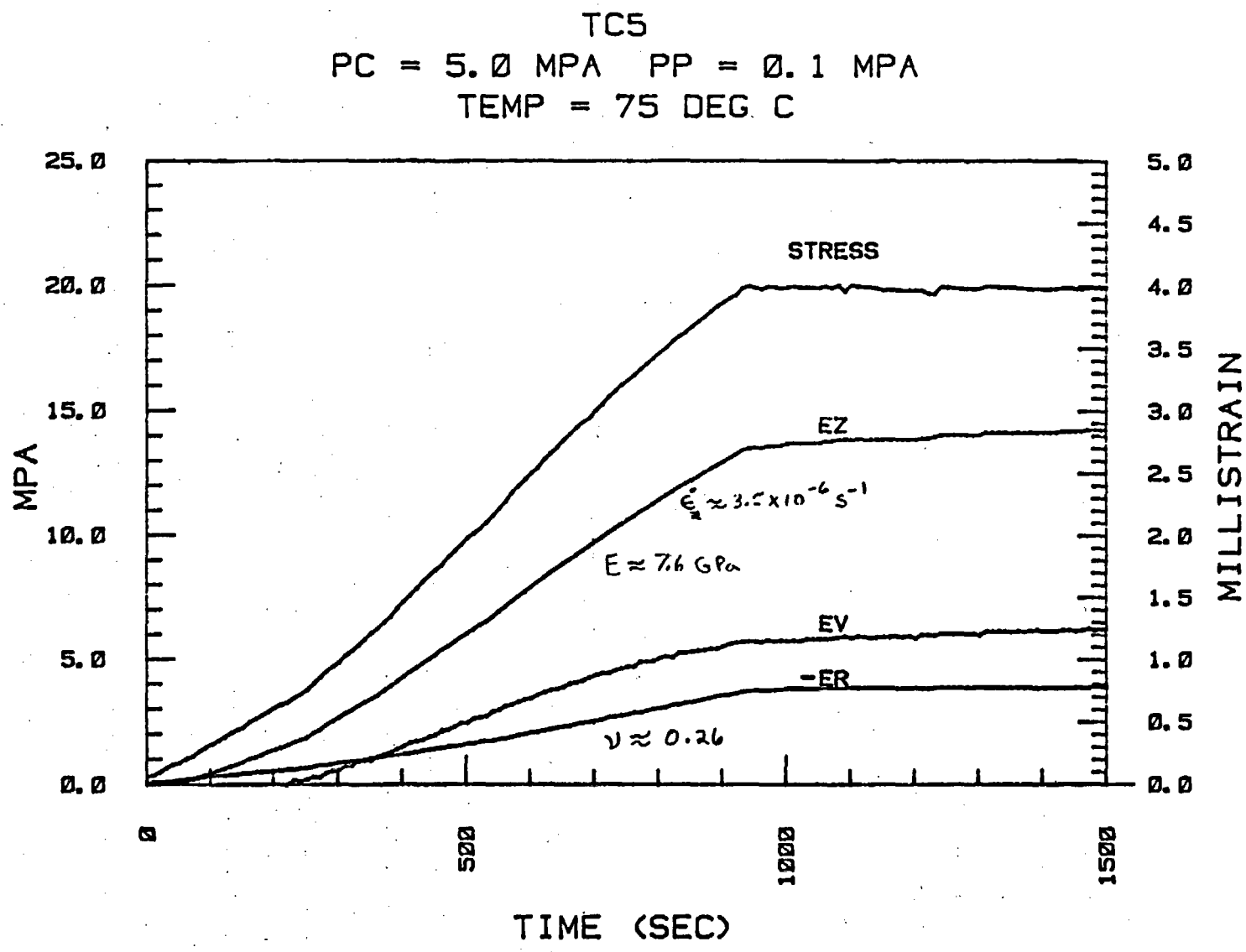

Fig. 6. Stress, axial strain (EZ), volume strain (EV), and circumferential strain (ER) vs time.

A summary of the thermomechanical properties determined to date in this test is given below:

Grain density: 2.27 g/cm^3 (ambient conditions)
Bulk density: 1.62 g/cm^3 (ambient conditions)
Porosity: 0.286 (ambient conditions)
Permeability: 7×10^{-19} m^2 (25°C, 2 MPa P_{eff})
Bulk modulus: 3.8 GPa (25°C, 4.9 MPa P_{eff})
Young's modulus: 7.6 GPa (75°C, 4.9 MPa P_{eff})
Poisson's ratio: 0.26 (75°C, 4.9 MPa P_{eff})
Coefficient of volume thermal expansion: -7×10^{-6}/degree (25 to 75°C, 4.9 P_{eff}).

Figure 7 shows the volume strain vs time curve to date. The creep curve can be characterized as showing a slow but accelerating dilation. Average strain rate over the last 50 hours is about 1×10^{-9}/second. This sample will be taken to failure if it is possible in a reasonable amount of time. However, in view of the limited amount of time available to work on the Calico Hills tuff, this test will probably be cut off at 500 hours.

VI. SHAFT AND BOREHOLE SEALING (R. J. Vidale and D. M. Roy)

Any sealing material will react with the tuff host rock at some rate because of chemical differences and because the tuff contains fine reactive mineral and glass particles. To choose an appropriate sealant, it is necessary to determine reaction products and their properties and to modify the sealant material to minimize reaction or reaction rates if the effects of reaction are deleterious to the sealing function.

The purpose of this project is to evaluate the chemical stability of potential sealing materials in the felsic tuff of Yucca Mountain. Concretes are being proposed as one major type of sealing material for use in a tuff repository. An experimental program was instituted to evaluate the chemical stability of concrete formulations that have potential use in sealing in the Yucca Mountain area. A thermodynamic property survey was made to predict stability of concretes in host environments. Tests are being done to evaluate the reactivity of experimental concretes in a tuff environment under accelerated exposure conditions.

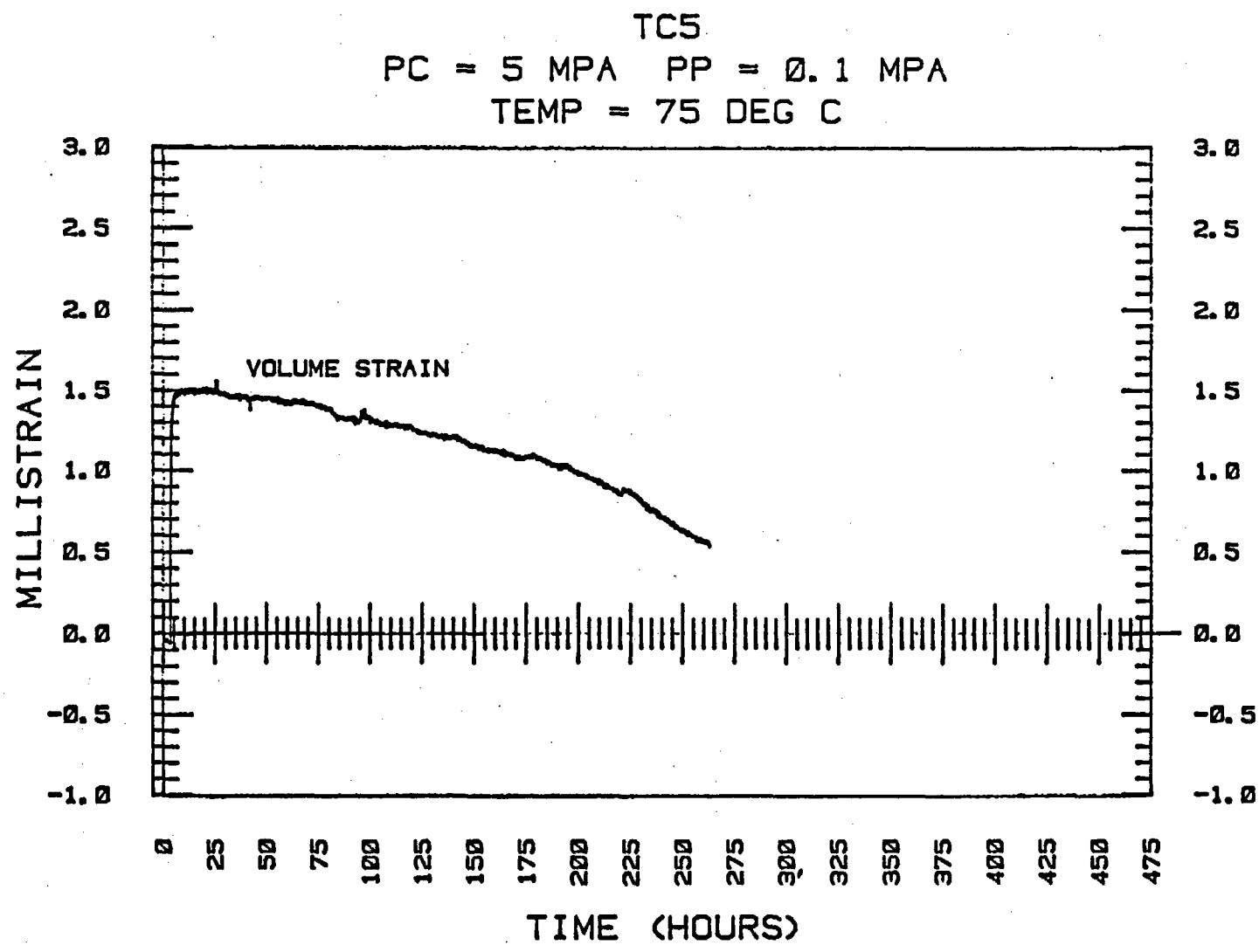

Fig. 7. Volume strain vs time.

The concrete formulation CON-14 was supplied to Los Alamos Laboratory as an example of a general type of concrete that was potentially compatible with Yucca Mountain tuffs. The concrete has a cementitious matrix that incorporates fine aggregate from the vicinity of the NTS and coarse aggregate from G-tunnel tuff. To study their possible interactions, crushed combinations of matrix and aggregate were exposed to accelerated test conditions under agitation in hydrothermal reaction vessels at Pennsylvania State University. Preliminary results of studies have been summarized.[44] The solid and the aqueous fluid reaction products of the experiments indicated that chemical reactions took place in both the tuff aggregate and the cementitious matrix of the concrete.

A second type of experiments uses crushed samples (less than -100 mesh powder) of matrix and aggregates under static cold-seal pressure-vessel conditions to quantify the alteration. These experiments apply a less severe acceleration, and the reaction proceeds at a slower rate. Materials are sampled at weekly intervals for the first 4 weeks and again at the end of 8 and 32 weeks. The pH of the capsule fluids was found to be about 5 after 1- to 4-weeks reaction, and the solutions contained mostly calcium, sodium, silicon, and potassium. Solid-phase characterization results to date generally support the results found in the agitated experiments. The x-ray diffraction and SEM characterization of the powders and chemical analyses of the fluid phases will be made at intervals to 32 weeks. The results will be compared with those observed in the agitated vessel powder experiments and in the tests with monolithic bulk concrete.

Additional experiments investigate reaction of bulk concrete; they are conducted at elevated temperature (200°C) and samples are either suspended in the vapor phase above water or immersed in water and pressurized at 6.8 to 10 MPa. The test conditions bracket the actual conditions that might exist for a repository host rock unsaturated with respect to water (including the 200°C vapor phase reaction experiments). Two disks of the CON-14 concrete were cut from a 3-in. by 6-in. cylinder; each was subdivided into four 1-in.-diam disks. Some SEM imagery photomosaics were prepared. After exposure to the two sets of conditions at various test intervals, the disks are examined again. The disks from the vapor phase reaction experiments were sampled at monthly intervals for the first 3 months, and the final sample will be examined after 6 months. The 2- to 3-month tests show that the samples are

generally more altered when immersed in liquid than when exposed to vapor phase. The cementitious matrix generally does not appear to have been substantially attacked, whereas the tuff shows more alteration.

Modifications have been made to the initial test plan. (1) A tuff from the Topopah Spring Member is being used in subsequent tests to address more specifically the proposed repository environment conditions, and (2) a sealing material (mixture #82-22) with higher silica content (nearer a tuff composition) is being tested to achieve greater chemical compatibility between host and sealing material. The geometry of monolithic test specimens will also help with better quantification of the test results.

Hydrothermal alteration studies of a physical mixture of powdered #82-22 and a sample of the Topopah Spring Member of the Paintbrush tuff (1:2 by weight) are now being conducted at 200°C and 6.8 to 10 MPa in a rocking autoclave. Alterations of the -20 + 30 mesh mixture are being monitored using the solution chemistry, and the solid alteration products will be characterized at the end of the experiments. The temperature dependence of the alteration will be investigated by conducting the tests at least three different temperatures.

A second set of experiments is being conducted using monolithic disks prepared with the mortar #82-22 cast around a square cross-sectional prism of Topopah Spring tuff that was cured at 60°C for 11 weeks. These tests will be conducted and monitored in a manner similar to that described for the above procedure. The alteration in this case will be carried out in an agitated Parr vessel. The disks will be examined for crystal growth and alteration of either the cementitious matrix or the tuff aggregates. Chemical alteration across the matrix/aggregate interface will be examined by SEM/EDS and/or microprobe to identify transport of cations/anions. Any aggregate alteration will be noted and compared to the phases and textures present in thin sections of concrete and tuff. X-ray diffraction will be used to characterize the disk mineralogy before the runs. When the runs are completed, the disks will be cut to remove two sections: one to be used for thin sections and another to be impregnated with a fluorescent dye and examined optically.

The second set of disks are being sampled on a weekly basis for the first 3 weeks and the final sample will be taken on the 8th week of hydrothermal treatment. A series of characterization sets that is parallel to the above described procedures will be followed. In addition, the fluids in contact with the disks are sampled at each interval and will be chemically analyzed.

Thermodynamic studies to evaluate the potential stability of concrete in a tuff environment have been completed.[45] Three different sources of data have been used: thermochemical measurements and thermodynamic calculations; phase equilibrium studies; and natural occurences of relevant phase assemblages. Only limited data were available from each source; the findings, though tentative, suggest that siliceous concretes may be compatible with tuff (whereas high-lime concretes are probably not) and that tuffs may be compatible with aluminous or siliceous clays but that even siliceous concretes are not compatible with clays.

VII. EXPLORATORY SHAFT

A. Design

Three ES Project Review Meetings were held at DOE/NTSSO during the report period. At the April 14, 1983 meeting, the Title II design status was discussed. Also, it was determined that the shaft collar is to be considered as part of the shaft, and therefore, cannot be built ahead of time. This decision resulted in a 3-month schedule delay. The start of shaft sinking, which now includes the shaft collar, was delayed to January 9, 1984. The combined effect of the two changes is a 6-month delay. On May 19, 1983, the main subjects of the ES Project Review Meeting were the shaft-sinking contract, Title II design, and quality assurance (QA). On June 23, 1983, the Title II design, QA, and additional schedule changes were discussed. Site preparation was delayed to January 15, 1984, and the start of shaft sinking was similarly delayed to July 16, 1984.

Three Design Criteria Letters (DCLs) were issued during the report period. The DCL-6 addressed (1) an additional drill room near the bottom of the completed shaft, (2) an upper breakout at about 950 ft below the surface, (3) new shaft water-chemistry requirements, and (4) saving topsoil from the borrow pit. The DCL-7 was an official request for Title II engineering cost estimates for the ES from the architect-engineers. The DCL-8 requested changes to the ES subsurface facilities Title II design. These changes include, among other things, a thicker shaft liner in the Calico Hills formation, a new layout of the underground openings, and downhole electrical and instrumentation requirements.

A second review of the ES subsurface facilities Title II design was completed. The design package consisted of 32 drawings and 14 sets of speci-

fications. This design review was required because of changes requested in DCL-6, and as a result of DCL-8, it will be necessary to perform yet another review.

The site access road and water line were completed to the NTS boundary. All construction work has temporarily ceased.

REECo has awarded contracts for much of the equipment required for the ES. The two major items are refurbishing of the two NTS hoists and procuring the headframe. The request for proposals on the shaft-sinking subcontract is now expected in October 1983.

The Finding of No Significant Impact and the Land Use Agreement between DOE and the US Air Force have been signed.

B. Test Plan

Work by the Exploratory Shaft Test Plan (ESTP) Committee continued at a high level this quarter. Test proposals for both the construction phase tests and the in situ phase tests were completed by the committee and reviewed by the Waste Management Project Office (WMPO) management. Approved test proposals, listed below, are now being developed into test plans.

The ESTP Committee planned and participated in a geologic field trip to the Yucca Mountain area on May 19. USGS members of the ESTP Committee led the field trip to familarize the entire group with the geomorphology, geology, and lithology of Yucca Mountain. Significant insights were gained regarding the fractured nature of the tuff layers, the distinction between void content and alteration halos around lithophysal cavities in the Topopah Spring Member, and the geologic section within the Topopah Spring. The Committee visited the USGS core library at Mercury and conducted detailed study and inspections of the significant USW G-4 core sections.

An initial QA matrix for the ESTP Committee activities was developed. This matrix of individual tests vs required QA procedures, inspections, and evaluations will be the basis for an overall QA procedure for ESTP implementation. The Committee reviewed the Integrated Data System (IDS) support in relation to enhanced QA monitoring with respect to ES test data calibration and recording.

The Los Alamos proposal for an IDS was submitted with the March 24 test plan proposals; the data aquisition phase was partially approved. An economic analysis of the data management portion, requested by WMPO, is in progress.

Key topics and issues considered by the ESTP Committee during the quarter included:

- The impact of a second, higher breakout zone in the 10% lithophysal unit above the current target unit. The committee concluded that limited new testing and a breakout room without a muck pocket may be required.

- The committee modified the drilling and coring procedures to be used by the shaft-sinking subcontractor. The selection of the breakout level would require the 100-ft of air drilling/coring (if possible) to commence at a depth about 50 ft above the proposed breakout. The cores produced by this operation would be used to select the exact depth for breakout. This procedure would be used at both breakout levels.

- After several reviews, the preferred orientation of the breakout rooms was decided, and a revised layout of the underground facilities was prepared.

- The proposal for air drilling/coring technology tests was drafted and is being reviewed. The ESTP Committee agreed to carry the proposal forward following review and revision; development of this technology is a continuing problem.

- Questions have been raised regarding penetration of the Calico Hills formation by the ES. The current ESTP requires testing in the upper Calico Hills and investigation of the Calico Hills/Topopah Spring contact. Methods of conducting these tests with minimum penetration are being considered and discussed.

- There were detailed discussions of the purposes, needs, and requirements for an upper breakout. The pros and cons of having this breakout at 950-ft depth instead of 520 ft were discussed, but the issue is not yet resolved.

Changes in the test-plan preparation schedule were brought about by postponing the start of shaft construction from January 1984 to July 1984. As directed by the TPO meeting in May, the Test Plan is now scheduled to be avail-

able to the NRC in February 1984. This allows about 3 months more time than the previous November 1983 due date. The majority of the Committee members felt that the additional time could be most profitably used for an external peer review process. Due dates for the initial versions of individual Test Plans were delayed until July and August, and the initial draft of the ESTP was scheduled for October 1983. Support for this new schedule was sought from WMPO management and TPOs.

Approved test proposals for the ES are listed below.

- Shaft-wall mapping, photography, and hand specimen sampling
- Large-block sampling and pore water analysis
- Groundwater sampling
- Shaft mechanical testing 1: rock extensometers and pressure cells
- Vertical core drilling from within the shaft
- Lateral drilling at the breakout level
- Overcore testing
- Breakout room testing
- Drift-wall mapping
- Radial borehole testing from within shaft
- Lateral core drilling from drifts
- Sampling and testing intact fractures
- Bulk permeability test
- Infiltration test
- Hydrologic testing/Calico Hills
- Waste package testing
- Drift and pillar deformation test
- Enhanced heated block testing
- Canister scale heater testing
- Borehole and drift seal testing
- Diffusion test

VIII. QUALITY ASSURANCE

A. Los Alamos

An audit of the INC-11 counting room was conducted and closed out. Six detailed procedures and a revised work plan were reviewed and approved for Los Alamos NNWSI activities. A quality assurance training program was presented,

and ten documents were issued to holders of the NNWSI Manual of QA Procedures. A proposed records system was presented to the TPOs.

More than 30 specifications and 50 drawings for Title I and Title II of the ES were reviewed, and QA requirements were added as necessary. Two draft documents for the Los Alamos ES program were prepared: the QA Program Plan and the Document Control Program Plan draft were revised to incorporate comments from the WMPO. The new drafts included the matrix as an attachment and were submitted to DOE/NV by June 15, 1983. The Holmes and Narver, REECo, and Fenix and Scisson QA Manuals were reviewed, and comments will be submitted to the WMPO.

B. USGS

A response was drafted for DOE audit 83-01 conducted in January. Three audits were performed to the USGS NNWSI activities. A systems audit of the overall QA program was performed in Denver. Audits were performed of geophysics records control in Menlo Park and Denver.

Two detailed procedures were prepared, reviewed, and routed for approvals. The QA requirements for test probe calibration and hardness testing were investigated.

ACKNOWLEDGMENTS

The following Los Alamos National Laboratory personnel are acknowledged for their efforts: D. A. Mann (technical assistance); P. A. Elder, M. E. Lark, and S. Lermuseaux (sample counting and gamma-spectra analyses); and L. M. Mitchell and C. E. Gallegos (typing of drafts and final manuscript).

REFERENCES

1. W. R. Daniels, B. R. Erdal, and D. T. Vaniman, Comps., "Research and Development Related to the Nevada Nuclear Waste Storage Investigations, July 1--September 30, 1982," Los Alamos National Laboratory report LA-9577-PR (March 1983).

2. A. F. White, H. C. Claassen, and L. V. Benson, "The Effect of Dissolution of Volcanic Glass on the Water Chemistry in a Tuffaceous Aquifer, Rainier Mesa, Nevada," US Geological Survey Water-Supply Paper 1535-Q (1980).

3. J. F. Kerrisk, "Reaction-Path Calculations of Groundwater Chemistry and Mineral Formation at Rainier Mesa, Nevada," Los Alamos National Laboratory report LA-9912-MS (December 1983).

4. K. Wolfsberg, B. R. Erdal, and B. M. Crowe, Comps., "Research and Development Related to the Nevada Nuclear Waste Storage Investigations, July 1—September 30, 1980," Los Alamos National Laboratory report LA-8612-PR (February 1981).

5. W. R. Daniels, K. Wolfsberg, R. S. Rundberg, A. E. Ogard, J. F. Kerrisk, C. J. Duffy, et al., "Summary Report on the Geochemistry of Yucca Mountain and Environs," Los Alamos National Laboratory report LA-9328-MS (December 1982).

6. F. A. Caporuscio, D. T. Vaniman, D. L. Bish, D. E. Broxton, B. H. Arney, G. H. Heiken, F. M. Byers, Jr., R.C. Gooley, and R. E. Semarge, "Petrologic Studies of Drill Cores USW-G2 and UE25b-1H, Yucca Mountain, Nevada," Los Alamos National Laboratory report LA-9255-MS (July 1982).

7. K. Wolfsberg, D. T. Vaniman, A. E. Ogard, "Research and Development Related to the Nevada Nuclear Waste Storage Investigations, January 1--March 31, 1983," Los Alamos National Laboratory report LA-9793-PR (July 1983).

8. F. A. Caporuscio, "Preliminary Estimates of the Buffering Potential of FeMn Oxides at Yucca Mountain with Respect to Eh," Los Alamos National Laboratory report (in preparation, 1983).

9. Stability Constants of Metal-Ion Complexes, Sect. I, Inorganic Ligands, L. G. Sillen, Comp. (London, The Chemical Society, 1964).

10. B. Allard, H. Kipatsi, and J. O. Liljenzin, "Expected Species of Uranium Neptunium, and Plutonium in Neutral Aqueous Solutions," J. Inorg. Nucl. Chem. 42, 1015 (1980).

11. D. A. Costanzo, R. E. Biggers, and J. T. Bell, "Plutonium Polymerization," J. Inorg. Nucl. Chem. 35, 606 (1973).

12. L. M. Toth, H. A. Friedman, and M. M. Osborne, "Polymerization of Pu(IV) in Aqueous Nitric Acid Solutions," J. Inorg. Nucl. Chem. 43, 2929 (1981).

13. D. Rai and J. L. Swanson, "Properties of Plutonium(IV) Polymer of Environmental Importance," Nucl. Technol. 54, 107 (1981).

14. A. E. Ogard, W. R. Daniels, and D. T. Vaniman, Comps., "Research and Development Related to the Nevada Nuclear Waste Storage Investigations, October 1--December 31, 1982," Los Alamos National Laboratory report LA-9666-PR (May 1983).

15. Environmental Protection Agency, "Environmental Standards for the Management and Disposal of Spent Nuclear Fuel, High-Level, and Transuranic Radioactive Wastes," Federal Register 47, No. 250, 58196-58206 (1982).

16. G. W. Leddicotte, "The Radiochemistry of Selenium," National Academy of Science Monograph NAS-NS-3030 (National Academy of Science, National Research Council, Washington, DC, 1961), p. 5.

17. T. J. Wolery, "MCRT, A Data Base Building Code for the EQ3/6 Geochemical Modeling Software Package," Lawrence Livermore National Laboratory report (in preparation).

18. C. M. Criss and J. W. Cobble, "The Thermodynamic Properties," National Bureau of Standards Technical Note 270-4 (1969).

19. H. C. Helgeson, "Thermodynamics of Hydrothermal Systems of Elevated Temperatures and Pressures," Am. J. Sci. 267, 729-804 (1969).

20. D. D. Wagman, W. H. Evans, V. P. Parker, I. Halow, S. M. Bailey, and R. H. Schumm, "Selected Values of Chemical Thermodynamic Properties," National Bureau of Standards Technical Note 270-4 (1969).

21. R. A. Robie, B. S. Hemingway, and J. R. Fisher," Thermodynamic Properties of Minerals and Related Substances at 298.15K and 1 Bar (10^5 Pascals) Pressure and at Higher Temperatures," Geological Survey Bulletin 1452 (1978).

22. R. G. Burns and V. M. Burns, "Manganese Oxides," In Marine Minerals, Short Course Notes, Vol. 6, R. G. Burns, Ed. (Mineralogical Society of America, Washington, DC, 1979), pp. 1-46.

23. D. A. Crerar and H. L. Barnes, "Deposition of Deep-Sea Manganese Nodules," Geochim. Cosmochim. Acta 38, 279-300 (1974).

24. O. Bricker, "Some Stability Relations in the System $Mn-O_2-H_2O$ at 25° and One Atmosphere Total Pressure," Am. Mineral. 50, 1296-1354 (1965).

25. J. W. Ball, D. K. Nordstrom, and E. A. Jenne, "Additional and Revised Thermochemical Data and Computer Code for WATEQ2--A Computerized Chemical Model for Trace and Major Element Speciation and Mineral Equilibria of Natural Waters," US Geological Survey Water Resources Investigation WRI 78-116 (1980).

26. L. N. Plummer, B. F. Jones, and A. H. Truesdell, "WATEQF--A FORTRAN IV Version of WATEQ, A Computer Program for Calculating Chemical Equilibrium of Natural Waters," US Geological Survey Water Resources Investigation WRI 76-13 (1976).

27. L. V. Benson and L. S. Teague, "A Tabulation of Thermodynamic Data for Chemical Reactions Involving 58 Elements Common to Radioactive Waste Package Systems," Lawrence Berkeley Laboratory report LBL-11448 (1980).

28. S. V. Mattigod and G. Sposito, "Estimated Association Constants for Some Complexes of Trace Metals with Inorganic Ligands," Soil Sci. Soc. Am. J. 41, 1092-1097 (1977).

29. C. F. Baes, Jr., and R. E. Mesmer, The Hydrolysis of Cations (John Wiley and Sons, New York, 1976), pp. 219-226.

30. S. V. Mattigod and G. Sposito, "Chemical Modeling of Trace Metal Equilibria in Contaminated Soil Solutions Using the Computer Program GEOCHEM," in Chemical Modeling in Aqueous Systems, E. A. Jenne, Ed. (American Chemical Society, Washington, DC, 1979), Chap. 37, pp. 837-856.

31. V. B. Parker, D. D. Wagman, and W. H. Evans, "Selected Values of Chemical Thermodynamic Properties," National Bureau of Standards Technical Note 270-6 (1971).

32. S. L. Phillips, "Hydrolysis and Formation Constants at 25°C," Lawrence Berkeley Laboratory report LBL-14313 (May 1982).

33. H. C. Helgeson, J. M. Delany, H. W. Nesbitt, and D. K. Bird, "Summary and Critique of Thermodynamic Properties of Rock-Forming Minerals," Am. J. Sci. 278A, 1-229 (1978).

34. G. K. Johnson, H. E. Flotow, P. A. G. O'Hare, and W. S. Wise, "Thermodynamic Studies of Zeolites: Analcime and Dehydrated Analcime," Am. Mineral. 67, 736-748 (1982).

35. A. Iijima and M. Utada, "Present Day Zeolitic Diagenesis of the Neogene Geosynclinal Deposits in the Niigata Oil Field, Japan," Am. Chem. Soc. Advances in Chemistry Series 101, Molecular Sieve Zeolites I (American Chemical Society, 1971), pp. 342-349.

36. D. L. Bish, D. T. Vaniman, R. S. Rundberg, K. Wolfsberg, W. R. Daniels, and D. E. Broxton, "Natural Sorptive Barriers in Yucca Mountain, Nevada, for Long-Term Isolation of High-Level Waste," International Conference on Radioactive Waste Management, Seattle, Washington, May 16-20, 1983, Los Alamos National Laboratory document LA-UR-83-758.

37. A. N. Rohl, A. M. Langer, G. Moncure, J. J. Selikoff, and A. Fischbein, "Endemic Pleural Disease Associated with Exposure to Mixed Fibrous Dust in Turkey," Science 216, 518-520 (1982).

38. Y. Suzuki, "Carcinogenic and Fibrogenic Effects of Zeolites: Preliminary Observations," Environ. Res. 27, 433-445 (1982).

39. D. L. Bish, D. T. Vaniman, F. M. Byers, Jr., and D. E. Broxton, "Summary of the Mineralogy-Petrology of Tuffs of Yucca Mountain and Secondary-Phase Thermal Stability in Tuffs," Los Alamos National Laboratory report LA-9321-MS (November 1982).

40. D. T. Vaniman, D. L. Bish, D. E. Broxton, F. M. Byers, G. H. Heiken, B. A. Carlos, R. E. Semarge, F. A. Caporuscio, and R. C. Gooley, "Variations in Authigenic Mineralogy and Sorptive Zeolite Abundance at Yucca Mountain, Nevada, Based on Studies of Drill Cores USW GU-3 and G-3," Los Alamos National Laboratory report LA-9707-MS (January 1984).

41. B. M. Crowe, D. T. Vaniman, and W. J. Carr, "Status of Volcanic Hazard Studies for the Nevada Nuclear Waste Storage Investigations," Los Alamos National Laboratory report LA-9325-MS (March 1983).

42. B. Crowe, R. Amos, F. Perry, S. Self, and D. T. Vaniman, "Aspects of Possible Magmatic Disruptions of a High-Level Radioactive Waste Repository at the Nevada Test Site," J. Geology 91, 259-276 (1983).

43. P. J. Carroll, F. A. Caporuscio, and D. L. Bish, "Further Description of Topopah Spring Member of the Paintbrush Tuff in Drill Holes UE25a-1 and USW G-1 and of the Lithic-Rich Tuff in USW G-1, Yucca Mountain, Nevada," Los Alamos National Laboratory report LA-9000-MS (November 1982)

44. B. E. Sheetz and D. M. Roy, "Preliminary Accelerated Reaction Studies of the Hydrothermal Alteration of a Tuff-bearing Concrete," Pennsylvania State University report to Los Alamos National Laboratory on Subcontract 9-X53-36254-1 (1983).

45. W. P. Freeborn, M. W. Barnes, and D. M. Roy, "Low Temperature Phase Equilibria in the System Concrete-Tuff: Thermodynamic Calculations, Experimental Studies, and Natural Assemblages," Pennsylvania State University report to Los Alamos National Laboratory on Subcontract 9-X53-36254-1 (1983).

APPENDIX A

MANGANESE AND STRONTIUM THERMODYNAMIC DATA FOR THE EQ3/6 COMPUTER PROGRAM

This appendix contains listings of the data file for manganese and strontium thermodynamic data for the EQ3/6 computer program. For each element, the MDAQS file lists aqueous species data, the MDSOL file provides solid species data, the REAC file gives the chemical reactions involving the new species and the other EQ3/6 basis species, and the DFILE file enumerates the calculated equilibrium constants for these reactions.

Manganese MDAQS File

```
MDAQSMN  DATA FOR AQUEOUS COMPLEXES OF MANGANESE (SEE BOTTOM OF FILE)
LAST REVISED  1/20/83
MNCL+
        1.          1
    298.15         1.
   -86.700       500.       500.      WAGMAN ET AL. (1969)
2
MN 1.
CL 1.
MNCL2
        0.          0
    298.15         1.
   -117.34       500.       -9.3      WAGMAN ET AL. (1969)
2
MN 1.
CL 2.
MNCL3-
       -1.          1
    298.15         1.
   -148.27       500.      500.0      WAGMAN ET AL. (1969)
2
MN 1.
CL 3.
MNSO4
        0.
    298.15         1.
   -235.60       500.        8.7      WAGMAN ET AL. (1969)
3                                        HELGESON (1969) GIVES LOG K FOR
MN 1.                                    MN++ + SO4-- = MNSO4 AT 25-200C
S  1.                                    DELHOR=-3.7, DELSOR=-22.7
O  4.                                    LOG K=-2.25 AT 25 C
MNOH+
        1.          1
    298.15         1.
   -96.8         500.       -4.0      WAGMAN ET AL. (1969). MACDONALD(1976)
3                                        GIVES SO=-9.0. BAES AND MESMER
MN 1.                                    (1976) GIVE LOG K=-10.59 FOR
O  1.                                    MN++ + H2O = MNOH + H+
H  1.
MN(OH)2
        0.          0
    298.15         1.
  -137.6         500.       500.      BAES AND MESMER (1976) LOG K=-22.2 FOR
3                                        MN++ + 2H2O = MN(OH)2 + 2H+
MN 1.                                    (ESTIMATE)
O  2.
H  2.
MN(OH)3-
       -1.          3
    298.15         1.
  -177.9         500.       500.      WAGMAN ET AL. (1969)
3
MN 1.
O  3.
H  3.
MN(OH)4--
       -2.          3
    298.15         1.
  -215.4         500.       500.      BAES AND MESMER (1976) LOG K=-48.3 FOR
3                                        MN++ + 4H2O = MN(OH)4-- + 4H+
MN 1.
O  4.
H  4.
MNCO3
        0.          0
    298.15         1.
  -189.5         500.       -8.3      EQ3/6 DATAO FILE LOG K VS T DATA
3
MN 1.
C  1.
O  3.
MNF+
        1.          1
    298.15         1.
  -123.7         500.       -2.5      EQ3/6 DATAO FILE LOG K VS T DATA
2
MN 1.
F  1.
HMNO2-
       -1.          4
```

```
    298.15          1.
  -121.2          500.        15.      MACDONALD (1976). HEM (1980) GIVES
3                                          GOF=-120.9
MN 1.
H  1.
O  2.
MN(NO3)2
        0.          0
    298.15          1.
  -107.8        -151.9      500.       WAGMAN ET AL. (1969)
3
MN 1.
N  2.
O  6.
MNHCO3+
        1.          1
    298.15          1.
  -196.0          500.      500.       WAGMAN ET AL. (1969)
4
MN 1.
H  1.
C  1.
O  3.
MN+++
        3.          1
    298.15          1.
   -19.6          500.       -51.      GOF FROM MACDONALD (1976). SOF FROM
1                                          NAUMOV ET AL. (1974). MACDONALD
MN 1.                                      (1976) GIVES SOF=-90.5
MNO4--
       -2.          3
    298.15          1.
  -119.7          500.        14.0     WAGMAN ET AL. (1969). MACDONALD (1976)
2                                          GIVES SOF=24.0
MN 1.
O  4.
MNO4-
       -1.          3
    298.15          1.
  -106.9          500.        45.7     WAGMAN ET AL. (1969). MACDONALD (1976)
2                                          GIVES SOF=50.7.
MN 1.
O  4.
MN2(OH)3+
        1.          1
    298.15          1.
  -246.45         500.       500.      BAES AND MESMER (1976) LOG K=-23.90 FOR
3                                          2MN++ + 3H2O = MN2(OH)3+ + 3H+
MN 2.
O  3.
H  3.
MN2(OH)+++
        3.          1
    298.15          1.
  -151.28         500.       500.      BAES AND MESMER (1976) LOG K=-10.56 FOR
3                                          2MN++ + H2O = MN2(OH)+++ + H+
MN 2.
O  1.
H  1.
STOP.
MDAQSP
```

DATA ON AQUEOUS COMPLEXES OF MANGANESE

NOTE--
- DATA FOR MNPO4-, MNHPO4 AND MNH2PO4+ APPEAR ON PHOSPHOROUS FILE MDAQSP
- THE VALUE "500." MEANS NO DATA

DATA PER SPECIES:

NAME

CHARGE NUMBER
ION CODE:

0	NEUTRAL COMPLEX	(MAY BE LEFT BLANK)
1	CATION	(MAY BE LEFT BLANK)
2	SIMPLE ANION	(MAY BE LEFT BLANK)
3	OXYANION	
4	ACID OXYANION	

TEMPERATURE (K) AND PRESSURE (BARS) CORRESPONDING TO
THE ENTERED THERMODYNAMIC DATA
THE INTERNAL ELECTRONIC ENTROPY, IF THIS IS TO BE APPLIED
IN A CORRECTION TO THE CRISS-COBBLE METHOD

APPARENT STANDARD MOLAL GIBBS ENERGY, KCAL/MOL
APPARENT STANDARD MOLAL ENTHALPY, KCAL/MOL
ENTROPY, CAL/MOL/K

NO. OF ELEMENTS
ELEMENT NAME AND STOICHIOMETRIC COEFFICIENT
STOICHIOMETRY IN TERMS OF REFERENCE ELEMENTAL COMPOUND

NO. OF (KINDS OF) IONIC SPECIES APPEARING IN A DISSOCIATION
REACTION OF THE NEUTRAL SPECIES
STOICHIOMETRIC COEFFICIENT FOR THE DISSOCIATION REACTION
AND THE NAME FOR EACH CONSTITUENT ION

NOTATION--
-- DELGO = GIBBS ENERGY OF FORMATION
-- DELGOR = GIBBS ENERGY OF REACTION
-- DELHO = ENTHALPY OF FORMATION
-- DELHOR = ENTHALPY OF REACTION
-- SO = CONVENTIONAL ENTROPY
-- DELSOR = ENTROPY OF REACTION

REFERENCES

BAES, C. F. JR. AND MESMER, R. E., 1976, THE HYDROLYSIS OF CATIONS, JOHN WILEY AND SONS,NEW YORK, PP. 219-226.

HELGESON, H. C., 1969, THERMODYNAMICS OF HYDROTHERMAL SYSTEMS AT ELEVATED TEMPERATURES AND PRESSURES, AMER. JOUR. SCIENCE, 267, 729-804.

MACDONALD, D. D., 1976, THE THERMODYNAMICS AND THEORETICAL CORROSION BEHAVIOR OF MANGANESE IN AQUEOUS SYSTEMS AT ELEVATED TEMPERATURES, CORROSION SCIENCE, 16, 461-482.

NAUMOV, G. B., RYZHENKO, B. N., AND KHODAKOVSKY, I. L., 1974, HANDBOOK OF THERMODYNAMIC DATA, USGS WATER RECOURCES DIVISION TRANSLATION FROM RUSSIAN, REPORT PB 226 722.

WAGMAN, D.D., W.H. EVANS, V.B. PARKER, I. HALOW, S.M. BAILEY, AND R.H. SCHUMM, 1969, SELECTED VALUES OF CHEMICAL THERMODYNAMIC PROPERTIES, NATL. BUR. STANDARDS TECH. NOTE 270-4.

STOP.

Manganese MDSOL File

```
MDSOLMN      DATA FOR SOLIDS OF MANGANESE   (SEE BOTTOM OF FILE)
LAST REVISED  2/18/83
RHODOCHROSITE
    298.15        1.
    31.073                          ROBIE ET AL. (1978).
   -195.04      500.      23.9      ROBIE ET AL. (1978)
1
O    21.99       9.3     -4.69        0.     KELLEY (1960)
      660.                                    SEE ALSO MOORE (1943A)
3
MN 1.
C  1.
O  3.
ALABANDITE
    298.15        1.
     21.46                          ROBIE ET AL. (1978)
    -52.14      500.      21.46     ROBIE ET AL (1978)
1
O    11.40       1.8        0.        0.     KELLEY (1960)
     1800.                                    SEE ALSO COUGHLIN (1950)
2
MN 1.
S  1.
MANGANOSITE
    298.15        1.
    13.221                          ROBIE ET AL. (1978)
    -86.73      500.      10.54     ROBIE ET AL. (1978)
1
O    11.11      1.94     -0.88        0.     KELLEY (1960)
     1000.                                    SEE ALSO SOUTHARD AND SHOMATE (1942)
2
MN 1.
O  1.
MNSO4(C)
    298.15        1.
     43.62                          ROBIE ET AL. (1978)
  -228.806      500.      26.80     ROBIE ET AL. (1978)
1
O    29.26      8.92     -7.04        0.     KELLEY (1960)
     1000.                                    SEE ALSO SOUTHARD AND SHOMATE (1942)
3
MN 1.
O  4.
S  1.
MN(OH)2(C)
    298.15        1.
        0.     NO DATA
    -147.0      500.      23.7      WAGMAN ET AL. (1969)
1
O       0.        0.        0.        0.     NO DATA
     1000.
3
MN 1.
O  2.
H  2.
HAUSMANNITE
    298.15        1.
     46.95                          ROBIE ET AL. (1978)
   -306.59      500.      36.8      ROBIE ET AL. (1978)
1
O    34.64     10.82     -2.20        0.     KELLEY (1960)
     1400.                                    SEE ALSO SOUTHARD AND MOORE (1942)
2                                             FOR SLIGHTLY DIFFERENT CP
MN 3.
O  4.
BIXBYITE
    298.15        1.
     31.37                          ROBIE ET AL. (1978)
   -210.58      500.      26.4      ROBIE ET AL. (1978)
1
O    24.73      8.38     -3.23        0.     KELLEY (1960)
     1350.
2
MN 2.
O  3.
MANGANITE
    298.15        1.
        0.     NO DATA
   -133.20      500.      500.      BRICKER (1965)
1
```

```
O        0.        0.        0.        0.     NO DATA
     1000.
3
MN 1.
O  2.
H  1.
MN(OH)3(C)
    298.15        1.
        0.     NO DATA
    -181.0      500.      30.          PLUMMER ET AL. (1976) GIVE LOG K=-35.644,
1                                      DELHR=20.09 FOR MN(OH)3 = MN+++ + 3OH-
O        0.        0.        0.        0.     NO DATA
     1000.
3
MN 1.
O  3.
H  3.
PYROLUSITE
    298.15        1.
     16.61                             ROBIE ET AL. (1978)
   -111.17      500.     12.68         ROBIE ET AL. (1978)
1
O     16.6     2.44     -3.88         0.     KELLEY (1960)
      800.                                    SEE ALSO MOORE (1943A)
2
MN 1.
O  2.
RHODONITE
    298.15        1.
     35.16                            ROBIE ET AL. (1978)
  -297.103      500.     24.50        ROBIE ET AL. (1978)
1                                     SEE ALSO WAGMAN ET AL. (1969)
O    26.42     3.88     -6.16         0.    KELLEY (1960)
     1400.                                  SEE ALSO SOUTHARD AND MOORE (1942)
3
MN 1.
SI 1.
O  3.
TEPHROITE
    298.15        1.
     48.61                              ROBIE AND WALDBAUM (1968)
    -390.1      500.      39.0          WAGMAN ET AL. (1969)
1
O    31.04        0.        0.         0.     WAGMAN ET AL. (1969)
     1000.
3
MN 2.
SI 1.
O  4.
SCACCHITE
    298.15        1.
     28.26                             ROBIE AND WALDBAUM (1968)
   -105.29      500.     28.26         WAGMAN ET AL. (1969)
1
O    18.04     3.16     -1.37         0.       KELLEY (1960)
     1000.                                     SEE ALSO MOORE (1943B)
2
MN 1.
CL 2.
MNCL2.H2O
    298.15        1.
        0.                            NO DATA
    -166.4      500.      41.6        WAGMAN ET AL. (1969)
1
O        0.        0.        0.        0.    NO DATA
     1000.
4
MN 1.
CL 2.
O  1.
H  2.
MNCL2.2H2O
    298.15        1.
        0.                            NO DATA
    -225.2      500.      52.3        WAGMAN ET AL. (1969)
1
O        0.        0.        0.        0.    NO DATA
     1000.
4
MN 1.
```

```
CL 2.
O  2.
H  4.
MNCL2.4H2O
    298.15        1.
        0.                              NO DATA
    -340.3      500.      72.5          WAGMAN ET AL. (1969)
1
0       0.        0.        0.          0.     NO DATA
     1000.
4
MN 1.
CL 2.
O  4.
H  8.
TODOROKITE
    298.15        1.
        0.                              NO DATA
   -923.38      500.      500.          CRERAR AND BARNES (1974) ESTIMATE
1                                       OF STABILITY RELATIVE TO MANGANITE
0       0.        0.        0.          0.     NO DATA
     1000.
3
MN 7.
O 15.
H  6.
BIRNESSITE
    298.15        1.
        0.                              NO DATA
  -1145.12      500.      500.          CRERAR AND BARNES (1974) ESTIMATE
1                                       OF STABILITY RELATIVE TO MANGANITE
0       0.        0.        0.          0.     NO DATA
     1000.
3
MN 8.
O 19.
H 10.
STOP.
MDSOLMN
```

DATA ON MINERALS AND RELATED SUBSTANCES OF MANGANESE

DATA PER SPECIES:

NAME OF SPECIES

BASE POINT TEMPERATURE (K) AND PRESSURE (BARS); THESE USUALLY BUT NOT NECESSARILY CORRESPOND TO THE REFERENCE TEMPERATURE (298.15 K) AND REFERENCE PRESSURE (1 BAR)

THE MOLAR VOLUME OF THE SOLID AT THE BASE TEMPERATURE AND PRESSURE, CC/MOL

THE APPARENT GIBBS ENERGY OF FORMATION FROM THE ELEMENTS AT THE BASE POINT TEMPERATURE AND PRESSURE, KCAL/MOL. (THIS IS THE SAME GIBBS ENERGY FUNCTION USED IN SUPCRT; HELGESON ET AL., 1978)

THE APPARENT ENTHALPY OF FORMATION FROM THE ELEMENTS AT AT THE BASE TEMPERATURE AND PRESSURE, KCAL/MOL. (THIS IS THE SAME ENTHALPY FUNCTION USED IN SUPCRT; HELGESON ET AL., 1978)

THE ENTROPY AT THE BASE TEMPERATURE AND PRESSURE, CAL/MOL-K

(NOTE: IF VALUES ARE ENTERED FOR ANY TWO OF THE THREE ABOVE FUNCTIONS, THE VALUE OF THE THIRD WILL BE CALCULATED AUTOMATICALLY USING THE 298.15 K AND 1 BAR ENTROPIES OF THE ELEMENTS IN THEIR STANDARD STATES AS STORED ON THE DATA FILE MDELEM.)

NUMBER OF HEAT CAPACITY RANGES TO FOLLOW

HEAT CAPACITY EQUATION CODE
- 0 EQ. ^4.1 OF BARNER AND SCHEURMAN (1978, P. 94)
- 1 EQ. ^4.2 , IBID.

(NOTE: WITHOUT THE D-TERM, BOTH EQUATIONS REDUCE TO THE STANDARD MAYER-KELLEY EXPRESSION)

THE HEAT CAPACITY COEFFICIENTS A, B, C, AND D

THE UPPER TEMPERATURE LIMIT OF THE HEAT CAPACITY EXPRESSION

NO. OF PHASE TRANSITIONS

THE TRANSITION VOLUME, CC/MOL
THE CLAPEYRON SLOPE, BAR/K

THE GIBBS ENERGY OF TRANSITION, KCAL/MOL
(USUALLY CALCULATED FROM THE ENTHALPY AND ENTROPY OF TRANSITION)
THE ENTHALPY OF TRANSITION, KCAL/MOL
THE ENTROPY OF TRANSITION, CAL/MOL-K
(USUALLY CALCULATED FROM THE TRANSITION VOLUME AND THE CLAPEYRON SLOPE)

THE UPPER TEMPERATURE LIMIT OF THE HEAT CAPACITY EXPRESSION

NO. OF ELEMENTS MAKING UP THE SOLID

ELEMENT NAME
STOICHIOMETRY IN TERMS THE ELEMENTS

NOTATION--
-- DELGO = GIBBS ENERGY OF FORMATION
-- DELGOR = GIBBS ENERGY OF REACTION
-- DELHO = ENTHALPY OF FORMATION
-- DELHOR = ENTHALPY OF REACTION
-- SO = CONVENTIONAL ENTROPY
-- DELSOR = ENTROPY OF REACTION

REFERENCES

BRICKER, O., 1965, SOME STABILITY RELATIONS IN THE SYSTEM MN-O2-H2O AT 25 DEG AND ONE ATMOSPHERE TOTAL PRESSURE, AMER. MINERALOGIST, 50, 1296-1354.

COUGHLIN, J. P., 1950, HIGH-TEMPERATURE HEAT CONTENTS OF MANGANOUS SULFIDE, FERROUS SULFIDE AND PYRITE, AMER. CHEM. SOC. JOUR., 72, 5445-5447.

CRERAR, D. A. AND BARNES, H. L., 1974, DEPOSITION OF DEEP-SEA MANGANESE NODULES, GEOCHIMICA ET COSMOCHIMICA ACTA, 38, 279-300.

HELGESON, H. C., DELANY, J. M., NESBITT, H. W., AND BIRD, D. K., 1978, SUMMARY AND CRITIQUE OF THE THERMODYNAMIC PROPERTIES OF ROCK-FORMING MINERALS, AMER. JOUR. OF SCIENCE, 278A, 1-229.

HEM, J. D., 1980, REDOX COPRECIPITATION MECHANISM OF MANGANESE OXIDES, PP. 45-72 IN KAVANAUGH, M. C. AND LECKIE, J. O. (ED.), PARTICULATES IN WATER, ADVANCES IN CHEMISTRY SERIES 189, AMER. CHEMICAL SOC., WASHINGTON D. C.

HEM, J. D., 1978, REDOX PROCESSES AT SURFACES OF MANGANESE OXIDE AND THEIR EFFECTS ON AQUEOUS METAL IONS, CHEMICAL GEOLOGY, 21, 199-218.

KELLEY, K. K., 1960, CONTRIBUTIONS TO THE DATA ON THEORETICAL METALLURGY, XIII. HIGH-TEMPERATURE HEAT-CONTENT, HEAT-CAPACITY, AND ENTROPY DATA FOR THE ELEMENTS AND INORGANIC COMPOUNDS, U. S. BUREAU OF MINES BULLETIN 584, 117-122.

MACDONALD, D. D.,1976, THE THERMODYNAMICS AND THEORETICAL CORROSION BEHAVIOR OF MANGANESE IN AQUEOUS SYSTEMS AT ELEVATED TEMPERATURES, CORROSION SCIENCE, 16, 461-482.

MOORE, G. E., 1943A, HEAT CONTENT OF MANGANESE DIOXIDE AND CARBONATE AT HIGH TEMPERATURE, AMER. CHEM. SOC. JOUR., 65, 1398-1399.

MOORE, G. E., 1943B, HEAT CONTENTS AT HIGH TEMPERATURE OF THE ANHYDROUS CHLORIDES OF CALCIUM, IRON, MAGNESIUM AND MANGANESE, AMER. CHEM. SOC. JOUR., 65, 1700-1703.

PLUMMER, L.N., JONES, B.F., AND TRUESDELL, A.H., 1976, WATEQF - A FORTRAN IV VERSION OF WATEQ, A COMPUTER PROGRAM FOR CALCULATING CHEMICAL EQUILIBRIUM OF NATURAL WATERS, U.S. GEOL. SURV. WATER RESOURCES INVESTIGATIONS 76-13.

ROBIE, R.A., B.S. HEMINGWAY, AND J.R. FISHER, 1978, THERMODYNAMIC PROPERTIES OF MINERALS AND RELATED SUBSTANCES AT 298.15 K AND 1 BAR ("10**5" PASCALS) PRESSURE AND AT HIGHER TEMPERATURES, GEOLOGICAL SURVEY BULLETIN 1452, U.S. GOVT. PRINTING OFFICE,

WASHINGTON, D.C.

ROBIE, R. A. AND WALDBAUM, D. R., 1968, THERMODYNAMIC PROPERTIES OF MINERALS AND RELATED SUBSTANCES AT 298.15 K (25.0 DEG C) AND ONE ATMOSPHERE (1.013 BARS) PRESSURE AND AT HIGHER TEMPERATURES, GEOLOGICAL SURVEY BULLETIN 1259, U. S. GOVT. PRINTING OFFICE, WASHINGTON D. C.

SOUTHARD, J. C. AND MOORE, G. E., 1942, HIGH TEMPERATURE HEAT CONTENT OF MN3O4, MNSIO3 AND MN3C, AMER. CHEM. SOC. JOUR., 64, 1769-1770.

SOUTHARD, J. C. AND SHOMATE, H., 1942, HEAT OF FORMATION AND HIGH-TEMPERATURE HEAT CONTENT OF MANGANOUS OXIDE AND MANGANOUS SULFATE. HIGH-TEMPERATURE HEAT CONTENT OF MANGANESE, AMER. CHEM. SOC. JOUR., 64, 1770-1774.

WAGMAN, D.D., W.H. EVANS, V.B. PARKER, I. HALOW, S.M. BAILEY, AND R.H. SCHUMM, 1969, SELECTED VALUES OF CHEMICAL THERMODYNAMIC PROPERTIES, NATL. BUR. STANDARDS TECH. NOTE 270-4.

STOP.

Manganese REAC File

```
AQUEOUS SPECIES OF MANGANESE
     MN++                          1
       1.00000 MN++
     MNCL+                         3
       -1.00000 MNCL+                          1.00000 MN++
       1.00000 CL-
     MNCL2                         3
       -1.00000 MNCL2                          1.00000 MN++
       2.00000 CL-
     MNCL3-                        3
       -1.00000 MNCL3-                         1.00000 MN++
       3.00000 CL-
     MNSO4                         3
       -1.00000 MNSO4                          1.00000 MN++
       1.00000 SO4--
     MNOH+                         4
       -1.00000 MNOH+                         -1.00000 H+
       1.00000 MN++                            1.00000 H2O
     MN(OH)2                       4
       -1.00000 MN(OH)2                       -2.00000 H+
       1.00000 MN++                            2.00000 H2O
     MN(OH)3-                      4
       -1.00000 MN(OH)3-                      -3.00000 H+
       1.00000 MN++                            3.00000 H2O
     MN(OH)4--                     4
       -1.00000 MN(OH)4--                     -4.00000 H+
       1.00000 MN++                            4.00000 H2O
     MNCO3                         4
       -1.00000 MNCO3                         -1.00000 H+
       1.00000 MN++                            1.00000 HCO3-
     MNF+                          3
       -1.00000 MNF+                           1.00000 MN++
       1.00000 F-
     HMNO2-                        4
       -1.00000 HMNO2-                        -3.00000 H+
       1.00000 MN++                            2.00000 H2O
     MN(NO3)2                      3
       -1.00000 MN(NO3)2                       1.00000 MN++
       2.00000 NO3-
     MNHCO3+                       3
       -1.00000 MNHCO3+                        1.00000 MN++
       1.00000 HCO3-
     MN+++                         5
       -4.00000 MN+++                         -2.00000 H2O
       4.00000 MN++                            4.00000 H+
       1.00000 O2(G)
     MNO4--                        5
       -1.00000 MNO4--                        -4.00000 H+
       1.00000 MN++                            2.00000 H2O
       1.00000 O2(G)
     MNO4-                         5
       -4.00000 MNO4-                         -12.0000 H+
       4.00000 MN++                            6.00000 H2O
       5.00000 O2(G)
     MN2(OH)3+                     4
       -1.00000 MN2(OH)3+                     -3.00000 H+
       2.00000 MN++                            3.00000 H2O
     MN2(OH)+++                    4
       -1.00000 MN2(OH)+++                    -1.00000 H+
       2.00000 MN++                            1.00000 H2O
SOLIDS OF MANGANESE
     RHODOCHROSITE                 4
       -1.00000 RHODOCHROSITE                 -1.00000 H+
       1.00000 MN++                            1.00000 HCO3-
     ALABANDITE                    4
       -1.00000 ALABANDITE                    -1.00000 H+
       1.00000 MN++                            1.00000 HS-
     MANGANOSITE                   4
       -1.00000 MANGANOSITE                   -2.00000 H+
       1.00000 MN++                            1.00000 H2O
     MNSO4(C)                      3
       -1.00000 MNSO4(C)                       1.00000 MN++
       1.00000 SO4--
     MN(OH)2(C)                    4
       -1.00000 MN(OH)2(C)                    -2.00000 H+
       1.00000 MN++                            2.00000 H2O
     HAUSMANNITE                   5
       -1.00000 HAUSMANNITE                   -6.00000 H+
       3.00000 MN++                            3.00000 H2O
```

```
      0.50000 O2(G)
BIXBYITE                    5
     -1.00000 BIXBYITE                  -4.00000 H+
      2.00000 MN++                       2.00000 H2O
      0.50000 O2(G)
MANGANITE                   5
     -4.00000 MANGANITE                 -8.00000 H+
      4.00000 MN++                       6.00000 H2O
      1.00000 O2(G)
MN(OH)3(C)                  5
     -4.00000 MN(OH)3(C)                -8.00000 H+
      4.00000 MN++                       10.0000 H2O
      1.00000 O2(G)
PYROLUSITE                  5
     -2.00000 PYROLUSITE                -4.00000 H+
      2.00000 MN++                       2.00000 H2O
      1.00000 O2(G)
RHODONITE                   5
     -1.00000 RHODONITE                 -2.00000 H+
      1.00000 MN++                       1.00000 H2O
      1.00000 SIO2(AQ)
TEPHROITE                   5
     -1.00000 TEPHROITE                 -4.00000 H+
      2.00000 MN++                       2.00000 H2O
      1.00000 SIO2(AQ)
SCACCHITE                   3
     -1.00000 SCACCHITE                  1.00000 MN++
      2.00000 CL-
MNCL2.H2O                   4
     -1.00000 MNCL2.H2O                  1.00000 MN++
      2.00000 CL-                        1.00000 H2O
MNCL2.2H2O                  4
     -1.00000 MNCL2.2H2O                 1.00000 MN++
      2.00000 CL-                        2.00000 H2O
MNCL2.4H2O                  4
     -1.00000 MNCL2.4H2O                 1.00000 MN++
      2.00000 CL-                        4.00000 H2O
TODOROKITE                  5
     -1.00000 TODOROKITE                -14.0000 H+
      7.00000 MN++                       10.0000 H2O
      2.50000 O2(G)
BIRNESSITE                  5
     -1.00000 BIRNESSITE                -16.0000 H+
      8.00000 MN++                       13.0000 H2O
      3.00000 O2(G)
STOP.
```

Manganese DFILE File

```
MN++                        1    1    0    0    0
        54.938    2.   0.0   5.0
       1.000 MN
       MCRT FILE MDAQSO., REV. 10/22/80, MDAQSO DATA GRID
       1.000 MN++
        43.9503    39.9477    35.3461    31.1507
        27.0288    23.7624    21.0581    18.6427
MNCL+                       2    3    0    0    0
        90.391    1.   0.0   4.0
       1.000 MN                1.000 CL
       MCRT FILE MDAQSMN, REV.  1/20/83, INSUFFICIENT DATA
      -1.000 MNCL+             1.000 MN++              1.000 CL-
        -.6010     -.6010   500.0000   500.0000
       500.0000   500.0000   500.0000   500.0000
MNCL2                       2    3    0    0    0
        125.844    0.   0.0   4.0
       1.000 MN                2.000 CL
       MCRT FILE MDAQSMN, REV.  1/20/83, DQUANT METHOD
      -1.000 MNCL2             1.000 MN++              2.000 CL-
        -.4026     -.0586      .4339      .9617
        1.6385     2.3912   500.0000   500.0000
MNCL3-                      2    3    0    0    0
        161.297   -1.   0.0   4.0
       1.000 MN                3.000 CL
       MCRT FILE MDAQSMN, REV.  1/20/83, INSUFFICIENT DATA
      -1.000 MNCL3-            1.000 MN++              3.000 CL-
         .2712      .2712   500.0000   500.0000
       500.0000   500.0000   500.0000   500.0000
MNSO4                       3    3    0    0    0
        150.996    0.   0.0   4.0
       1.000 MN                1.000 S                 4.000 O
       MCRT FILE MDAQSMN, REV.  1/20/83, DQUANT METHOD
      -1.000 MNSO4             1.000 MN++              1.000 SO4--
        -2.1232    -2.3082    -2.6221    -3.0034
        -3.5602    -4.2519   500.0000   500.0000
MNOH+                       3    4    0    0    0
        71.945    1.   0.0   4.0
       1.000 MN                1.000 O                 1.000 H
       MCRT FILE MDAQSMN, REV.  1/20/83, CRISS-COBBLE METHOD
      -1.000 MNOH+            -1.000 H+                1.000 MN++
       1.000 H2O
        11.4478    10.5447     9.5103     8.5673
         7.6403     6.8801     6.1848     5.4106
MN(OH)2                     3    4    0    0    0
        88.953    0.   0.0   4.0
       1.000 MN                2.000 O                 2.000 H
       MCRT FILE MDAQSMN, REV.  1/20/83, INSUFFICIENT DATA
      -1.000 MN(OH)2          -2.000 H+                1.000 MN++
       2.000 H2O
        22.1889    22.1889   500.0000   500.0000
       500.0000   500.0000   500.0000   500.0000
MN(OH)3-                    3    4    0    0    0
        105.960   -1.   0.0   4.0
       1.000 MN                3.000 O                 3.000 H
       MCRT FILE MDAQSMN, REV.  1/20/83, INSUFFICIENT DATA
      -1.000 MN(OH)3-         -3.000 H+                1.000 MN++
       3.000 H2O
        34.1996    34.1996   500.0000   500.0000
       500.0000   500.0000   500.0000   500.0000
MN(OH)4--                   3    4    0    0    0
        122.967   -2.   0.0   4.0
       1.000 MN                4.000 O                 4.000 H
       MCRT FILE MDAQSMN, REV.  1/20/83, INSUFFICIENT DATA
      -1.000 MN(OH)4--        -4.000 H+                1.000 MN++
       4.000 H2O
        48.2626    48.2626   500.0000   500.0000
       500.0000   500.0000   500.0000   500.0000
MNCO3                       3    4    0    0    0
        114.947    0.   0.0   4.0
       1.000 MN                1.000 C                 3.000 O
       MCRT FILE MDAQSMN, REV.  1/20/83, DQUANT METHOD
      -1.000 MNCO3            -1.000 H+                1.000 MN++
       1.000 HCO3-
         3.9521     3.8716     3.8144     3.8370
         3.9774     4.2527   500.0000   500.0000
MNF+                        2    3    0    0    0
        73.936    1.   0.0   4.0
       1.000 MN                1.000 F
       MCRT FILE MDAQSMN, REV.  1/20/83, CRISS-COBBLE METHOD
      -1.000 MNF+              1.000 MN++              1.000 F-
```

```
        -1.1830   -1.3758   -1.7059   -2.1182
        -2.6696   -3.3002   -4.0945   -5.2898
HMNO2-                  3    4    0    0    0
         87.945  -1.  0.0  4.0
       1.000 MN              1.000 H                2.000 O
       MCRT FILE MDAQSMN, REV.  1/20/83, CRISS-COBBLE METHOD
      -1.000 HMNO2-          -3.000 H+              1.000 MN++
       2.000 H2O
        37.3836   34.2099   30.7212   27.6993
        24.9409   22.9543   21.4420   20.1470
MN(NO3)2                3    3    0    0    0
        178.948   0.  0.0  4.0
       1.000 MN              2.000 N                6.000 O
       MCRT FILE MDAQSMN, REV.  1/20/83, INSUFFICIENT DATA
      -1.000 MN(NO3)2        1.000 MN++             2.000 NO3-
         -.2067    -.2067  500.0000  500.0000
       500.0000  500.0000  500.0000  500.0000
MNHCO3+                 4    3    0    0    0
        115.955   1.  0.0  4.0
       1.000 MN              1.000 H                1.000 C
       3.000 O
       MCRT FILE MDAQSMN, REV.  1/20/83, INSUFFICIENT DATA
      -1.000 MNHCO3+         1.000 MN++             1.000 HCO3-
         -.8928    -.8928  500.0000  500.0000
       500.0000  500.0000  500.0000  500.0000
MN+++                   1    5    0    0    0
         54.938   3.  0.0  8.0
       1.000 MN
       MCRT FILE MDAQSMN, REV.  1/20/83, CRISS-COBBLE METHOD
      -4.000 MN+++           -2.000 H2O             4.000 MN++
       4.000 H+              1.000 O2(G)
        17.9467   19.2247   20.6187   21.9614
        23.4263   24.5975   25.4179   25.4930
MNO4--                  2    5    0    0    0
        118.936  -2.  0.0  4.0
       1.000 MN              4.000 O
       MCRT FILE MDAQSMN, REV.  1/20/83, CRISS-COBBLE METHOD
      -1.000 MNO4--          -4.000 H+              1.000 MN++
       2.000 H2O             1.000 O2(G)
        37.5954   35.3093   32.8669   30.8208
        28.9880   27.6999   26.7508   25.9144
MNO4-                   2    5    0    0    0
        118.936  -1.  0.0  4.0
       1.000 MN              4.000 O
       MCRT FILE MDAQSMN, REV.  1/20/83, CRISS-COBBLE METHOD
      -4.000 MNO4-          -12.000 H+              4.000 MN++
       6.000 H2O             5.000 O2(G)
       102.7188   95.6662   87.9382   81.2761
        75.1730   70.6576   67.0095   63.4939
MN2(OH)3+               3    4    0    0    0
        160.898   1.  0.0  4.0
       2.000 MN              3.000 O                3.000 H
       MCRT FILE MDAQSMN, REV.  1/20/83, INSUFFICIENT DATA
      -1.000 MN2(OH)3+       -3.000 H+              2.000 MN++
       3.000 H2O
        23.9012   23.9012  500.0000  500.0000
       500.0000  500.0000  500.0000  500.0000
MN2(OH)+++              3    4    0    0    0
        126.883   3.  0.0  8.0
       2.000 MN              1.000 O                1.000 H
       MCRT FILE MDAQSMN, REV.  1/20/83, INSUFFICIENT DATA
      -1.000 MN2(OH)+++      -1.000 H+              2.000 MN++
       1.000 H2O
        10.5594   10.5594  500.0000  500.0000
       500.0000  500.0000  500.0000  500.0000
RHODOCHROSITE           3    4    0    0    0
        114.947   0.  0.0  0.0
       1.000 MN              1.000 C                3.000 O
       MCRT FILE MDSOLMN, REV.  2/18/83, HEAT CAPACITY INTEGRATION
      -1.000 RHODOCHROSIT    -1.000 H+              1.000 MN++
       1.000 HCO3-
          .1199    -.1891    -.6238   -1.0992
        -1.6745   -2.2744   -2.9808   -4.0062
ALABANDITE              2    4    0    0    0
         86.998   0.  0.0  0.0
       1.000 MN              1.000 S
       MCRT FILE MDSOLMN, REV.  2/18/83, HEAT CAPACITY INTEGRATION
      -1.000 ALABANDITE      -1.000 H+              1.000 MN++
       1.000 HS-
          .0213    -.3811    -.9477   -1.5684
```

```
        -2.3130   -3.0686   -3.9207   -5.0904
MANGANOSITE              2    4    0    0    0
         70.937   0.  0.0  0.0
       1.000 MN              1.000 O
       MCRT FILE MDSOLMN, REV.  2/18/83, HEAT CAPACITY INTEGRATION
      -1.000 MANGANOSITE    -2.000 H+                1.000 MN++
       1.000 H2O
        19.7962   17.9259   15.7892   13.8629
        11.9955   10.5258    9.2906    8.1010
MNSO4(C)                 3    3    0    0    0
        150.996   0.  0.0  0.0
       1.000 MN              4.000 O                 1.000 S
       MCRT FILE MDSOLMN, REV.  2/18/83, HEAT CAPACITY INTEGRATION
      -1.000 MNSO4(C)        1.000 MN++              1.000 SO4--
         3.6185    2.6717    1.3613    -.0491
        -1.7116   -3.3501   -5.1138   -7.3663
MN(OH)2(C)               3    4    0    0    0
         88.953   0.  0.0  0.0
       1.000 MN              2.000 O                 2.000 H
       MCRT FILE MDSOLMN, REV.  2/18/83, CONSTANT APPARENT ENTHALPY
      -1.000 MN(OH)2(C)     -2.000 H+                1.000 MN++
       2.000 H2O
        16.8827   15.2989   13.5574   12.0678
        10.7199    9.7390  500.0000  500.0000
HAUSMANNITE              2    5    0    0    0
        228.812   0.  0.0  0.0
       3.000 MN              4.000 O
       MCRT FILE MDSOLMN, REV.  2/18/83, HEAT CAPACITY INTEGRATION
      -1.000 HAUSMANNITE    -6.000 H+                3.000 MN++
       3.000 H2O               .500 O2(G)
        21.8788   19.7671   17.3742   15.2637
        13.2728   11.7122   10.3110    8.6456
BIXBYITE                 2    5    0    0    0
        157.874   0.  0.0  0.0
       2.000 MN              3.000 O
       MCRT FILE MDSOLMN, REV.  2/18/83, HEAT CAPACITY INTEGRATION
      -1.000 BIXBYITE       -4.000 H+                2.000 MN++
       2.000 H2O               .500 O2(G)
         9.5111    8.6434    7.6704    6.8338
         6.0690    5.4725    4.8970    4.0823
MANGANITE                3    5    0    0    0
         87.945   0.  0.0  0.0
       1.000 MN              2.000 O                 1.000 H
       MCRT FILE MDSOLMN, REV.  2/18/83, INSUFFICIENT DATA
      -4.000 MANGANITE      -8.000 H+                4.000 MN++
       6.000 H2O             1.000 O2(G)
        18.5562   18.5562  500.0000  500.0000
       500.0000  500.0000  500.0000  500.0000
MN(OH)3(C)               3    5    0    0    0
        105.960   0.  0.0  0.0
       1.000 MN              3.000 O                 3.000 H
       MCRT FILE MDSOLMN, REV.  2/18/83, CONSTANT APPARENT ENTHALPY
      -4.000 MN(OH)3(C)     -8.000 H+                4.000 MN++
      10.000 H2O             1.000 O2(G)
        48.3195   44.6094   40.7566   37.7535
        35.4037   33.9973  500.0000  500.0000
PYROLUSITE               2    5    0    0    0
         86.937   0.  0.0  0.0
       1.000 MN              2.000 O
       MCRT FILE MDSOLMN, REV.  2/18/83, HEAT CAPACITY INTEGRATION
      -2.000 PYROLUSITE     -4.000 H+                2.000 MN++
       2.000 H2O             1.000 O2(G)
         -.4075     .0235     .5437    1.0713
         1.6486    2.1084    2.3852    2.2724
RHODONITE                3    5    0    0    0
        131.022   0.  0.0  0.0
       1.000 MN              1.000 SI                3.000 O
       MCRT FILE MDSOLMN, REV.  2/18/83, HEAT CAPACITY INTEGRATION
      -1.000 RHODONITE      -2.000 H+                1.000 MN++
       1.000 H2O             1.000 SIO2(AQ)
        10.7943    9.7289    8.4369    7.2366
         6.0609    5.1292    4.3270    3.4859
TEPHROITE                3    5    0    0    0
        201.959   0.  0.0  0.0
       2.000 MN              1.000 SI                4.000 O
       MCRT FILE MDSOLMN, REV.  2/18/83, HEAT CAPACITY INTEGRATION
      -1.000 TEPHROITE      -4.000 H+                2.000 MN++
       2.000 H2O             1.000 SIO2(AQ)
        25.6555   23.0612   20.0255   17.2630
        14.5897   12.4936   10.7165    8.9134
```

Manganese DFILE File (cont)

```
SCACCHITE                2    3    0    0    0
        125.844    0.   0.0  0.0
       1.000 MN                2.000 CL
       MCRT FILE MDSOLMN, REV.  2/18/83, HEAT CAPACITY INTEGRATION
      -1.000 SCACCHITE         1.000 MN++              2.000 CL-
         9.8751     8.7738     7.3241     5.8043
         4.0537     2.3657      .5885    -1.6317
MNCL2.H2O                4    4    0    0    0
        143.859    0.   0.0  0.0
       1.000 MN                2.000 CL                1.000 O
       2.000 H
       MCRT FILE MDSOLMN, REV.  2/18/83, CONSTANT APPARENT ENTHALPY
      -1.000 MNCL2.H2O         1.000 MN++              2.000 CL-
       1.000 H2O
         6.2990     5.5311     4.5459     3.5444
         2.4144     1.3136   500.0000   500.0000
MNCL2.2H2O               4    4    0    0    0
        161.874    0.   0.0  0.0
       1.000 MN                2.000 CL                2.000 O
       4.000 H
       MCRT FILE MDSOLMN, REV.  2/18/83, CONSTANT APPARENT ENTHALPY
      -1.000 MNCL2.2H2O        1.000 MN++              2.000 CL-
       2.000 H2O
         4.5032     3.9816     3.3209     2.6627
         1.9261     1.1845   500.0000   500.0000
MNCL2.4H2O               4    4    0    0    0
        197.905    0.   0.0  0.0
       1.000 MN                2.000 CL                4.000 O
       8.000 H
       MCRT FILE MDSOLMN, REV.  2/18/83, CONSTANT APPARENT ENTHALPY
      -1.000 MNCL2.4H2O        1.000 MN++              2.000 CL-
       4.000 H2O
         2.8879     2.7150     2.5383     2.4161
         2.3181     2.1780   500.0000   500.0000
TODOROKITE               3    5    0    0    0
        630.604    0.   0.0  0.0
       7.000 MN               15.000 O                6.000 H
       MCRT FILE MDSOLMN, REV.  2/18/83, INSUFFICIENT DATA
      -1.000 TODOROKITE      -14.000 H+               7.000 MN++
      10.000 H2O               2.500 O2(G)
        18.3100    18.3100   500.0000   500.0000
       500.0000   500.0000   500.0000   500.0000
BIRNESSITE               3    5    0    0    0
        753.572    0.   0.0  0.0
       8.000 MN               19.000 O               10.000 H
       MCRT FILE MDSOLMN, REV.  2/18/83, INSUFFICIENT DATA
      -1.000 BIRNESSITE      -16.000 H+               8.000 MN++
      13.000 H2O               3.000 O2(G)
        20.3755    20.3755   500.0000   500.0000
       500.0000   500.0000   500.0000   500.0000
```

Strontium MDAQS File

```
MDAQSSR  DATA FOR AQUEOUS COMPLEXES OF STRONTIUM (SEE BOTTOM OF FILE)
LAST REVISED  4/20/83
SROH+
        1.          1
    298.15         1.
  -172.400     500.0       -2.4     DELGO FROM PARKER ET AL. (1971);
3                                   SO FROM SMITH AND MARTELL (1976) AS
SR 1.                               DELSOR=+8. FOR SR2+ + OH- = SROH+
O  1.
H  1.
SRCL2
        0.          0
    298.15         1.
   -196.45      500.       19.2     PARKER ET AL. (1971)
2
SR 1.
CL 2.
SRBR2
        0.          0
    298.15         1.
   -183.41      500.       31.6     PARKER ET AL. (1971)
2
SR 1.
BR 2.
SRSO4
        0.
    298.15         1.
   -315.14      500.       -3.0     DELGO FROM SMITH AND MARTELL (1976);
3                                   SO FROM PARKER ET AL. (1971);
SR 1.                               SEE NOTE A.
S  1.
O  4.
SRI2
        0.          0
    298.15         1.
   -158.37      500.       45.4     PARKER ET AL. (1971)
2
SR 1.
I  2.
SRNO3+
        1.          1
    298.15         1.
  -161.31       500.       19.3     SMITH AND MARTELL (1976) GIVE
3                                      LOGK=+0.8 AND DELSOR=-8.
SR 1.                                  FOR SR++ + NO3- = SRNO3+
O  3.
N  1.
SR(NO3)2
        0.          0
    298.15         1.
   -186.93      500.       62.2     PARKER ET AL. (1971)
3
SR 1.
O  6.
N  2.
SRCO3
        0.          0
    298.15         1.
  -259.88       500.      -21.4     PARKER ET AL. (1971)
3
SR 1.
O  3.
C  1.
SRF+
        1.          1
    298.15         1.
  -202.06       500.        3.0     SMITH AND MARTELL (1976) GIVE
2                                      LOGK=+0.1 AND DELSOR=14. FOR
SR 1.                                  SR++ + F- = SRF+ AT I=1.0
F  1.
STOP.
MDAQSSR
```

DATA ON AQUEOUS COMPLEXES OF STRONTIUM

NOTE--

- DATA FOR SRPO4-, SRHPO4 AND SRH2PO4+ APPEAR ON PHOSPHOROUS FILE MDAQSP
- THE VALUE "500." MEANS NO DATA

```
NOTE A - PARKER ET AL. GIVE DELGO OF -311.68 FOR SRSO4.
         THIS GIVES LOGK=0.014 FOR SR++ + SO4-- = SRSO4.
         OTHER ALKALINE EARTH SULFATES ALSO HAVE THIS
         SAME APPROX LOGK FROM PARKER ET AL. (1971).
         SMITH AND MARTELL (1976) LOGK IS IN BETTER
         AGREEMENT WITH OTHER REPORTS.

DATA PER SPECIES:

   NAME

   CHARGE NUMBER
   ION CODE:
      0   NEUTRAL COMPLEX    (MAY BE LEFT BLANK)
      1   CATION             (MAY BE LEFT BLANK)
      2   SIMPLE ANION       (MAY BE LEFT BLANK)
      3   OXYANION
      4   ACID OXYANION

   TEMPERATURE (K) AND PRESSURE (BARS) CORRESPONDING TO
      THE ENTERED THERMODYNAMIC DATA
   THE INTERNAL ELECTRONIC ENTROPY, IF THIS IS TO BE APPLIED
      IN A CORRECTION TO THE CRISS-COBBLE METHOD

   APPARENT STANDARD MOLAL GIBBS ENERGY, KCAL/MOL
   APPARENT STANDARD MOLAL ENTHALPY, KCAL/MOL
   ENTROPY, CAL/MOL/K

   NO. OF ELEMENTS
   ELEMENT NAME AND STOICHIOMETRIC COEFFICIENT
   STOICHIOMETRY IN TERMS OF REFERENCE ELEMENTAL COMPOUND

   NO. OF (KINDS OF) IONIC SPECIES APPEARING IN A DISSOCIATION
      REACTION OF THE NEUTRAL SPECIES
   STOICHIOMETRIC COEFFICIENT FOR THE DISSOCIATION REACTION
      AND THE NAME FOR EACH CONSTITUENT ION

NOTATION--
   -- DELGO = GIBBS ENERGY OF FORMATION
   -- DELGOR = GIBBS ENERGY OF REACTION
   -- DELHO = ENTHALPY OF FORMATION
   -- DELHOR = ENTHALPY OF REACTION
   -- SO = CONVENTIONAL ENTROPY
   -- DELSOR = ENTROPY OF REACTION
```

REFERENCES

BAES, C. F. JR. AND MESMER, R. E., 1976, THE HYDROLYSIS OF CATIONS, JOHN WILEY AND SONS,NEW YORK, PP. 98-103.

PARKER, V.B., D.D. WAGMAN, W.H. EVANS, 1971, SELECTED VALUES OF CHEMICAL THERMODYNAMIC PROPERTIES, NATL. BUR. STANDARDS TECH. NOTE 270-6.

PLUMMER, L.N., JONES, B.F., AND TRUESDELL, A.H., 1976, WATEQF - A FORTRAN IV VERSION OF WATEQ, A COMPUTER PROGRAM FOR CALCULATING CHEMICAL EQUILIBRIUM OF NATURAL WATERS, U.S. GEOL. SURV. WATER RESOURCES INVESTIGATIONS 76-13.

SILLEN, L.G., A.E. MARTELL, 1971, STABILITY CONSTANTS OF METAL-ION COMPLEXES, SUPPLEMENT NO. 1, THE CHEMICAL SOC., LONDON.

SMITH, R.M. AND A.E. MARTELL, 1976, CRITICAL STABILITY CONSTANTS, VOL. 4, INORGANIC COMPLEXES, PLENUM PRESS, NEW YORK.

STOP.

Strontium MDSOL File

```
MDSOLSR     DATA FOR SOLIDS OF STRONTIUM   (SEE BOTTOM OF FILE)
LAST REVISED  4/15/83
SRO(C)
    298.15        1.
    20.686                          ROBIE ET AL. (1978).
   -134.30      500.      13.0     PARKER ET AL. (1971)
1
O    12.13      1.26     -1.55        O.     KELLEY (1960)
     1100.
2
SR 1.
O  1.
SRF2(C)
    298.15        1.
      0.0                           NO DATA
   -278.40      500.      19.63    PARKER ET AL. (1971)
1
O    16.28      4.36     -0.62        O.     SEE NOTE A
     1100.
2
SR 1.
F  2.
SRCL2(C)
    298.15        1.
     0.00                           NO DATA
   -186.70      500.      27.45    PARKER ET AL. (1971)
1
O    18.20      2.45      0.00        O.     KELLEY (1960)
     1000.
2
SR 1.
CL 2.
SRCL2.H2O
    298.15        1.
      0.00                          NO DATA
    -247.7      500.      41.0     PARKER ET AL. (1971)
1
O    28.7       0.0       0.0         O.     PARKER ET AL. (1971)
     1000.
4
SR 1.
CL 2.
O  1.
H  2.
SRCL2.2H2O
    298.15        1.
      0.00                          NO DATA
    -306.4      500.      52.0     PARKER ET AL. (1971)
1
O    38.3       0.0       0.0         O.     PARKER ET AL. (1971)
     1000.
4
SR 1.
CL 2.
O  2.
H  4.
SRCL2.6H2O
    298.15        1.
      0.00                          NO DATA
   -535.67      500.      93.4     PARKER ET AL. (1971)
1
O     0.0       0.0       0.0         O.     NO DATA
     1000.
4
SR 1.
CL 2.
O  6.
H 12.
SRBR2(C)
    298.15        1.
    58.31                           ROBIE ET AL. (1978)
   -166.60      500.      32.29    PARKER ET AL. (1971)
1
O    14.39      9.32      0.88        O.     SEE NOTE B
      900.
2
SR 1.
BR 2.
SRBR2.H2O
    298.15        1.
```

```
      0.00                                NO DATA
    -228.1        500.        43.0       PARKER ET AL. (1971)
1
O     28.9         0.0         0.0          0.      PARKER ET AL. (1971)
      1000.
4
SR 1.
BR 2.
O  1.
H  2.
SRBR2.6H2O
    298.15          1.
      0.00                                NO DATA
   -519.70        500.        97.0       PARKER ET AL. (1971)
1
O     82.1         0.0         0.0          0.      PARKER ET AL. (1971)
      1000.
4
SR 1.
BR 2.
O  6.
H 12.
SRS(C)
    298.15          1.
        0.       NO DATA
    -107.2        500.        16.3       PARKER ET AL. (1971)
1
O     11.64         0.          0.          0.      PARKER ET AL. (1971)
      1000.
2
SR 1.
S  1.
CELESTITE
    298.15          1.
     46.25                               ROBIE ET AL. (1978)
   -320.50        500.        28.0       PARKER ET AL. (1971)
1
O     21.80       13.30        0.0          0.      KELLEY (1960)
      1400.
3
SR 1.
O  4.
S  1.
SR(NO3)2(C)
    298.15          1.
     70.93                                ROBIE ET AL. (1978)
   -186.46        500.        46.5        PARKER ET AL. (1971). ROBIE ET AL.
1                                         (1978) GIVES -186.21 FOR DELGO
O     40.80       22.82      -11.32          0.      SEE NOTE B
       900.
3
SR 1.
O  6.
N  2.
SR(NO3)2.4H2O
    298.15          1.
      0.0                                 NO DATA
   -413.65        500.        88.2        PARKER ET AL. (1971)
1
O      0.0         0.0         0.0          0.      NO DATA
       900.
4
SR 1.
O 10.
N  2.
H  8.
STRONTIANITE
    298.15          1.
     39.01                               ROBIE ET AL. (1978)
   -272.50        500.        23.2       PARKER ET AL. (1971). SEE NOTE C.
1
O     19.69       10.62       -2.51          0.      SEE NOTE B
      1000.
3
SR 1.
O  3.
C  1.
SRSIO3(C)
    298.15          1.
        0.       NO DATA
```

```
    -370.4      500.      23.1          PARKER ET AL. (1971)
1
O    21.16        0.        0.          0.     PARKER ET AL. (1971)
     1000.
3
SR 1.
O  3.
SI 1.
SR2SIO4(C)
    298.15        1.
       0.0                              NO DATA
   -523.70      500.      36.3          PARKER ET AL. (1971)
1
O    32.09      0.0        0.0          0.     PARKER ET AL. (1971)
      800.
3
SR 2.
O  4.
SI 1.
SRI2(C)
    298.15        1.
       0.0                             NO DATA
   -133.54      500.      38.03        CHASE ET AL. (1975)
1
O    16.68      6.56   -0.0088          0.    SEE NOTE A
      900.
2
SR 1.
I  2.
SR(OH)2(C)
    298.15        1.
       0.0
   -210.85      500.      23.2           CHASE ET AL. (1978)
1
O     8.45     31.74    -0.015          0.     SEE NOTE A
      700.
3
SR 1.
O  2.
H  2.
STOP.
MDSOLSR
```

DATA ON MINERALS AND RELATED SUBSTANCES OF STRONTIUM

NOTE - -

NOTE A - SMOOTHED DATA FROM CHASE ET AL. (1975) OR CHASE ET AL. (1978) FIT TO MAIER-KELLEY HEAT CAPACITY EQUATION FOR SRF2(C), SRI2(C), AND SR(OH)2(C) BY J. F. KERRISK, LOS ALAMOS NATIONAL LABORATORY.

NOTE B - SMOOTHED DATA FROM ROBIE ET AL. (1978) FIT TO MAIER-KELLEY HEAT CAPACITY EQUATION FOR SRBR2(C), SR(NO3)2(C), AND STRONTIANTITE BY J. F. KERRISK, LOS ALAMOS NATIONAL LABORATORY.

NOTE C - STRONTIANITE DELGO - ROBIE ET AL. (1978) GIVES -271.90; HELGESON ET AL. (1978) GIVES -275.47; ROBIE AND WALDBAUM (1968) GIVES -275.45.

DATA PER SPECIES:

NAME OF SPECIES

BASE POINT TEMPERATURE (K) AND PRESSURE (BARS); THESE USUALLY BUT NOT NECESSARILY CORRESPOND TO THE REFERENCE TEMPERATURE (298.15 K) AND REFERENCE PRESSURE (1 BAR)

THE MOLAR VOLUME OF THE SOLID AT THE BASE TEMPERATURE AND PRESSURE, CC/MOL

THE APPARENT GIBBS ENERGY OF FORMATION FROM THE ELEMENTS AT THE BASE POINT TEMPERATURE AND PRESSURE, KCAL/MOL. (THIS IS THE SAME GIBBS ENERGY FUNCTION USED IN SUPCRT; HELGESON ET AL., 1978)

THE APPARENT ENTHALPY OF FORMATION FROM THE ELEMENTS AT
AT THE BASE TEMPERATURE AND PRESSURE, KCAL/MOL.
(THIS IS THE SAME ENTHALPY FUNCTION USED IN SUPCRT;
HELGESON ET AL., 1978)
THE ENTROPY AT THE BASE TEMPERATURE AND PRESSURE, CAL/MOL-K

(NOTE: IF VALUES ARE ENTERED FOR ANY TWO OF THE THREE
ABOVE FUNCTIONS, THE VALUE OF THE THIRD WILL BE
CALCULATED AUTOMATICALLY USING THE 298.15 K AND 1 BAR
ENTROPIES OF THE ELEMENTS IN THEIR STANDARD STATES
AS STORED ON THE DATA FILE MDELEM.)

NUMBER OF HEAT CAPACITY RANGES TO FOLLOW

HEAT CAPACITY EQUATION CODE
0 EQ. ^4.1 OF BARNER AND SCHEURMAN (1978, P. 94)
1 EQ. ^4.2 , IBID.
(NOTE: WITHOUT THE D-TERM, BOTH EQUATIONS REDUCE
TO THE STANDARD MAYER-KELLEY EXPRESSION)
THE HEAT CAPACITY COEFFICIENTS A, B, C, AND D

THE UPPER TEMPERATURE LIMIT OF THE HEAT CAPACITY EXPRESSION

NO. OF PHASE TRANSITIONS

THE TRANSITION VOLUME, CC/MOL
THE CLAPEYRON SLOPE, BAR/K

THE GIBBS ENERGY OF TRANSITION, KCAL/MOL
(USUALLY CALCULATED FROM THE ENTHALPY AND ENTROPY
OF TRANSITION)
THE ENTHALPY OF TRANSITION, KCAL/MOL
THE ENTROPY OF TRANSITION, CAL/MOL-K
(USUALLY CALCULATED FROM THE TRANSITION VOLUME AND
THE CLAPEYRON SLOPE)

THE UPPER TEMPERATURE LIMIT OF THE HEAT CAPACITY EXPRESSION

NO. OF ELEMENTS MAKING UP THE SOLID

ELEMENT NAME
STOICHIOMETRY IN TERMS THE ELEMENTS

NOTATION--
-- DELGO = GIBBS ENERGY OF FORMATION
-- DELGOR = GIBBS ENERGY OF REACTION
-- DELHO = ENTHALPY OF FORMATION
-- DELHOR = ENTHALPY OF REACTION
-- SO = CONVENTIONAL ENTROPY
-- DELSOR = ENTROPY OF REACTION

REFERENCES

CHASE, M.W., J.L. CURNUTT, H. PROPHET, R.A. MCDONALD, AND A.N. SYVERUD, 1975, JANAF THERMOCHEMICAL TABLES, 1975 SUPPLEMENT, JOUR. PHYS. CHEM. REF. DATA, 4, 1-175.

CHASE, M.W., JR., J.L. CURNUTT, R.A. MCDONALD, AND A.N. SYVERUD, 1978, JANAF THERMOCHEMICAL TABLES, 1978 SUPPLEMENT, JOUR. PHYS. CHEM. REF. DATA, 7, 793-940.

HELGESON, H. C., DELANY, J. M., NESBITT, H. W., AND BIRD, D. K., 1978, SUMMARY AND CRITIQUE OF THE THERMODYNAMIC PROPERTIES OF ROCK-FORMING MINERALS, AMER. JOUR. OF SCIENCE, 278A, 1-229.

KELLEY, K. K., 1960, CONTRIBUTIONS TO THE DATA ON THEORETICAL METALLURGY, XIII. HIGH-TEMPERATURE HEAT-CONTENT, HEAT-CAPACITY, AND ENTROPY DATA FOR THE ELEMENTS AND INORGANIC COMPOUNDS, U. S. BUREAU OF MINES BULLETIN 584, 117-122.

PARKER, V.B., D.D. WAGMAN, W.H. EVANS, 1971, SELECTED VALUES OF CHEMICAL THERMODYNAMIC PROPERTIES, NATL. BUR. STANDARDS TECH. NOTE 270-6.

PLUMMER, L.N., JONES, B.F., AND TRUESDELL, A.H., 1976, WATEQF - A FORTRAN IV VERSION OF WATEQ, A COMPUTER PROGRAM FOR CALCULATING CHEMICAL EQUILIBRIUM OF NATURAL WATERS, U.S. GEOL. SURV. WATER

RESOURCES INVESTIGATIONS 76-13.

ROBIE, R.A., B.S. HEMINGWAY, AND J.R. FISHER, 1978, THERMODYNAMIC PROPERTIES OF MINERALS AND RELATED SUBSTANCES AT 298.15 K AND 1 BAR ("10**5" PASCALS) PRESSURE AND AT HIGHER TEMPERATURES, GEOLOGICAL SURVEY BULLETIN 1452, U.S. GOVT. PRINTING OFFICE, WASHINGTON, D.C.

ROBIE, R. A. AND WALDBAUM, D. R., 1968, THERMODYNAMIC PROPERTIES OF MINERALS AND RELATED SUBSTANCES AT 298.15 K (25.0 DEG C) AND ONE ATMOSPHERE (1.013 BARS) PRESSURE AND AT HIGHER TEMPERATURES, GEOLOGICAL SURVEY BULLETIN 1259, U. S. GOVT. PRINTING OFFICE, WASHINGTON D. C.

STOP.

Strontium REAC File

```
AQUEOUS SPECIES OF STRONTIUM
     SR++                          1
        1.00000 SR++
     SROH+                         4
       -1.00000 SROH+                      -1.00000 H+
        1.00000 SR++                        1.00000 H2O
     SRCL2                         3
       -1.00000 SRCL2                       1.00000 SR++
        2.00000 CL-
     SRBR2                         3
       -1.00000 SRBR2                       1.00000 SR++
        2.00000 BR-
     SRI2                          3
       -1.00000 SRI2                        1.00000 SR++
        2.00000 I-
     SRSO4                         3
       -1.00000 SRSO4                       1.00000 SR++
        1.00000 SO4--
     SRNO3+                        3
       -1.00000 SRNO3+                      1.00000 SR++
        1.00000 NO3-
     SR(NO3)2                      3
       -1.00000 SR(NO3)2                    1.00000 SR++
        2.00000 NO3-
     SRCO3                         4
       -1.00000 SRCO3                      -1.00000 H+
        1.00000 SR++                        1.00000 HCO3-
     SRF+                          3
       -1.00000 SRF+                        1.00000 SR++
        1.00000 F-
SOLIDS OF STRONTIUM
     SRO(C)                        4
       -1.00000 SRO(C)                     -2.00000 H+
        1.00000 SR++                        1.00000 H2O
     SRF2(C)                       3
       -1.00000 SRF2(C)                     1.00000 SR++
        2.00000 F-
     SRCL2(C)                      3
       -1.00000 SRCL2(C)                    1.00000 SR++
        2.00000 CL-
     SRCL2.H2O                     4
       -1.00000 SRCL2.H2O                   1.00000 SR++
        2.00000 CL-                         1.00000 H2O
     SRCL2.2H2O                    4
       -1.00000 SRCL2.2H2O                  1.00000 SR++
        2.00000 CL-                         2.00000 H2O
     SRCL2.6H2O                    4
       -1.00000 SRCL2.6H2O                  1.00000 SR++
        2.00000 CL-                         6.00000 H2O
     SRBR2(C)                      3
       -1.00000 SRBR2(C)                    1.00000 SR++
        2.00000 BR-
     SRBR2.H2O                     4
       -1.00000 SRBR2.H2O                   1.00000 SR++
        2.00000 BR-                         1.00000 H2O
     SRBR2.6H2O                    4
       -1.00000 SRBR2.6H2O                  1.00000 SR++
        2.00000 BR-                         6.00000 H2O
     SRS(C)                        4
       -1.00000 SRS(C)                     -1.00000 H+
        1.00000 SR++                        1.00000 HS-
     CELESTITE                     3
       -1.00000 CELESTITE                   1.00000 SR++
        1.00000 SO4--
     SR(NO3)2(C)                   3
       -1.00000 SR(NO3)2(C)                 1.00000 SR++
        2.00000 NO3-
     SR(NO4)2.4H2O                 4
       -1.00000 SR(NO3)2.4H2O               1.00000 SR++
        2.00000 NO3-                        4.00000 H2O
     STRONTIANITE                  4
       -1.00000 STRONTIANITE               -1.00000 H+
        1.00000 SR++                        1.00000 HCO3-
     SRSIO3(C)                     5
       -1.00000 SRSIO3(C)                  -2.00000 H+
        1.00000 SR++                        1.00000 SIO2(AQ)
        1.00000 H2O
     SR2SIO4(C)                    5
       -1.00000 SR2SIO4(C)                 -4.00000 H+
```

Strontium REAC File (cont)

```
        2.00000 SR++                        1.00000 SIO2(AQ)
        2.00000 H2O
     SRI2(C)                      3
       -1.00000 SRI2(C)                     1.00000 SR++
        2.00000 I-
     SR(OH)2(C)                   4
       -1.00000 SR(OH)2(C)                 -2.00000 H+
        1.00000 SR++                        2.00000 H2O
STOP.
```

Strontium DFILE File

```
SR++                        1    1    0    0    0
        87.620    2.   0.0  5.0
       1.000 SR
       MCRT FILE MDAQSO., REV. 10/22/80, MDAQSO DATA GRID
       1.000 SR++
       107.1119    98.0074    87.5292    77.9731
        68.5846    61.1790    55.1455    50.0236
SROH+                       3    4    0    0    0
        104.627    1.   0.0  4.0
       1.000 SR                1.000 O                    1.000 H
       MCRT FILE MDAQSSR, REV.  4/20/83, CRISS-COBBLE METHOD
      -1.000 SROH+            -1.000 H+                   1.000 SR++
       1.000 H2O
        14.1563    13.1908    12.0655    11.0474
        10.0589     9.2676     8.5686     7.8358
SRCL2                       2    3    0    0    0
        158.526    0.   0.0  4.0
       1.000 SR                2.000 CL
       MCRT FILE MDAQSSR, REV.  4/20/83, DQUANT METHOD
      -1.000 SRCL2             1.000 SR++                 2.000 CL-
         -.1460      .0147     -.1117     -.0936
         -.0742     -.0565    500.0000   500.0000
SRBR2                       2    3    0    0    0
        247.428    0.   0.0  4.0
       1.000 SR                2.000 BR
       MCRT FILE MDAQSSR, REV.  4/20/83, DQUANT METHOD
      -1.000 SRBR2             1.000 SR++                 2.000 BR-
         -.1532      .0235     -.1175     -.0988
         -.0788     -.0607    500.0000   500.0000
SRI2                        2    3    0    0    0
        341.429    0.   0.0  4.0
       1.000 SR                2.000 I
       MCRT FILE MDAQSSR, REV.  4/20/83, DQUANT METHOD
      -1.000 SRI2              1.000 SR++                 2.000 I-
         -.0044      .1202     -.0926     -.1495
         -.2238     -.3080    500.0000   500.0000
SRSO4                       3    3    0    0    0
        183.678    0.   0.0  4.0
       1.000 SR                1.000 S                    4.000 O
       MCRT FILE MDAQSSR, REV.  4/20/83, DQUANT METHOD
      -1.000 SRSO4             1.000 SR++                 1.000 SO4--
        -2.9700    -2.5501    -2.4472    -2.1940
        -1.9473    -1.7562    500.0000   500.0000
SRNO3+                      3    3    0    0    0
        149.625    1.   0.0  4.0
       1.000 SR                3.000 O                    1.000 N
       MCRT FILE MDAQSSR, REV.  4/20/83, CRISS-COBBLE METHOD
      -1.000 SRNO3+            1.000 SR++                 1.000 NO3-
        -1.0783     -.7997     -.5661     -.3976
         -.2755     -.2572     -.3945     -.8451
SR(NO3)2                    3    3    0    0    0
        211.630    0.   0.0  4.0
       1.000 SR                6.000 O                    2.000 N
       MCRT FILE MDAQSSR, REV.  4/20/83, DQUANT METHOD
      -1.000 SR(NO3)2          1.000 SR++                 2.000 NO3-
         -.3524     -.1481     -.2809     -.2447
         -.2074     -.1757    500.0000   500.0000
SRCO3                       3    4    0    0    0
        147.629    0.   0.0  4.0
       1.000 SR                3.000 O                    1.000 C
       MCRT FILE MDAQSSR, REV.  4/20/83, DQUANT METHOD
      -1.000 SRCO3            -1.000 H+                   1.000 SR++
       1.000 HCO3-
        10.4076    10.3439    10.0329    10.0847
        10.4446    11.1584   500.0000   500.0000
SRF+                        2    3    0    0    0
        106.618    1.   0.0  4.0
       1.000 SR                1.000 F
       MCRT FILE MDAQSSR, REV.  4/20/83, CRISS-COBBLE METHOD
      -1.000 SRF+              1.000 SR++                 1.000 F-
         -.6040     -.7528    -1.0486    -1.4162
        -1.9029    -2.4577    -3.1626    -4.2336
SRO(C)                      2    4    0    0    0
        103.619    0.   0.0  0.0
       1.000 SR                1.000 O
       MCRT FILE MDSOLSR, REV.  4/15/83, HEAT CAPACITY INTEGRATION
      -1.000 SRO(C)           -2.000 H+                   1.000 SR++
       1.000 H2O
        44.9476    41.1175    36.7108    32.7166
        28.8227    25.7686    23.2708    21.0816
```

Strontium DFILE File (cont)

```
SRF2(C)                    2    3    0    0    0
        125.617   0.  0.0  0.0
       1.000 SR                2.000 F
       MCRT FILE MDSOLSR, REV.  4/15/83, HEAT CAPACITY INTEGRATION
      -1.000 SRF2(C)           1.000 SR++              2.000 F-
        -7.4594   -7.3621   -7.4569   -7.7122
        -8.1900   -8.8579   -9.8148  -11.3986
SRCL2(C)                   2    3    0    0    0
        158.526   0.  0.0  0.0
       1.000 SR                2.000 CL
       MCRT FILE MDSOLSR, REV.  4/15/83, HEAT CAPACITY INTEGRATION
      -1.000 SRCL2(C)          1.000 SR++              2.000 CL-
         7.8854    7.1613    6.1208    4.9772
         3.6019    2.2202     .7048   -1.2635
SRCL2.H20                  4    4    0    0    0
        176.541   0.  0.0  0.0
       1.000 SR                2.000 CL                1.000 O
       2.000 H
       MCRT FILE MDSOLSR, REV.  4/15/83, HEAT CAPACITY INTEGRATION
      -1.000 SRCL2.H20         1.000 SR++              2.000 CL-
       1.000 H20
         4.3780    3.9992    3.3745    2.6322
         1.6777     .6509    -.5584   -2.2588
SRCL2.2H20                 4    4    0    0    0
        194.556   0.  0.0  0.0
       1.000 SR                2.000 CL                2.000 O
       4.000 H
       MCRT FILE MDSOLSR, REV.  4/15/83, HEAT CAPACITY INTEGRATION
      -1.000 SRCL2.2H20        1.000 SR++              2.000 CL-
       2.000 H20
         2.6600    2.5229    2.1957    1.7468
         1.1068     .3509    -.6210   -2.1109
SRCL2.6H20                 4    4    0    0    0
        266.617   0.  0.0  0.0
       1.000 SR                2.000 CL                6.000 O
      12.000 H
       MCRT FILE MDSOLSR, REV.  4/15/83, CONSTANT APPARENT ENTHALPY
      -1.000 SRCL2.6H20        1.000 SR++              2.000 CL-
       6.000 H20
          .2264     .6714    1.2674    1.9503
         2.7646    3.4563  500.0000  500.0000
SRBR2(C)                   2    3    0    0    0
        247.428   0.  0.0  0.0
       1.000 SR                2.000 BR
       MCRT FILE MDSOLSR, REV.  4/15/83, HEAT CAPACITY INTEGRATION
      -1.000 SRBR2(C)          1.000 SR++              2.000 BR-
        13.3913   12.3449   10.9331    9.4526
         7.7586    6.1461    4.4706    2.4128
SRBR2.H20                  4    4    0    0    0
        265.443   0.  0.0  0.0
       1.000 SR                2.000 BR                1.000 O
       2.000 H
       MCRT FILE MDSOLSR, REV.  4/15/83, HEAT CAPACITY INTEGRATION
      -1.000 SRBR2.H20         1.000 SR++              2.000 BR-
       1.000 H20
         9.4263    8.8163    7.9228    6.9347
         5.7460    4.5489    3.2197    1.4512
SRBR2.6H20                 4    4    0    0    0
        355.519   0.  0.0  0.0
       1.000 SR                2.000 BR                6.000 O
      12.000 H
       MCRT FILE MDSOLSR, REV.  4/15/83, HEAT CAPACITY INTEGRATION
      -1.000 SRBR2.6H20        1.000 SR++              2.000 BR-
       6.000 H20
         2.3318    2.8279    3.2914    3.6378
         3.8754    3.9024    3.6442    2.8228
SRS(C)                     2    4    0    0    0
        119.680   0.  0.0  0.0
       1.000 SR                1.000 S
       MCRT FILE MDSOLSR, REV.  4/15/83, HEAT CAPACITY INTEGRATION
      -1.000 SRS(C)           -1.000 H+                1.000 SR++
       1.000 HS-
        19.0280   17.3204   15.2361   13.2359
        11.1431    9.3384    7.6549    5.8378
CELESTITE                  3    3    0    0    0
        183.678   0.  0.0  0.0
       1.000 SR                4.000 O                 1.000 S
       MCRT FILE MDSOLSR, REV.  4/15/83, HEAT CAPACITY INTEGRATION
      -1.000 CELESTITE         1.000 SR++              1.000 SO4--
        -6.5595   -6.4788   -6.6341   -6.9850
```

```
        -7.5933    -8.3813    -9.4331   -11.0507
SR(NO3)2(C)              3     3    0    0    0
        211.630    0.   0.0   0.0
       1.000 SR                6.000 O                    2.000 N
       MCRT FILE MDSOLSR, REV.  4/15/83, HEAT CAPACITY INTEGRATION
      -1.000 SR(NO3)2(C)       1.000 SR++                 2.000 NO3-
         -.1905      .1965      .4462      .5079
          .3656      .0197     -.5772    -1.6515
SR(NO3)2.4H2O            4     4    0    0    0
        283.691    0.   0.0   0.0
       1.000 SR               10.000 O                    2.000 N
       8.000 H
       MCRT FILE MDSOLSR, REV.  4/15/83, CONSTANT APPARENT ENTHALPY
      -1.000 SR(NO3)2.4H2      1.000 SR++                 2.000 NO3-
       4.000 H2O
         -.9577     -.1305      .8725     1.9104
         3.0755     4.0715   500.0000   500.0000
STRONTIANITE             3     4    0    0    0
        147.629    0.   0.0   0.0
       1.000 SR                3.000 O                    1.000 C
       MCRT FILE MDSOLSR, REV.  4/15/83, HEAT CAPACITY INTEGRATION
      -1.000 STRONTIANITE     -1.000 H+                   1.000 SR++
       1.000 HCO3-
         1.2935     1.0936      .7627      .3874
         -.0792     -.5771    -1.1795    -2.0742
SRSIO3(C)                3     5    0    0    0
        163.704    0.   0.0   0.0
       1.000 SR                3.000 O                    1.000 SI
       MCRT FILE MDSOLSR, REV.  4/15/83, HEAT CAPACITY INTEGRATION
      -1.000 SRSIO3(C)        -2.000 H+                   1.000 SR++
       1.000 SIO2(AQ)          1.000 H2O
        15.2843    14.0630    12.5709    11.1960
         9.8631     8.8283     7.9664     7.1201
SR2SIO4(C)               3     5    0    0    0
        267.323    0.   0.0   0.0
       2.000 SR                4.000 O                    1.000 SI
       MCRT FILE MDSOLSR, REV.  4/15/83, HEAT CAPACITY INTEGRATION
      -1.000 SR2SIO4(C)       -4.000 H+                   2.000 SR++
       1.000 SIO2(AQ)          2.000 H2O
        45.0343    41.2538    36.8135    32.7767
        28.8620    25.8087    23.2861    20.9399
SRI2(C)                  2     3    0    0    0
        341.429    0.   0.0   0.0
       1.000 SR                2.000 I
       MCRT FILE MDSOLSR, REV.  4/15/83, HEAT CAPACITY INTEGRATION
      -1.000 SRI2(C)           1.000 SR++                 2.000 I-
        19.8055    18.3202    16.4132    14.4815
        12.3345    10.3549     8.3732     6.0639
```

APPENDIX B

Los Alamos

Los Alamos National Laboratory
Los Alamos, New Mexico 87545

memorandum

TO: B. Erdal, CNC-7, MS 514

DATE: June 24, 1982

FROM: D. Bish Dave Bish

MAIL STOP/TELEPHONE: J978/7-4337

SYMBOL: ESS-2

TWS-ESS-2-6/82-14
page 1 of 2

SUBJECT: RE-EXAMINATION OF JA AND YM SAMPLES POSSIBLY CONTAINING ERIONITE AND PHILLIPSITE

As you know, there is mention of erionite and phillipsite in Los Alamos reports. Heiken and Bevier (1979, LA-7563-MS) reported erionite in JA-15, JA-32, and JA-33BC, and phillipsite in JA-13. These analyses were based primarily on electron microprobe data, although the discussion of JA-32 included the x-ray diffraction (XRD) identification of "Er'ionite'(?)." Sykes, Heiken, and Smyth (1979, LA-8139-MS) reported the occurrence of erionite in YM-34 based on scanning electron microscope (SEM) examination.

I have re-examined all of the above samples by x-ray diffraction and find no evidence for the occurrence of either erionite or phillipsite. The results of my analyses are included, and they agree with previously published analyses of JA-32 (reported in memo from M. Sykes to B. Erdal, Aug. 6, 1981, #CNC7-81-180) and YM-34 (published in Carroll, Caporuscio, and Bish, 1981, LA-9000-MS). The minimum detection limits for phases such as erionite, phillipsite, mordenite, and clinoptilolite are on the order of 1-3%. In addition, the x-ray patterns of these zeolites are distinctive and their identification by XRD is usually unambiguous.

There are several explanations for the previous erionite and phillipsite identifications. All of the JA erionite and phillipsite analyses relied upon microprobe data. It is difficult, if not impossible, to obtain reliable chemical data for hydrous, finely intergrown materials, and identifications based upon analyses of such materials are suspect. Furthermore, it is possible for several different zeolites to yield similar chemical analyses, particularly erionite and mordenite.

The tentative identification of erionite in YM-34 was based on the morphology observed with the SEM. However, we have since observed identical morphologies in mordenite-rich tuffs containing no phillipsite. I suggest that the fibrous material in YM-34 is mordenite even though no mordenite peaks appeared in the x-ray diffraction pattern; we have often seen mordenite in tuffs (Topopah Spring, soak test samples) using the SEM when no mordenite peaks appeared in the x-ray diffraction patterns.

cc: B. Crowe, CNC7, MS 514
W. Myers, ESS-1, MS D461
W. Morris, ESS-2, MS K586
TWS file, MS K586

X-RAY ANALYSES OF JA AND YM SAMPLES

JA-13

Smectite	1-3%
Mica	1-3%
Quartz	10-20%
Alkali Feldspar	70-90%

JA-15

Mica	1-3%
Quartz	30-40%
Alkali Feldspar	60-70%

JA-32

Smectite	1-3%
Mica	2-5%
Quartz	30-40%
Alkali Feldspar	55-65%

JA-33

Smectite	2-4%
Mica	3-5%
Quartz	30-45%
Alkali Feldspar	50-60%

YM-34

Smectite	∿5%
Clinoptilolite	60-80%
Mordenite	5-10%
Quartz	5-15%
Alkali Feldspar	5-10%

☆U.S. GOVERNMENT PRINTING OFFICE: 1984-0-776-026/121

Printed in the United States of America
Available from
National Technical Information Service
US Department of Commerce
5285 Port Royal Road
Springfield, VA 22161

Microfiche (A01)

Page Range	NTIS Price Code	Page Range	NTIS Price Code	Page Range	NTIS Price Code	Page Range	NTIS Price Code
001-025	A02	151-175	A08	301-325	A14	451-475	A20
026-050	A03	176-200	A09	326-350	A15	476-500	A21
051-075	A04	201-225	A10	351-375	A16	501-525	A22
076-100	A05	226-250	A11	376-400	A17	526-550	A23
101-125	A06	251-275	A12	401-425	A18	551-575	A24
126-150	A07	276-300	A13	426-450	A19	576-600	A25
						601-up*	A99

*Contact NTIS for a price quote.

Los Alamos